'Neural stem cell recruitment in prion disease'

Kanella Prodromidou

MRC Prion Unit
Institute of Neurology
UCL

A thesis submitted for the degree of Doctor of Philosophy
to the University of London

Primary supervisor: Professor Sebastian Brandner
Secondary supervisor: Dr Peter Kloehn

ProQuest LLC
789 East Eisenhower Parkway
P.O. Box 1346
Ann Arbor, MI 48106-1346

Acknowledgments

I would like to thank my supervisors Sebastian Brandner and Peter Kloehn for their help and particularly professor Brandner for his guidance and advice. I also have to thank my colleagues in the Prion Unit, including Heike Naumann, who have provided precious assistance towards the completion of this project and others for the interesting discussions on the purpose of it all.

I am grateful to my brothers Nikos and Dimitris and my friends Alexandra, Ntomi and Fotoula for their important encouragement and support during the last years and even longer before.

This thesis is dedicated to my parents Adamantions and Kassandra Prodromidis who made this possible by giving me the opportunity to study abroad.

'Not everything that counts can be counted and not everything that can be counted counts.'

Albert Einstein

Abstract

Neurogenesis can be induced by several physiological and pathological conditions, such as environmental enrichment, stroke, epilepsy or inflammatory demyelination. The aim of this project was to investigate the possible effect of prion disease on neurogenesis, i.e. proliferation and differentiation of neural stem cells with a particular focus on the hippocampus and the neurogenic area of the dentate gyrus. We studied stem cell recruitment in non-infected and prion infected wild type mice. In addition, we examined transgenic mice which express prion protein at 3 times wt level (tg37), show profound hippocampal degeneration upon scrapie infection and that can be rescued by Cre-mediated inactivation of the *Prnp* gene in neurons.

Stem cell proliferation and differentiation was analysed by immunostaining of vibratome sections. To study stem cell *proliferation*, scrapie-infected and control mice received one intraperitoneal injection of BrdU (50 μg/g body weight) 30 minutes before culling. BrdU gets incorporated into proliferating cells. To study differentiation of labelled cells, animals were culled at different time points after BrdU injection (e.g. 7 and 8 days). BrdU-labelled cells were further characterised by the expression of astroglial (GFAP) and early neuronal (β-tubulin) markers using double labelling immuno-fluorescence. Also, we identified proliferating microglial cells using the marker Iba-1. Neuropathology of prion infected animals was assessed by immunostaining of paraffin-embedded brain sections. Cellular morphology was examined by haematoxylin and eosin staining. Astrogliosis and microglia activation was analyzed by immunostainings for the astroglial marker GFAP and the microglial marker Iba-1 respectively. Finally, PrP^{Sc} accumulation was verified by immunostaining with the PrP-specific antibody ICSM35.

Late-stage scrapie increased cell proliferation in the hippocampus but not the dentate gyrus of wild type mice while it profoundly increased cell proliferation throughout the area of the hippocampus of tg37 transgenic mice. BrdU-labelled proliferating cells in the dentate gyrus of wt mice acquired a neuronal phenotype within 8 days, thus confirming that BrdU labelling identifies proliferating progenitor cells, and further that the cell proliferation we estimated in the dentate gyrus partly reflects proliferation of stem cells. Proliferating cells in the dentate gyrus of prion-infected tg37 mice were identified as astrocytes and microglial cells. Also there was a significant increase in BrdU-labelled cells expressing β-tubulin.

Inactivation of PrP expression in neuronal cells during scrapie incubation, significantly decreased cell proliferation in the hippocampus. This decrease in part corresponded to a reduction in the number of proliferating astrocytes and microglial cells in the dentate gyrus. However, the

number of proliferating cells acquiring a neuronal phenotype (β-tubulin positive) was unaffected by PrP depletion (and the subsequent reversal of clinical prion disease) at least at an early time point following PrP depletion. Depletion of neuronal PrP also led to reduced proliferation in the hippocampus of un-inoculated mice, suggesting that PrP plays a role in cell proliferation.

We have demonstrated that prion disease and the resulting neuronal loss in the hippocampus increases neurogenesis (BrdU-labelled cells acquiring a neuronal phenotype) and also increases the numbers of proliferating astrocytes and microglia cells in the dentate gyrus of PrP over-expressing mice (tg37).

Contents

Index of figures and tables

Abbreviations

All amino acid abbreviations as standard

A	Adenin
BCA	Bicichoninic acid
BDNF	Brain derived neurotrophic factor
BMP	Bone morphogenetic protein
bp	Base pairs
BrdU	5' Bromo-2'deoxyuridine
BSA	Bovine serum albumin
BSE	Bovine spongiform encephalopathy
C	Cytosine
CA	Cornu ammonis (Ammons Horn)
cAMP	Cyclic adenine monophosphate
°C	Degrees Celsius
CJD	Creutzfeldt Jakob Disease
CNS	Central nervous system
CO_2	Carbon dioxide
CWD	Chronic wasting disease
DAB	3.3 Diaminobenzidine
DCX	Doublecortin
ddH2O	Distilled water
DG	Dentate gyrus
DGCs	Dentate granular cells
DMSO	Dimethyl sulphoxide
DNA	Deoxyribonucleic acid
dNTP	Deoxyribonucleotide triphosphate
Dpl	Doppel protein
EAE	Experimental auto-immune encephalomyelitis
EDTA	Ethylenediaminetetraacetic acid
EEG	Electroencephalogram
FDCs	Follicular dendritic cells
FFI	Fatal familial insomnia
G	Guanine
GABA	Gamma aminobutyric acid

GSS	Gerstmann-Sträussler-Scheinker syndrome
GFAP	Glial fibrillary acid protein (astrocyte intermediate filament)
GPI	Glycosyl-phosphatidylinositol
Ha	Hamster
HC	Hippocampus
HCl	Hydrochloric acid
HD	Huntington's Disease
HLA	Human leukocyte antigen
HRP	Horse radish peroxidase
HSCs	Haematopoietic stem cells
I4096	RML inoculum 4096 (MRC Prion Unit identifier code)
I5035	Mock inoculum 5035, 1% CD-1 brain homogenate (MRC Prion Unit identifier code)
Iba-1	Ionized calcium binding adaptor molecule 1 (microglial marker)
i.c.	Intracerebrally
i.p.	Intraperitoneal
kDa	Kilo daltons
KO	Knock-out
Lck	Promoter
LTD	Long term depression
LTP	Long term potentiation
M	Molar
ME7	Mouse-adapted scrapie strain
MAPK	Mitogen-activated protein kinase
MEK1	Mitogen-activated protein kinase kinase
min	Minutes
MoPrP	Mouse PrP
NaCl	Sodium chloride
NCAM	Neuronal cell adhesion molecule
NFH	Neurofilament heavy chain
NSE	Neuron-specific Enolase
OB	Olfactory bulb
ORF	Open reading frame
ORPD	octapeptide repeat deletion

ORPI	octapeptide repeat insertions
p75NTR	p75 neurotrophin receptor
PBS	Phosphate buffered saline
PBST	PBS containing Tween-20
PCNA	Proliferating cell nuclear antigen
PCR	Polymerase chain reaction
PK	Proteinase K
PKA	Protein kinase A
p.i.	Post-inoculation
PMCA	Protein misfolding cyclic amplification
prions	Infectious agent associated with transmission and/or clinical prion disease
Prnd	Mouse doppel gene
PRNP	Human PrP gene
Prnp	Mouse PrP gene
$Prnp^{0/0}$	Transgenic mice lacking PrP gene
PrP	Prion protein
PrP^{c}	Cellular prion protein
PrP^{res}	PrP protein resistant to proteolysis
PrP^{Sc}	The abnormal isoform of the prion protein
RMS	Rostral migratory stream
RB	Retinoblastoma
RE1/NRSE	Repressor element 1/neuron-restrictive silencer element
REST/NRSF	RE1/NRSE binding protein
RML	Mouse-adapted scrapie strain (Rocky Mountain Laboratory)
rpm	Revolutions per minute
RT	Room temperature
s	seconds
sCJD	Sporadic CJD
SDS	Sodium dodecyl sulphate
SGL	Subgranular layer
SVZ	Subventricular zone
T	Thymine
TAE	Tris acetate EDTA

TE	Tris EDTA
tg	Transgenic
TME	Transmissible mink encephalopathy
Tris	2,3-dibromopropyl phosphate
TrkB	Tyrosine receptor kinase B
TSA	Tyramide signal amplification
TSE	Transmissible spongiform encephalopathy
Tween-20	Polyoxyethylene (20) sorbitan monolaurate
U	Unit
vCJD	Variant CJD
wk	Week(s)
wt	Wild type

1 Introduction

1.1 Prion disease: Introduction

Transmissible Spongiform Encephalopathies (TSEs) or prion diseases are fatal neurodegenerative diseases that affect humans and both domestic and free ranging animals. Scrapie is a prion disease that affects sheep and it has been known for at least 200 years. Scrapie was demonstrated to be transmissible between sheep and goats following remarkably prolonged incubation periods in 1936 (Cuille, 1936). TSEs are transmissible by inoculation or ingestion of contaminated tissues. The incubation period, which is defined as the time from exposure to the infectious agent until clinical onset, can range from months to decades (Chesebro, 2003; Collinge, 2006). The molecular pathology of prion diseases involves the conversion of a normal cellular protein called prion protein (PrP^{c}) into an abnormal isoform which is partially protease resistant (denoted PrP scrapie or PrP^{Sc}). Prion protein is a membrane-associated glycoprotein of uncertain function. In the CNS it is expressed by neurons and astrocytes. The protease resistant isoform of the prion protein was isolated in 1982 by Prusiner and co-workers. It was found to be the major constituent of infective fractions as it forms aggregates in affected brains. All animal and human conditions share common histopathological features. Apart from accumulation of abnormal PrP, they include spongiform vacuolation (affecting any part of the cerebral grey matter), neuronal loss which varies from moderate to very severe, microglial activation and astrocytic proliferation which can be accompanied by plaques in which some of the PrP may be in the form of amyloid (Neuropathology, 2000, Ellison D, Love S; Collinge, 2005).

1.2 Prion disease in animals

Prion diseases in animals include scrapie in sheep which was the first prion disease to be shown as experimentally transmissible. Another form of prion disease that affects animals is the bovine spongiform encephalopathy (BSE or 'mad cow disease'), which became widespread among cattle in the UK in the mid-1980s (Anderson et al., 1996; Nathanson et al., 1997). The mean incubation time for BSE is about 5 years. Most cattle did not manifest disease as they were culled between 2 and 3 years of age (Stekel et al., 1996). It is believed that BSE was spread by feeding of protein supplements contaminated with the rendered tissues of BSE positive cattle. Controls were put in place in 1988 to ban the feeding of ruminant protein to ruminants. As a result the epidemic of

BSE in the UK has declined by 25–45% per year since 1992. The occurrence of BSE affected cattle born after the feeding ban remains unexplained, but their number is small and given the control measures in place, it is unlikely they will have significant impact on animal or public health (Ferguson and Donnelly, 2003). Transmission of BSE to humans was suspected when the first cases of an atypical form of CJD in teenagers and young adults occurred in Britain after the outbreak of BSE epidemic in 1994. The patients exhibited distinct clinical and neuropathological features and this new form of CJD was named variant CJD (vCJD).

Chronic wasting disease (CWD) in deer and Rocky Mountain elk in the US and Canada is another example of animal prion disease of unknown origin. In both species, the incidence of CWD in contaminated farms can be much higher than in wild populations. As clinical disease progresses, more noticeable signs arise such as hypotonic facial muscles, excessive salivation, and polyuria. Deer may survive up to 7–8 months after onset of clinical signs, elk may survive even longer (Miller et al., 1998).

Transmissible mink encephalopathy (TME) is an animal prion disease believed to be acquired by feeding animal tissues from scrapie-infected sheep or prion-infected cattle. The incubation period of natural TME has been estimated at 7–12 months. Clinical signs, which include ataxia and circling, can range from one week to several months prior to death (Marsh et al., 1991)

1.3 Prion disease in humans

Prion diseases in humans are identified as inherited, sporadic or transmitted. Inherited or familial human prion diseases are associated with *PRNP* mutations, and include familial Creutzfeldt-Jakob disease (CJD), fatal familial insomnia (FFI) and Gerstmann-Sträussler-Scheinker syndrome (GSS).

Sporadic prion diseases include sporadic CJD and sporadic fatal familial insomnia (FFI). In transmitted prion disease there is clear exposure to infectious agent. This group of prion diseases in humans comprises iatrogenic Creutzfeldt-Jakob disease (CJD), variant CJD (vCJD) and Kuru.

1.3.1 Sporadic human prion disease

At present sporadic CJD accounts for the majority of prion disease cases in humans (85%) and occurs at an incidence of 1 in 1 million people worldwide (Wadsworth, 2003). There is no

association with a mutant *PRNP* allele, nor is there any epidemiological evidence for exposure to infectious agent (Will, 1993; Harries-Jones et al., 1988). However, heterozygosity (Met/Val) at the polymorphic codon 129 of the *PRNP* gene appears to be associated with a lower risk of sporadic CJD (Palmer et al., 1991). Sporadic CJD occurs in males and females at equal frequencies. The age of onset is usually between 50–70 years of age, but can range from as low as 16 years and as high as 80 years. The main clinical symptom is usually dementia associated with cognitive disturbances such as confusion and memory loss. This usually progresses to severe dementia which can also be associated with myoclonus, cerebellar symptoms such as ataxia, visual disturbance and seizures. Clinical duration may last between 1–12 months.

1.3.2 Transmitted human prion disease

1.3.2.1 Iatrogenic CJD and Kuru

For kuru and iatrogenic CJD, the sufferers are exposed to human tissue contaminated with the infectious agent. Kuru mainly affected the people of the fore linguistic group at the eastern highlands of Papua New Guinea and their neighbours with whom they intermarried. Transmission occurred through handling and consumption of tissue from dead relatives as a mark of respect and mourning (Collinge et al., 2006). Prohibition of cannibalism by Australian authorities in the mid-1950s resulted in inhibition of transmission and cessation of the epidemic. However recent cases of kuru-affected individuals reveal that incubation periods can exceed 50 years (Collinge et al., 2006).

Iatrogenic CJD has been transmitted by transplantation of corneal or dural tissue from patients with prion disease, or by neurosurgical procedures using instruments previously used on patients with subclinical prion disease (Duffy et al., 1974; Will, 1993; Bernoulli et al., 1977; Fradkin et al., 1991). Iatrogenic CJD has also been transmitted by treatment with growth hormone extracted from cadaveric pituitary glands of undiagnosed CJD patients (Fradkin et al., 1991). The clinical symptoms vary in the different forms of iatrogenic prion diseases. In kuru and in prion disease caused by inoculation of contaminated growth hormone extracts, cerebellar ataxia is the primary sign. Dementia is less prominent and usually occurs late in the disease course. The incubation period is long, ranging from 2 years to greater than 10 years (Chesebro, 2003).

In prion disease caused by corneal or dural transplant or use of contaminated neurosurgical instruments (Guiroy et al., 1991) dementia is more prominent and latency is shorter (1–2 years) It is

likely that direct introduction of agent into the brain in the latter instances might account for the clinical differences.

Transmitted prion diseases are not associated with mutations of the *PRNP* gene, however, susceptibility may be influenced by *PRNP* codon 129 genotype, where Valine/Methionine (129V/M) heterozygosity is associated with longer incubation periods or even protection against transmission (Will, 1993; Pocchiari, 1994). In accordance to that observation it has been shown that most elderly survivors of the kuru epidemic are V/M heterozygotes (Collinge et al., 2006).

1.3.2.2 Variant Creutzfeldt-Jakob disease (vCJD)

In 1996, variant CJD (vCJD) , a new form of CJD, was first described in the UK (Will et al., 1996). Recent transmission studies on transgenic mice support the hypothesis that vCJD represents transmission of BSE from cattle to humans (Asante et al., 2002; Bruce et al., 1997; Hill et al., 1997; Lasmezas et al., 1996; Lasmezas et al., 2001). vCJD can be distinguished from sporadic CJD by the early age of onset, absence of distinct EEG (Electroencephalogram) features, and distinct neuropathology (Wieser, 2006). Moreover, whereas sporadic CJD is predominantly a late-onset disease with a peak onset at 60–65 years, the median age of onset of vCJD is 26 years (Spencer et al., 2002; Collee et al., 2006). The duration of disease is longer in vCJD with mean patient survival times of about 13 months, compared with about 4 months for sporadic CJD. Predominant clinical presentation of vCJD resembles kuru more than sCJD and is characterised by behavioural and psychiatric symptoms, peripheral sensory disturbance and cerebellar ataxia. Common early psychiatric features include anxiety, depression and withdrawal. All vCJD cases to date are homozygous for methionine at *PRNP* codon 129 (Collinge et al., 1996b; Wadsworth, 2003). A reduced frequency of human leukocyte antigen (HLA) class-II type DQ7 has been described in patients with vCJD, but not in those with sporadic CJD, which may have important implications for understanding host susceptibility to infection by BSE prions (Jackson et al., 2001).

As of 2007, there are over 200 cases of vCJD reported, mostly from the UK. It has now been 14 years since the peak of the BSE epidemic in the UK. This long time period without a clear peak in annual incidence of vCJD suggests that humans might be partially resistant to BSE-induced disease and/or that the dose of BSE infectivity to which people have been exposed is quite low. There is now concern that some individuals exposed to BSE might be asymptomatic carriers of the agent (Race and Chesebro, 1998; Race et al., 2001), and these people might, in turn, pose a risk of

further transmission of the infection for example by blood transfusion or surgical procedures. There has been wide concern that the blood supply might be contaminated with the vCJD agent as 3 cases of possible prion disease transmission through blood transfusion have been reported (Llewelyn, 2004 ; Peden, 2004 ; Wroe, 2006). This possibility is supported by evidence that BSE in sheep can be transmitted by blood transfusion (Houston et al., 2000).

1.3.3 Inherited human prion disease

Inherited prion disease is associated with the presence of an autosomal dominant mutation of the *PRNP* gene (Hsiao et al., 1989; Doh-ura et al., 1989) (Fig.1). The clinical and pathological characteristics, age of onset, and duration are variable and depend on the particular *PRNP* mutation involved. However, in some cases the same mutation can be associated with different clinical manifestations. The clinical symptoms include ataxia, dementia or sleep abnormality (Chapman, 1993). For most *PRNP* mutations, all carriers eventually develop the disease; however, for E200L mutation, this is not the case, suggesting that other factors may contribute to the onset of prion disease (Goldfarb et al., 1991). Such factors can be involvement of other genes, age of onset, and dietary or environmental factors.

In addition to point mutations in the *PRNP* gene, insertions in the octapeptide repeat coding region of *PRNP* have been associated with familial prion disease. In particular, addition of 2, 5, 6, 7, 8, or 9 extra octapeptide repeats have been detected in various families. In these cases clinical disease usually begins at an early age and is of long duration. The clinical symptoms are variable and include dementia and ataxia.

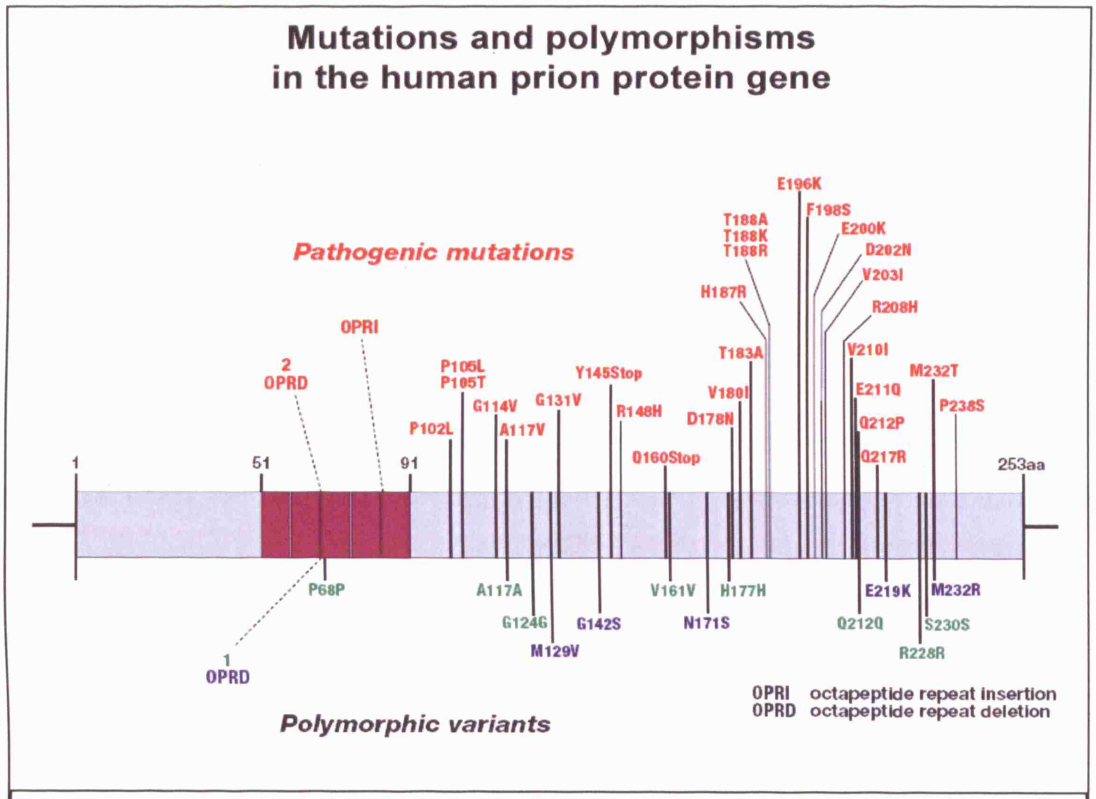

Figure 1: Mutations and polymorphisms in the human prion protein gene. The pathogenic mutations associated with human prion disease are depicted in red colour. These consist of 1, 2 or 4–9 octapeptide repeat insertions (ORPI) within the octapeptide repeat region between codons 51 and 91, a 2 octapeptide repeat deletion (ORPD) and various point mutations causing missense or stop amino-acid substitutions. To indicate point mutations the wild-type amino acid is shown before the codon number, followed by the mutant residue, using single letter amino-acid nomenclature. Polymorphic variants are shown below the PrP coding sequence. Deletion of one octapeptide repeat is not associated with prion disease in humans. (adapted from Wadsworth et.al, 2003).

1.4 The nature of the infectious agent and the protein-only hypothesis

The nature of the infectious agent for prion diseases remains elusive. There is no evidence for a virus-like particle or a nucleic acid genome. Both UV and ionizing radiation inactivation studies have eliminated the possibility of a large nucleic acid hiding within purified preparations of prions (Bellinger-Kawahara et al., 1987; Bellinger-Kawahara et al., 1987; Bellinger-Kawahara et al., 1988). Prusiner defined prions as proteinaceous infectious particles that lack nucleic acid (Prusiner, 1982; Prusiner, 1997). More importantly, PrP^{Sc} and scrapie (prion) infectivity co-purify when biochemical and immunological procedures are used (Gabizon et al., 1988). These observations led to the *protein only hypothesis* which states that the prion is devoid of informational nucleic acid and

that the essential pathogenic component is protein. However, the association with other 'non-informational' molecules (such as lipids or glycosamino glycans) is not excluded (Aguzzi and Weissmann, 1997).

The hallmark of all prion diseases whether sporadic, inherited, or transmitted, is that they involve the conversion of a normal cellular protein called prion protein (PrP^{c}) into an abnormal isoform (PrP^{Sc}) which is partially protease resistant (Prusiner, 1991) . The conversion of PrP^{C} into PrP^{Sc} involves a conformational change whereby the α-helical content diminishes and the amount of β-sheet increases (Pan et al., 1993).

One hypothesis that explains the conversion of PrP^{c} to PrP^{Sc} is the nucleation-dependent polymerization of PrP^{C} to form the ordered aggregate PrP^{Sc} (Harper and Lansbury, 1997). According to this theory prion protein exists in equilibrium between a predominantly α-helical native state (PrP^{c}) and a series of other β-sheet rich conformations, one of which, under certain conditions, can self-associate to produce a stable 'seed' ($PrP^{Sc)}$. PrP^{Sc} can then recruit PrP molecules towards the formation of an ordered aggregate, leading to an auto-catalytic cascade which is essentially irreversible (Fig. 2).

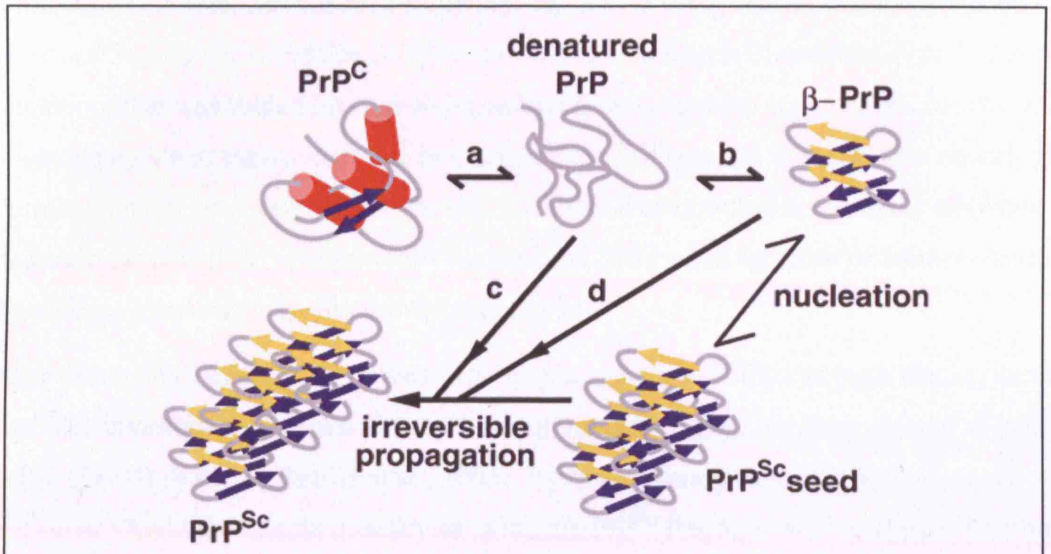

Figure 2: Proposed mechanism for prion replication. The predominantly α-helical PrP^{C} proceeds via an unfolded state to (a-b) refold into a rich in β-sheet conformation (β-PrP), which aggregates into a 'seed' and ultimately to the ordered aggregate PrP^{Sc}. Further recruitment of unfolded PrP (c) or β-PrP monomers (d) then occurs as an irreversible process (adapted from Collinge, 2005).

In support of the protein-only hypothesis it has been shown that antibodies to PrP inhibit prion replication and clear cell cultures from infectivity while *in vivo* engagement of PrP delays the development of prion disease (Peretz et al., 2001; White et al., 2003; Heppner et al., 2001). A limitation of the protein only hypothesis is that prions in animals and humans (Fig. 3) can be distinguished in different strains according to distinct glycoform ratios of the prion protein (diglycosylated, monoglycosylated, and un-glycosylated PrP), distinct incubation periods and also patterns of neuropathology (Kuczius, 1999; Kuczius, 1998; Somerville, 1997; Wadsworth, 2003). Moreover prion strains can be re-isolated in mice after passage in intermediate species with different PrP primary structures (Bruce et al., 1994;). These observations can argue in favour of a virus-like behavior where the characteristics of the infectious material are maintained after passaging. Alternatively it has been proposed that these data strongly support the 'protein-only' hypothesis by suggesting that strain variation could be encoded by a combination of PrP conformation and glycosylation (Collinge, 2005).

The ultimate proof of the 'protein only hypothesis' would be the *in vitro* production of prion protein that is both protease resistant and infectious. The first demonstration of *in vitro* production

of prion infectious material came from a study that has shown the synthesis of an aggregated peptide from a 55-amino acid peptide composed of MoPrP (mouse PrP) residues 89 to 143 with the P101L mutation, that was folded into a β-rich conformation (Legname et.al., 2004). Inoculation of the aggregated peptide to transgenic mice over-expressing PrP resulted in a TSE-like neurologic dysfunction within almost 1 year. However, this work received criticism since the tg mice that were inoculated over-expressed PrP and previous studies have shown that this type of animals develop a prion-like disease spontaneously (Westaway et.al., 1994)

Other recent and elegantly-conceived experiments were more efficient in producing *in vitro* infectivity. The investigators devised an amplification method to produce large amount of protease resistant PrP (PrP^{res}) *in vitro* (Castilla et.al., 2005). By this system (protein misfolding cyclic amplification or PMCA), a minute quantity of inoculum PrP^{res} (seed) is incubated with PrP^{c} (normal brain homogenate) which provides the substrate for conversion into more PrP^{res} (amplification). The amplified material was subjected to a series of dilutions into normal brain homogenate and subsequent amplification cycles to achieve the de novo production of a large amount of misfolded protein, free from brain PrP^{res} inoculum.

They further demonstrated that PrP^{res} generated in vitro has the same structural and biochemical properties as the disease-associated PrP, such as similar secondary structure and Western blot profile. Moreover, inoculation of in vitro produced PrP^{res} to wild type animals caused a disease that has clinical, histological and biochemical properties identical to the illness caused by the prion infectious agent.

However, the caveat of the PMCA method is that it is not readily reproducible, which may be explained by the differential organization of protein molecules into infectious units. For example, a large production of PrP^{res} *in vitro* may have led to the formation of big aggregates that might be less efficient for propagating infectivity *in vivo*, or sonication (part of the PMCA method procedure) may have produced too small aggregates that were not very efficient in maintaining infectivity.

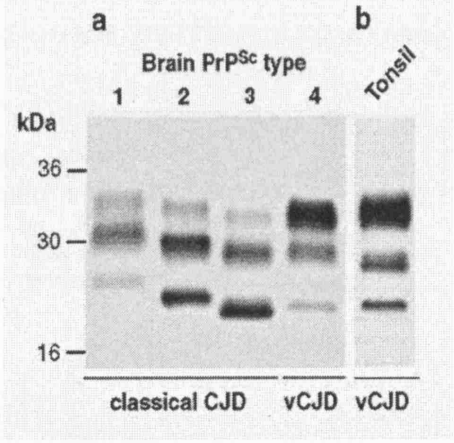

Figure 3: Molecular classification of human prion strains.

(a) Different strains are identified in human prion disease according to different glycoform ratios of PrP^{Sc}. There are 3 different strains of PrP^{Sc} (types 1-3) associated with human sporadic CJD (otherwise termed classical CJD) while a fourth strain (type 4) identifies vCJD. (b) PrP^{Sc} seen uniquely in tonsil of vCJD cases. In all cases samples were treated with PK and Western blots developed with monoclonal antibody 3F4. (from Wadsworth, 2003)

1.4.1 The species barrier

The concept of a 'species barrier' has been introduced to describe the difficulty of transmission of prion disease between different mammalian species. Upon transmission within the same species all inoculated animals succumb with a remarkably consistent incubation period. However upon transmission to another species not all animals develop the disease and those that do show much longer incubation periods than what is observed with transmission of prions within the same species. Moreover, upon transmission to another species the length of incubation varies among the successfully infected animals.

Transmission studies on transgenic mice have shown that transgenic mice expressing hamster PrP were, unlike wild type mice, highly susceptible to infection with Sc237 hamster prions and exhibited neuropathologic changes characteristic of hamsters with scrapie (Prusiner et al., 1990) (Fig.4). Similarly, transgenic mice expressing only human PrP, again unlike wt mice, were highly susceptible to CJD prions, with 100% attack rate and consistent short incubation periods (Hill et al., 1997a; Collinge et al., 1995). These results argued that prion synthesis is initiated by species specific interaction between PrP^{Sc} in the inoculum and homologous PrP^{c} of the inoculated host (Prusiner et al., 1990).

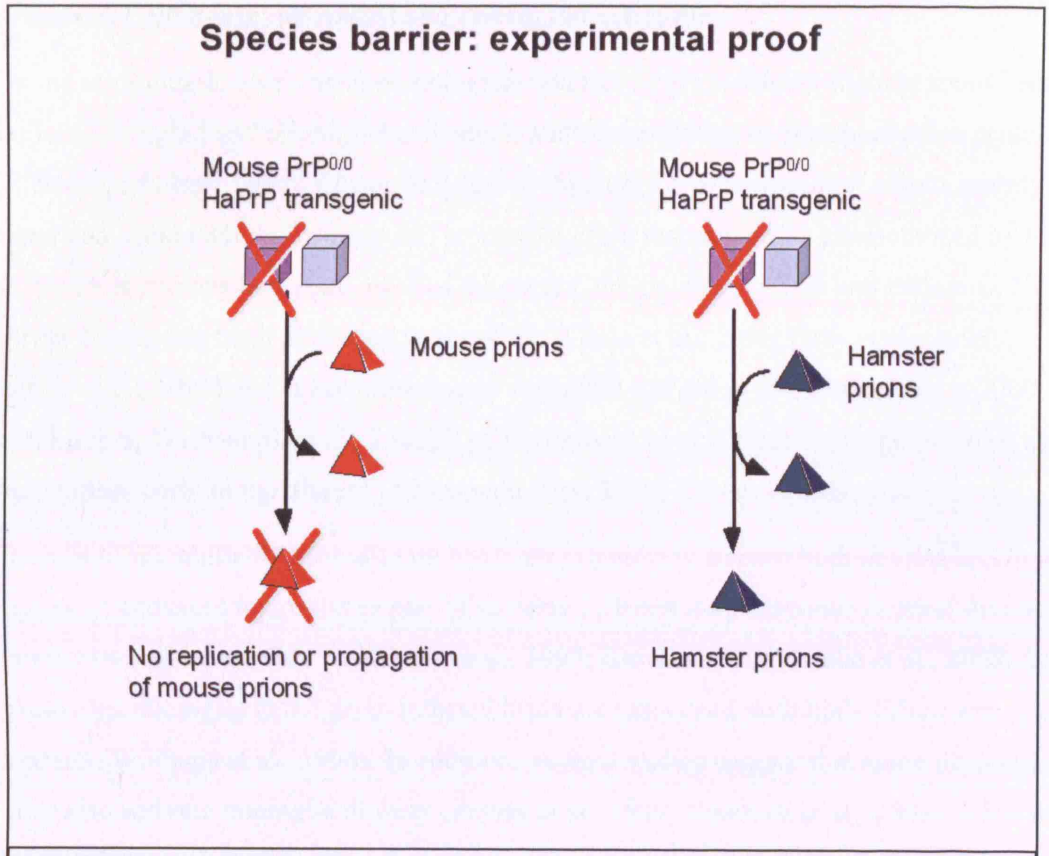

Figure 4: The effect of a species barrier in prion disease was demonstrated in transmission studies showing that transgenic mice expressing hamster PrP are, unlike wild type mice, highly susceptible to infection with hamster prions and exhibit neuropathological changes characteristic of hamsters with scrapie.

1.5 Neuropathology of prion disease

1.5.1 Macroscopic changes in prion disease

Neuropathology of human prion disease sometimes includes atrophy which in rare instances can result in reduction in brain weight to as low as 850g (Neuropathology, 2000, Ellison D, Love S). However, in most instances there is no atrophy. Rarely atrophy results in ventricular enlargement, reduction of the size of the caudate nucleus, the thalamus and the cerebellar foliae. The hippocampus is usually spared (Neuropathology, 2000, Ellison D, Love S). Loss of brain parenchyma affects the grey matter while white matter appears relatively unaffected. There are no pathological changes observed in meninges and blood vessels.

1.5.2 Neuronal cell death, astroglial and microglial activation

On the microscopic level, neuropathological features of prion disease include spongiosis, neuronal loss, astroglial and microglial activation, and accumulation of abnormal prion protein (PrP^{Sc}) (Neuropathology, 2000, Ellison D, Love S). Spongiosis or vacuolation affects mainly the grey matter and occurs within the neuronal processes. Prion disease is also characterised by loss of neurons, which is greatest in certain areas of the cortex, the caudate nucleus and thalamus. Neuronal loss in prion disease has been attributed to apoptosis (Giese et al., 1995; Gray et al., 1999; Kretzschmar et al., 1997) and is accompanied by astroglial activation (Neuropathology, 2000, Ellison D, Love S; Wadsworth et al., 2003; Van Everbroeck et al., 2002). Damage of axons and dendrites happens early in the disease (Neuropathology, 2000, Ellison D, Love S).

The role of microglia in prion disease has been extensively studied both *in vitro* and *in vivo*. The presence of activated microglia as part of an early inflammatory response in prion disease has been reported by various studies (Williams et al., 1997; Brown, 2001; Marella et al., 2005; Szpak, 2006). Activated microglia in the prion infected brain are associated with both diffuse and plaque PrP^{Sc} deposits (Williams et al., 1994). In addition, *in vitro* studies suggest that some fibrillar forms of PrP may also activate microglia directly (Peyrin et al., 1999; Veerhuis et al., 2002). It has been argued that PrP^{Sc} accumulation rather than neuronal loss is responsible for recruitment of microglial cells (Williams et al., 1997). The neuronal mitogen-activated protein kinase pathway was suggested to be involved in this process (Marella et al., 2005; Brown, 2001). However, it has been demonstrated *in vitro* that the complementary response of neurons and astrocytes to prion infection leads to microglial cell recruitment (Marella and Chabry, 2004).

An active role for microglia in removing neurons in prion disease has been demonstrated in tissue culture studies where the extent of neuronal death caused by prions was greatly increased in the presence of microglia (Brown et al., 1996; Bate et al., 2001). In support of these observations extensive numbers of microglial cells in the brain have been reported in a study of autopsy material from sCJD patients. Microglia cells were identified to be in a homing activation stage. In this stage microglia cells are able to distinguish between degenerating and surviving neurons, and selectively respond to signals from injured neurons and eliminate them (Szpak, 2006).

1.5.3 Absence of immune response, neuroinvasion and accumulation of PrP^{Sc}

In contrast to most other infectious disorders, prion diseases are not associated with T cell-mediated immune response. It is believed that this is due to tolerance to PrP^{c} which is a protein expressed in various cell types (Mabbott and MacPherson, 2006).

For vCJD, CWD and sheep scrapie, following exposure much of the acquired PrP^{Sc} accumulates in lymphoid tissues such as the spleen, lymph nodes, tonsils, appendix and Peyer's patches before spreading to the CNS, a process termed neuroinvasion (Hill et al., 1999; Hill et al., 1997; Mabbott and MacPherson, 2006). Follicular dendritic cells (FDCs) express PrP^{c} and play an important role in prion neuroinvasion. In the absence of FDCs , accumulation of PrP^{Sc} in the spleen is blocked, neuroinvasion is delayed and susceptibility is reduced (Burthem et al., 2001; Mabbott et al., 2000; Mabbott et al., 2003; Montrasio et al., 2000).

As PrP^{Sc} invades the CNS it accumulates in the brain where it can appear in various patterns: diffuse synaptic deposition, perivacuolar deposits around areas of vacuolation or larger deposits (or plaques) in which PrP^{Sc} appears in the form of amyloid (Neuropathology, 2000, Ellison D, Love S; Chesebro, 2003; Wadsworth et al., 2003). vCJD neuropathology shows striking amyloid plaques containing PrP^{Sc} throughout the forebrain and cerebellum, and these plaques are often surrounded by vacuoles giving rise to the characteristic 'florid plaque' morphology.

1.6 Mouse models of prion disease

1.6.1 Prion disease in wild type mouse strains.

Prion infection studies in mice revealed that in a given combination of mouse strain, prion strain, and inoculation path, incubation periods and vacuolar lesions in the brains appear strikingly constant (Bruce et al., 1991; Fraser and Dickinson, 1973). Kimberlin and Walker studied neuroinvasion and spread within the CNS and first proposed that clinical signs evolve when neuronal damage, caused by whichever mechanism, exceeds a certain threshold (Kimberlin and Walker, 1988). The duration of scrapie replication in mouse brains until clinical disease develops is always longer after i.c. infection than after infection by any of the non-neural, peripheral routes tested (Kimberlin and Walker, 1986). It has been suggested that the pathological processes must extend to a so-called 'clinical target area' before disease and death occur (Kimberlin et al., 1987). The application of different inoculation routes reflects the efficiency of different neural pathways through which infectivity spreads to these postulated clinical target areas (Kimberlin and Walker,

1986). This explains why agent entering from the thoracic cord (after i.p. injection) is transported more directly to these target areas than agent injected i.c. (Kimberlin et al., 1987).

1.6.2 Transgenic mouse models of inherited prion disease

Inherited human prion diseases have been associated with more than 30 mutations of the *PRNP* gene (Wadsworth, 2003). However, mice transgenic for human mutations of PrP gene have failed to develop transmissible disease. The only exception are mice over-expressing murine *Prnp* P101L (8-fold, on a $Prnp^{0/0}$ background). These mice harbor a mutation (P101L) analogous to the human prion protein mutation that causes Gerstmann-Straussler-Scheinker syndrome. They spontaneously developed neurodegeneration at 140 days of age, but little, if any PrP^{Sc} is detected (Hsiao et al., 1994; Telling et al., 1996). However, human P102L-linked GSS can be transmitted to both monkeys and wild type mice (Brown et al., 1994; Tateishi et al., 1996). It has been argued that the P101L mutation may be important susceptibility factor rather than a direct cause of GSS (Chesebro, 1999).

1.6.3 Prion disease in mice over-expressing PrP

In order to elucidate the role of host PrP in susceptibility and infection, transmission studies were carried out in mice over-expressing mouse PrP. Transgenic mice (tg37, tgc35, tga19, tga20) were generated that express PrP at 3 to 7-fold the level of wild-type mice (Fischer et al., 1996; Mallucci, 2002). Incubation of prion disease in these transgenic mice was significantly reduced following the inoculation of some scrapie isolates, and was shortened by half following inoculation of some mouse-adapted srapie strains, such as ME7 and RML (Fischer et al., 1996; Thackray et al., 2002; Mallucci, 2002). Moreover, the duration of clinical disease was greatly decreased in the transgenic animals over-expressing PrP as compared with wild-type animals. These experiments demonstrated that *Prnp* dosage affects the incubation time of prion disease.

An interesting finding that came from studies in mice over-expressing PrP was the discovery that un-inoculated older mice carrying high copy numbers of wild-type PrP transgenes, derived from Syrian hamsters (SHa) or sheep (She), developed spontaneously neurological symptoms, such as ataxia and hindlimb paralysis (Westaway, 1994). It was reported that these transgenic mice exhibited myopathy, demyelinating polyneuropathy and focal vacuolation of the CNS. Moreover, the onset of the disease was dependent on transgene dosage, as mice homozygous for the wt

transgene developed the disease earlier compared to mice hemizygous for the PrP transgene. These experiments contributed to the prion research by suggesting that over-expression of wt PrP can be pathogenic.

1.6.4 PrP knock-out mice

To investigate the function of PrP as a cellular protein and further its role in prion infection PrP knock-out mice (*Prnp*$^{0/0}$) were generated. *Prnp* is encoded by a single copy gene that comprises 3 exons with the entire open reading frame (ORF) contained in the 3rd exon (Basler et al., 1986). The first approach for generation of knock-out mice involved disruptive modifications restricted to the ORF and produced the Zurich I and Edinburgh knock-out mice which develop normally (Bueler et al., 1992; Manson et al., 1994). However, electrophysiological studies showed that long-term potentiation was impaired in these mice (Collinge et al., 1994; Manson et al., 1995; Whittington et al., 1995), while biochemical changes reported for Zürich-I-type knock-out mice suggest an impairment of enzymatic activity required for anti-oxidant defence (Klamt et al., 2001).

Another approach for generation of *Prnp*$^{0/0}$ mice involved the deletion of not only the open reading frame, but also of its flanking regions, in particular the splice acceptor site of the third exon (Sakaguchi et al., 1996). This type of *Prnp*$^{0/0}$ mice (Nagasaki) also develops normally, but exhibits severe ataxia and Purkinje cell loss later in life (Sakaguchi et al., 1996; Silverman et al., 2000; Rossi et al., 2001). As it was later found, Doppel, a novel PrP-like protein which normally is not detected in the brain of adult wild-type mice (Lu et al., 2000; Silverman et al., 2000), was upregulated in the brain of Nagasaki knockout mice (Moore et al., 1999). More specifically, in the Nagasaki knock-out line the acceptor splice site of the third *Prnp* exon is lost, causing exon skipping and formation of chimeric transcripts that place *Prnd* transcription under control of the *Prnp* promoter and therefore Doppel, is ectopically expressed in the brain of these animals (Moore et al., 1999; Li et al., 2000; Weissmann, 1996).

Wild type mice inoculated intracerebrally with mouse-adapted scrapie prions develop clinical symptoms at around 160 days and die about approximately 10 days later. By contrast, prion-infected PrP knock-out mice remain free of clinical symptoms, free of scrapie-specific neuropathology as late as 57 weeks after inoculation and they do not propagate prions (Bueler, 1993; Sailer, 1994). It was concluded that the host PrP is necessary for susceptibility to prion infection while its absence confers resistance (Fig. 5).

Finally, mice carrying a single *Prnp* allele (*Prnp* $^{0/+}$ mice) showed prolonged incubation of about 290 days until the onset of mild symptoms, as compared to 160 days in *Prnp*$^{+/+}$ mice. Both *Prnp* heterozygous and homozygous mice harbour high levels of infectivity and PrP^{Sc} at 140 days after inoculation, but only heterozygous mice survive thereafter for at least another 140 days without showing severe clinical symptoms (Bueler et al., 1994). Therefore, PrP gene dosage affects the incubation time of prion disease, but not the final pathology.

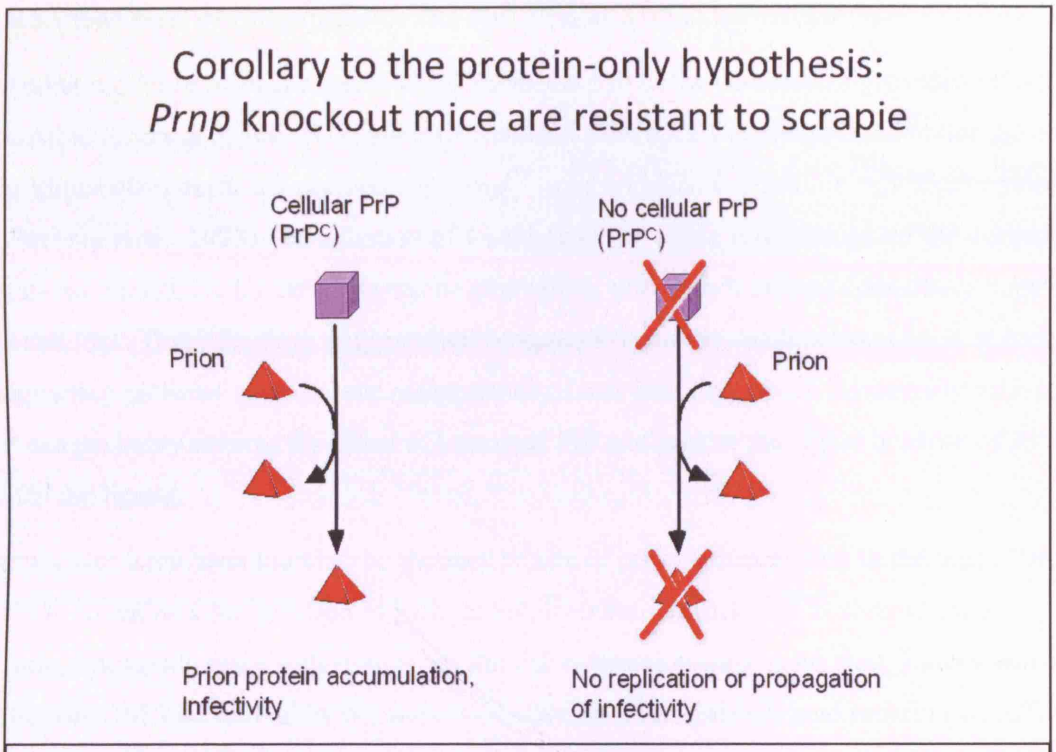

Figure 5: schematic drawing illustrating the prerequisite of prion protein expression for susceptibility to prion infection. In agreement with the *'protein only hypothesis'*, mice lacking the prion protein are resistant to prion infection and cannot further propagate infectivity.

1.6.5 Transgenic models of ectopic expression of PrP

The resistance of *Prnp*$^{0/0}$ mice against prion infection revealed that the expression of the prion protein is necessary for susceptibility and prion propagation (Fig. 5) (Bueler, 1993; Sailer, 1994). Various transgenic mouse models of ectopic expression of PrP have been generated to examine the competence of different cell types for prion replication. The ectopic expression of the PrP has been studied in neurons, astrocytes and in B and T lymphocytes.

Neuron-specific HaPrP expression was demonstrated to be sufficient to render mice susceptible to prion disease induced by the 263K hamster scrapie strain (Race et.al., 1995).

Specifically, transgenic mice expressing the hamster PrP (HaPrP) gene under control of the Neuron-specific Enolase (NSE) promoter, showed only PrP in brain tissue, with highest levels found in neurons of the cerebellum, hippocampus, thalamus, and cerebral cortex. These mice were susceptible to infection by the 263K strain of hamster scrapie with a longer incubation period compared to wild type hamsters. Interestingly some regions of high HaPrP expression, such as the cerebellar cortex and hippocampus, had no detectable abnormal PrP deposition, indicating that factors other than level of PrP expression can also influence prion accumulation.

Another model of ectopic expression of truncated PrP in the cerebellum provided information on the possible function of PrP. N-terminally truncated PrP (ΔPrP) was expressed under the control of the Purkinje cell-specific L7 promoter in *Prnp*$^{0/0}$ mice and lead to Purkinje cell degeneration and ataxia (Flechsig et.al., 2003). Introduction of a wild-type PrP allele fully abrogated the clinical manifestations elicited by L7-ΔPrP transgene expression, although it did not completely suppress Purkinje cell loss. These findings suggest that truncated PrP causes death perhaps by interfering with a signalling pathway essential for maintenance of cell viability, which is normally activated by PrP. PrP can probably reverse the effect of truncated PrP and restore the signal because of its higher affinity for the ligand.

Astrocytes have been found to be the earliest site of prion accumulation in the brain (Diedrich et al.,1991). To address the question of a direct involvement of astrocytes in scrapie agent propagation, transgenic mice with tissue-specific PrP expression were generated. Expression of HaPrP (hamster PrP) controlled by the astrocytic-specific glial fibrillary acid protein (GFAP) promoter in *Prnp*$^{0/0}$ mice rendered the animals susceptible to prion infection and led to clinical disease, suggesting that astrocytes are competent for prion replication. The neuropathological changes seen in these transgenic mice is quite similar to these found in scrapie-infected wild type mice (Raeber et al., 1997).

Other studies have also showed accumulation of PrP^{Sc} in astrocytes. In NFH-Cre/tg37 transgenic mice, Cre-mediated depletion of neuronal PrP during the course of prion infection and at a point of established spongiosis results in rescue of neuronal loss and reversal of clinical disease (Mallucci et al., 2003). However, PrP^{Sc} continued to accumulate in the brain of rescued animals after the Cre-mediated PrP depletion in neurons. Because astrocytes are the largest non-neuronal PrP-expressing population of cells in the brain, it was hypothesized that they are probably the major source of PrP^{Sc} generation. In line with this assumption, it was found that astrocytic proliferation was also increased over time, in parallel to and correlating with the pattern of continued PrP^{Sc}

deposition. Using double immunofluorescent labelling it was shown that PrP^{Sc} deposits co-localized with GFAP-positive astrocytes in the brains of infected mice with neuronal PrP depletion, which was not seen in scrapie-infected control animals without PrP depletion. These findings suggested that propagation of PrP^{Sc} was occurring in the PrP-expressing astrocytes. Despite the continued PrP^{Sc} accumulation and increased gliosis observed after neuronal PrP depletion, the animals remained asymptomatic. It was proposed by the authors that the conversion of PrP to disease-associated isoforms needs to take place specifically within neurons to be neurotoxic. However, this finding contradicted previous studies where ectopic expression of PrP in astrocytes led to clinical disease following prion inoculation (Raeber et al., 1997). This discrepancy could be attributed to the different mouse models used by the two studies: Mallucci and colleagues carried out their study on a transgenic mouse line overexpressing mouse PrP, while Raeber's work involved a transgenic mouse strain with ectopic expression of hamster PrP in astrocytes.

Mature B lymphocytes have been shown to carry PrP^{Sc} when isolated from spleens of wild-type mice after i.p. prion infection (Raeber et.al., 1999a). Ectopic expression of PrP in B lymphocytes has been investigated in follow up of data that showed impaired prion acumulation in the spleen of mice lacking B cells (Klein et.al., 1997). However, transgenic mice over-expressing PrP in B lymphocytes in a PrP-nul background, failed to accumulate prions in spleen after scrapie i.p. inoculation (Montrasio et.al., 2001), suggesting that in wild-type mice B cells must be acquiring prions from other cells. B lymphocytes are closely associated with and play an essential role in the maturation of follicular dendritic cells (FDCs), which are essential for the synthesis and accumulation of prions in spleen and to contribute directly or indirectly to neuroinvasion (Montrasio, 2000, Mabbot 2000). It has therefore been proposed that B cells acquire prions from FDCs, and that at least in mouse they are not instrumental in carrying infectivity to the CNS.

Finally, ectopic expression of PrP on T lymphocytes of PrP knock out mice is insufficient to maintain prion replication. Transgenic mice that over-express PrP exclusively on T lymphocytes under the control of the *Lck* promoter failed to replicate prions in the spleen or brain and showed no disease following i.p. challenge with mouse scrapie prions (Raeber et.al., 1999b).

1.6.6 Transgenic mouse model of reversal of prion disease

Studies of transgenic mice over-expressing PrP demonstrated that PrP depletion in neurons during the incubation of prion disease prevents progression to clinical disease and reverses neuronal

loss and spongiosis (Mallucci et al., 2003). Transgenic mice were raised on a *Prnp* null background and expressed PrP^c from M*lox*P transgenes at 3 (tg37) and 1 (tg46) times of wild-type levels. Double transgenic NFH-Cre/M*lox*P mice were generated from tg37 mice which express Cre recombinase in neurons under the control of the neurofilament heavy chain (NFH) promoter at 10 to 12 weeks of age (Mallucci et al., 2003). Expression of NFH coincides with Cre-mediated recombination of the floxed PrP transgenes in neuronal cells but not in astrocytes or other cell types (Mallucci et al., 2002).

Tg37 and tg46 mice normally succumb to scrapie at 12 and 18 weeks p.i., respectively, after intracerebral Rocky Mountain Laboratory (RML) scrapie prion inoculation. NFH-Cre/M*lox*P mice were inoculated with RML scrapie prions at 1 week of age and underwent Cre-mediated neuronal PrP^c depletion at 11 weeks post inoculation when spongiform change was already established. PrP^c depletion resulted in reversal of spongiosis even at this late stage of incubation. Specifically, in scrapie-infected tg37 mice without PrP depletion, hippocampal CA1 to CA3 neurons begin to degenerate from 10 weeks post-inoculation (wpi), with almost complete cell loss in CA1 to CA3 areas by 12 wpi and accompanying shrinkage of the entire hippocampus. In contrast prion-infected NFH-Cre/tg37, in which *Prnp* was inactivated due to Cre-mediated recombination, remained asymptomatic at 57 wpi , CA1 to CA3 neurons remained healthy, and hippocampal structure was completely preserved. However, there was increasing gliosis and PrP^{Sc} deposition in infected animals after PrP^c depletion. It was shown that PrP^{Sc} deposits co-localized with astrocytes in the brains of infected mice with neuronal PrP depletion which was not seen in scrapie-infected control animals without PrP depletion (Fig. 6).

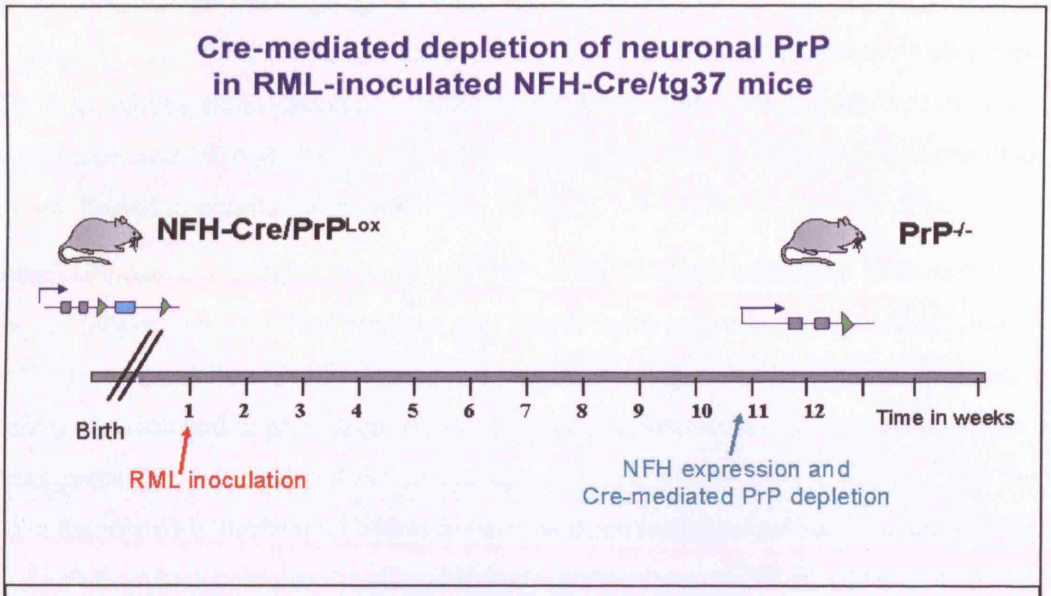

Figure 6: NFH-Cre/tg37 mice were RML-inoculated at 7-10 days of age. In this system Cre is expressed under the control of the NFH promoter when the animals reach 10-12 wk of age i.e. at approximately 10-11 wk of prion incubation. Cre expression results in splicing of the floxed PrP transgene in neuronal cells, which in turn results in reversal of the established spongiosis and neuronal loss and ultimately leads to the reversal of clinical prion disease.

1.7 Function of PrP^c

1.7.1 The role of prion protein in signalling and neuroprotection

Cellular prion protein (PrP^c) is a plasma membrane glycosyl-phosphatidylinositol-anchored protein present in neurons (Kretzschmar et al., 1986) but also in other cell types and is highly conserved among species. The prion protein gene contains three exons in mouse and rat and two exons in hamster and humans, with the third and second exons, respectively, encoding the entire protein of approximately 250 amino acids. Two signal peptides are present in the molecule, one at the N-terminus, which is cleaved during the biosynthesis of PrP^c in the rough endoplasmic reticulum and the second at the C-terminus, that allows for attachment to a glycosyl-phosphatidylinositol (GPI) anchor. Two glycosylation sites are also mapped to the C-terminus (reviewed in Prusiner, 1998).

The function of prion protein has been extensively investigated and different studies suggest a role for PrP in signalling, neurite outgrowth, cell survival and apoptosis. First a role in cell surface

signalling or cell adhesion was highlighted when it was found that PrP^c binds to the 37 kDa laminin receptor (Rieger et al., 1997; Gauczynski et al., 2001). Another cell surface protein that interacts with PrP^c, is NCAM (Santuccione et al., 2005; Schmitt-Ulms et al., 2001). Both the laminin receptor precursor and NCAM (Rieger et al., 1997; Gauczynski et al., 2001; Santuccione et al., 2005) are implicated in neurite outgrowth.

There is evidence to suggest that not only PrP and NCAM are associated with each other at the surface of hippocampal neurons but they also interact with each other in to mediate neurite outgrowth (Santuccione et al., 2005). Initially, it was observed that PrP partially co-localizes with NCAM along neurites and in growth cones. Immnoprecipitation studies of brain homogenate with antibodies against PrP, revealed that PrP immunoprecipitated with NCAM, indicating that the two proteins are associated in the brain. Further *in vitro* work on hippocampal neurons showed that binding of PrP-Fc(which contains the extracellular domain of mouse PrP fused to the Fc portion of IgG) to NCAM stabilizes NCAM in lipid-rich microdomains and promotes neurite outgrowth. Furthermore recombinant prion protein has been shown to promote neurite outgrowth, development of synapses and neuronal survival *in vitro* (Chen et al., 2003; Kanaani et al., 2005).

Also, there is evidence of an anti-apoptotic role for PrP. Initially it was demonstrated that $Prnp^{0/0}$ neuronal cells are more susceptible to apoptosis than wild type cells (Kuwahara et al., 1999). Subsequent studies on human primary neurons implicated PrP as a potent anti-apoptotic protein against Bax-mediated cell death (Bounhar et al., 2001). More recent experimental data contradicted the anti-apoptotic role of PrP by showing that cross-linking PrP^c in vivo with specific monoclonal antibodies triggered rapid and extensive apoptosis in hippocampal and cerebellar neurons. However apoptosis was not induced with all antibodies used and the findings may also be interpreted by loss of PrP function (Solforosi et al., 2004).

Other studies have demonstrated that peptide-mediated engagement of PrP^c induces neuroprotective signals against apoptosis through a cAMP/PKA –dependent pathway suggesting a role for PrP^c as a trophic receptor, the activation of which leads to a neuroprotective state (Chiarini et al., 2002). In agreement with a neuroprotective role for PrP it has been shown that $Prnp^{0/0}$ mice display significantly increased infarct volumes after both transient and permanent ischemia when compared with wild type animals. In the same study they demonstrated that in the absence of PrP^c the anti-apoptotic phosphatidylinositol 3-kinase/Akt pathway is impaired resulting in reduced postischemic phospho-Akt expression, followed by enhanced postischemic caspase-3 activation, and aggravated neuronal injury after transient and permanent cerebral ischemia (Weise et al., 2006).

Furthermore, over-expression of PrP in vivo by adenovirus-mediated gene targeting diminished the infarct volume in a stroke rat model (Shyu et al., 2005), while in other studies ischemia induced upregulation of cerebral PrP^c (Weise et al., 2004)) further reinforcing the notion of a neuroprotective role for PrP. Finally a role in cognition has been attributed to the prion protein as polymorphisms of the prion gene in humans have been associated with better long term memory (Papassotiropoulos et al., 2005).

1.7.2 The role of prion protein in stem cell proliferation and differentiation

Recent studies examined the role of prion protein in stem cell proliferation and differentiation: PrP^c is expressed in multipotent neural precursors as well as in mature neurons and its expression increases in fully differentiated mature neurons both *in vitro* and *in vivo* (Steele et al., 2006). In the same study they examined mice with different levels of PrP expression including wild type, $Prnp^{0/0}$, and PrP over-expressing mice. They isolated multipotent neural precursors from these mice and observed that PrP^c levels directly increase the rate of multipotent precursor differentiation. They also showed that PrP^c has a role on cellular proliferation in the adult subventricular zone (SVZ) and dentate gyrus (DG), indicated by increased proliferation in the SVZ of mice over-expressing PrP and reduced proliferation in the DG of $Prnp^{0/0}$ mice. However, they did not identify a corresponding reduction in the number of newborn neurons neither a change in the gross morphology of the hippocampus of knock-out mice, suggesting that neurogenesis in the adult brain depends on multiple factors, and PrP^c is probably only one factor involved in this complex process (Steele et al., 2006).

In another set of experiments the role of PrP in self-renewal of hematopoietic stem cell (HSCs) was investigated. The study involved transplantation of HSCs derived from either wild type or $Prnp^{0/0}$ bone marrow into lethally irradiated mouse recipients. It has been shown that HSCs from $Prnp^{0/0}$ bone marrow exhibited impaired self-renewal in serial transplantation (Zhang et al., 2006). Possible interpretations of these findings include a neuroprotective role for PrP against apoptosis and towards long-term self renewal of stem cells. Alternatively, it has been suggested that PrP might interact with proteins in the bone marrow extracellular matrix and support in this way the retention of transplanted HSCs within the bone marrow which may facilitate their integration.

Finally, NGF (nerve growth factor) known to induce differentiation has been shown *in vitro* to activate the *Prnp* promoter and subsequently lead to up-regulation of PrP expression through a pathway that involves MEK1 kinase. MEK 1 is an important component of the mitogen-activated

protein kinase (MAPK) signalling pathway, which is the common mechanism regulating cellular processes such as proliferation, differentiation and apoptosis (Zawlik, 2006).

1.8 Neurogenesis in the adult brain

Since the discovery of neurogenesis in the adult brain more that 40 years ago (Altman and Das, 1965) effort has been invested into unraveling the characteristics of neural stem cells and the mechanism that drives adult neurogenesis. An important step was the finding that neural stem cells persist in the adult mammalian brain and have the ability to divide, self renew and give rise to neurons, astrocytes, and oligodendrocytes *in vitro* (Davis and Temple, 1994; Reynolds and Weiss, 1992). There is *in vivo* evidence of both neurogenesis (generation of neurons) and gliogenesis (generation of astrocytes), although the latter occurs at a lesser extent and it is not clear if the same type of stem cell produces both neurons and astrocytes (Marshall et.al., 2003).

It is now well established that there are two main zones of neurogenesis in the adult rodent brain where proliferating neural stem cells reside before differentiating into mature neurons; the subventricular zone of the lateral ventricles and the dentate gyrus of the hippocampus. Neuronal differentiation in the neurogenic niche is facilitated by the presence of BMP antagonists, which bind to bone morphogenetic protein (BMP) and block its action against neurogenesis. Both noggin, which is secreted by the ependymal cells in the SVZ and neurogenesin-1 secreted by astrocytes in the subgranular zone (SGL) of the dentate gyrus act as BMP antagonists in the adult brain (Lim et.al., 2000; Ueki et.al., 2003).

Nestin-positive subependymal cells and GFAP-positive cells that resemble astrocytes (Fig. 7) have been shown to exhibit stem cell and progenitor properties in the adult brain (Fukuda et.al., 2003; Doetsch et al., 1999; Johansson et al., 1999; Seri B. et.al., 2001). The division of a stem cell gives rise to transiently amplifying progenitor cells, which have limited self-renewal, a greater proliferative capacity and a neuronal-restricted fate. Immature neurons, which are derived from progenitor cells, are distinguished by the expression of common markers such as β tubulin isoform III (clone Tuj-1) and also PSA-NCAM and doublecortin (DCX), both of which characterize migrating neuroblasts. At the next stage of the differentiation, the maturing cells become post-mitotic and express markers specific of mature neurons, such as the nuclear protein NeuN. This transient postmitotic stage, during which network connections are established and the selection for long-term survival occurs, is followed by the formation of terminally differentiated neuronal cells (Kempermann et.al., 2004; Ming and Song, 2005).

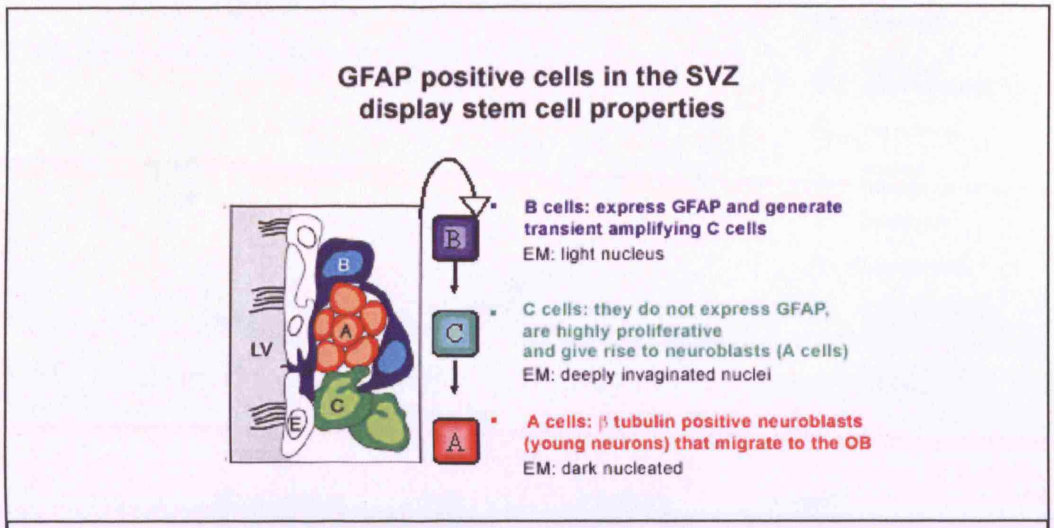

Figure 7: Schematic drawing of the organization of the SVZ. Ependymal cells (E) do not divide and form the lining of the lateral ventricle. GFAP-positive cells (type B cells) are the primary neuronal precursors that divide to give rise to transient precursors that are highly proliferative (type C cells), which in turn divide forming tight clusters and generate migrating neuroblasts (type A cells). (adapted from Doetsch, 2003)

1.8.1 Neurogenesis in the SVZ-OB pathway

In the subventricular zone (SVZ) of both rodents and humans (Sanai et al., 2004) (Quinones-Hinojosa et al., 2006; Lois and Alvarez-Buylla, 1993; Curtis, 2007) neural stem cells divide throughout life but the vast majority of these newly generated cells dies. Cells that survive migrate through the rostral migratory stream (RMS) to the olfactory bulb (OB) where they give rise to neurons (Lois and Alvarez-Buylla, 1993; Curtis, 2007) (Fig. 8). Subependymal cells and also GFAP-positive cells have been identified as neural stem cells and progenitor cells in the SVZ of the adult rodent brain (Doetsch et al., 1999; Johansson et al., 1999). Ependymal cells express several proteins, which are also expressed by neural stem cells during normal development, including nestin, musashi and Notch-1 receptors (Lendahl et al., 1990; Rietze et al., 2001; Sakakibara and Okano, 1997).

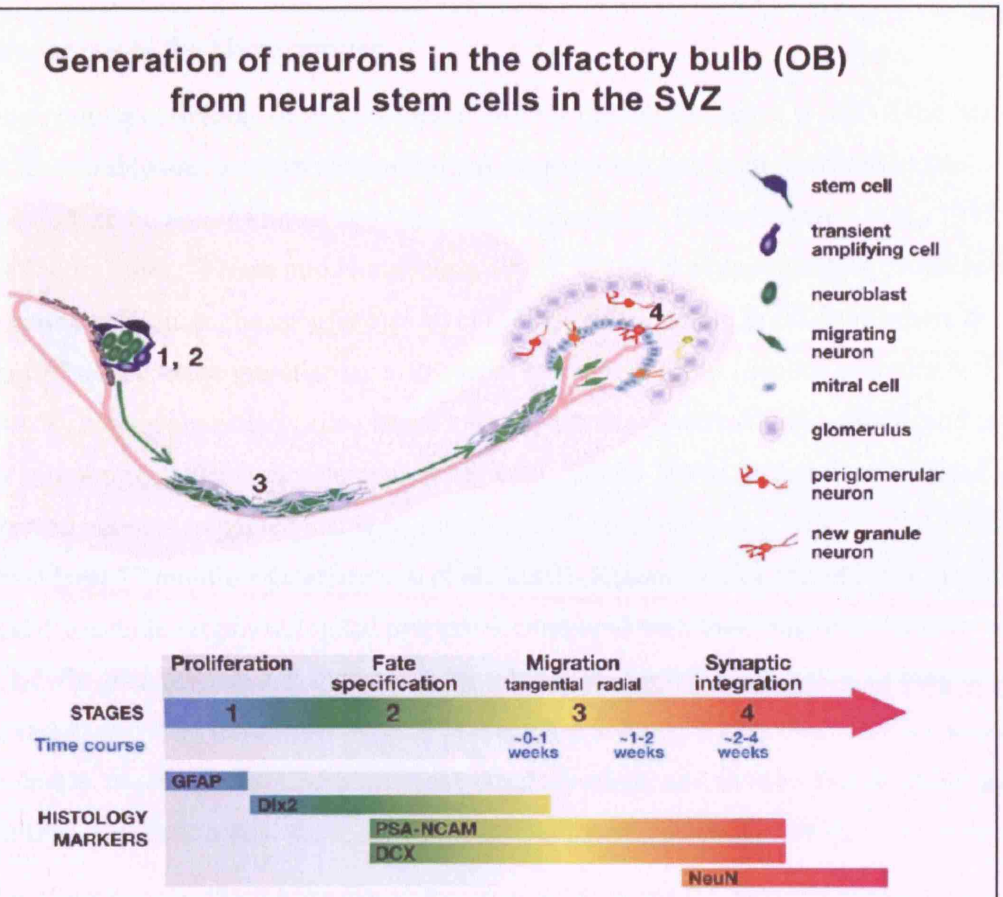

Figure 8: adult neurogenesis in the SVZ/olfactory system occurs in 4 developmental stages:
Stage 1. Proliferation: stem cells in the SVZ of the lateral ventricles give rise to transient amplifying GFAP-positive cells (*light blue*). Stage 2. Fate specification: transient amplifying cells differentiate into immature neurons which express markers such as DCX and PSA-NCAM (*green*). Stage 3. Migration: Immature neurons (*green*) migrate with each other in chains through the rostral migratory stream (RMS) to the olfactory bulb. The migrating neurons are ensheathed by astrocytes. Once reaching the bulb, new neurons then migrate radially to the outer cell layers. Stage 4. Synaptic integration: Immature neurons differentiate into either granule neurons or periglomerular neurons . These unusual interneurons lack an axon and instead release their neurotransmitter from the dendritic spines at specialized reciprocal synapses to dendrites of mitral or tufted cells. (reviewed in and adapted from Ming and Song, 2005).

1.8.2 Neurogenesis in the hippocampus

The other region of neurogenesis in the adult brain is the hippocampus, a part of the brain that is important for learning and memory. Hippocampal neurogenesis has been observed in adult animals from birds to humans (Altman and Das, 1965; Kuhn et al., 1996; Eriksson et al., 1998; Kornack and Rakic, 1999 ; Barnea and Nottebohm, 1994). Within the hippocampus, proliferating neural stem cells are found in the subgranular layer (SGL) of the dentate gyrus from where they migrate a short distance to the granular layer to become mature neurons (dentate granular cells (DGCs)) (Fig. 9). Newly generated cells mature into functional neurons within a month and reach a more mature morphology after 4 months (van Praag et al., 2002). It was further demonstrated that the newly formed neurons remained stable in number and in their relative position in the granule cell layer for at least 11 months (Kempermann et al., 2003). Recent studies showed that newborn DGCs exhibit distinct electrophysiological properties compared with their mature neighbors in the adult brain. Newly generated DGCs appear to have a lower threshold for induction of long term potentiation (LTP) and long term depression (LTD) leading to an enhanced bi-directional plasticity (Song et al., 2005). Studies in mice with different genetic background showed that there is a genetic influence on hippocampal neurogenesis of adult mice (Kempermann et al., 1997).

Studies aiming at elucidating the signalling process of neurogenesis in the dentate gyrus revealed that both NCAM (neuronal cell adhesion molecule) and Wnt signalling regulate the differentiation of hippocampal neural progenitor cells. Furthermore GABAergic inputs have been shown to promote neuronal differentiation and synaptic integration of newly generated hippocampal neurons (Amoureux et al., 2000; Tozuka et al., 2005)

It has been proposed that hippocampal neurogenesis might serve as a powerful mechanism for plasticity of brain circuits (Schinder and Gage, 2004). Another possible hypothesis is that new neurons may be required to replace dying neurons (Biebl et al., 2000).

Finally, the newly generated cells may have a function in cognition since factors that have been shown to increase neurogenesis such as enriched environment (Kempermann et al., 1997b) and exercise (van Praag et al., 1999b) are associated with improved memory function and enhanced synaptic plasticity (van Praag et al., 1999a), while stress has been related to decreased cell proliferation and memory impairment (Gould et al., 1992).

1.8.3 The role of astrocytes and microglia in neurogenesis

An active role in neurogenesis has been attributed to astrocytes. It has been reported that hippocampal astrocytes instruct the neuronal fate commitment of adult stem cells *in vitro* (Song et al., 2002), providing the suitable environment for adult neurogenesis. Other studies show that in vivo elimination of immature precursors and neuroblasts results in astrocytes dividing to generate immature precursors and neuroblasts. Furthermore SVZ astrocytes give rise to new neurons in the OB while *in vitro* can grow into multipotent neurospheres (Doetsch et al., 1999).

In vitro data provide evidence that microglia direct the migration of neural stem cells and can influence the differentiation of both adult and embryonic neural precursors toward a neuronal phenotype (Aarum et al., 2003). It has been argued that as microglial activation is a common feature of pathological processes they may have a role in directing the replacement of damaged cells in the CNS.

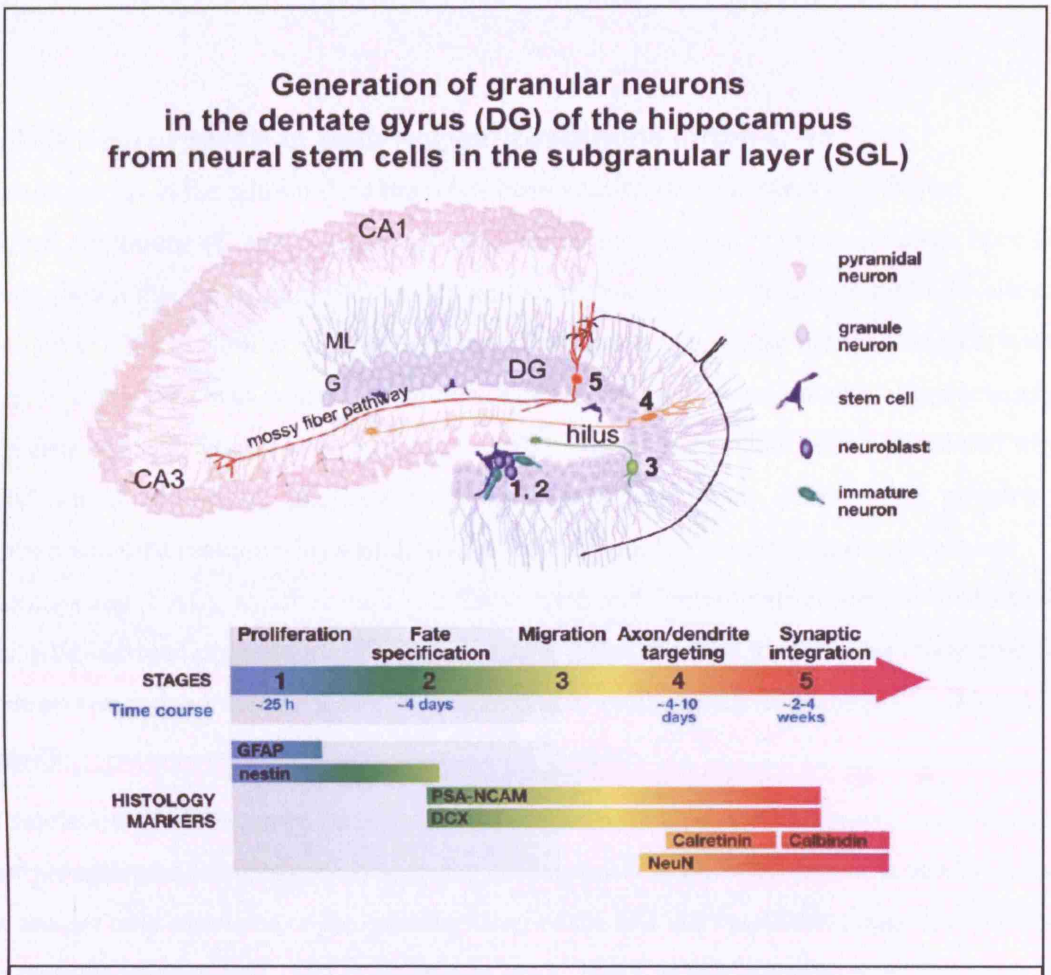

Figure 9: Adult neurogenesis in the dentate gyrus of the hippocampus undergoes five developmental stages.
Stage 1. Proliferation: Stem cells with their cell bodies located within the subgranular layer in the dentate gyrus have radial processes that project through the granular cell layer and short tangential processes that extend along the border of the granule cell layer and hilus. These stem cells give rise to GFAP-positive and Nestin-positive transient amplifying cells (*light blue*). Stage 2. Differentiation: transient amplifying cells differentiate into immature neurons, which are positive for DCX and/or PSA-NCAM (*green*). Proliferating progenitors in the SGL are tightly associated with astrocytes. Stage 3. Migration: Immature neurons (*light green*) migrate a short distance into the granule cell layer. Stage 4. Axon/dendrite targeting: Immature neurons extend their axonal projections along mossy fibre pathways to the CA3 pyramidal cell layer. They send their dendrites in the opposite direction toward the molecular layer. Stage 5. Synaptic integration: New granule neurons (*red*) receive inputs from the entorhinal cortex and send outputs to the CA3 and hilus regions. DG, dentate gyrus region; ML, molecular cell layer; GL, granular cell layer.
(reviewed in and adapted from Ming and Song, 2005)

1.9 Adult neurogenesis in pathological conditions of the CNS

Neurogenesis in the adult rodent brain has been studied in the context of different pathological conditions of the CNS such as stroke/ischemia, seizures or demyelination. Specifically, it has been shown that ischemia results in generation of neurons that are migrating to the site of injury (Jin et al., 2003). Similar observations have been made in a mouse model of stroke, where proliferation in the SVZ was enhanced and newly generated neurons migrated into the severely damaged area of the striatum (Arvidsson et al., 2002). However it remains to be elucidated whether the newly formed neurons are functional and contribute to brain repair. Additionally, progenitor proliferation and differentiation was studied in a mouse model of experimental autoimmune encephalomyelitis (EAE), which results in inflammation and demyelination, similar to multiple sclerosis. SVZ-derived progenitor cells migrate to the lesioned white matter where they give rise to astrocytes and oligodendrocytes possibly contributing to replacement of the lost cells (Picard-Riera et al., 2002).

Stimulation of hippocampal neurogenesis has also been observed in response to brain injury. For example epileptic seizures greatly increase neurogenesis in the adult DG. The newly formed neurons are not only restricted to the granular layer of the DG but they also migrate ectopically to the dentate hilus (Parent et al., 1997; Scharfman et al., 2000). It has been proposed that these ectopic neurons might play a key role in the pathogenesis of epilepsy. Moreover, other pathological conditions may induce functional neurogenesis in otherwise non-neurogenic regions of the hippocampus. Neurogenesis is also induced in transient forebrain ischemia that causes a selective and massive degeneration of CA1 pyramidal neurons in the dorsal hippocampus of adult rats (Nakatomi et al., 2002). This study revealed a strong correlation between neurogenesis and recovery when the mice showed improved performance in the Morris water maze, a behavioral test that assesses spatial learning and memory. In addition, it has been shown that new neurons are generated in the hippocampus after stroke (Liu et al., 1998).

1.10 The role of BDNF in neurogenesis and neuronal function

Brain-derived neurotrophic factor (BDNF) is a member of the nerve growth factor family of neurotrophins. Expression of BDNF is detected in many areas of the brain and spinal cord (Kawamoto et al., Dreyfus et.al., 1999) and is increased in the postnatal brain. Although widely expressed in the adult mammalian central nervous system (CNS), BDNF is particularly abundant in the hippocampus and cerebral cortex (Hofer et al., 1990) and is anterogradely transported via the corticostriatal afferents to striatal neurons, which require BDNF for their activity and survival (Altar et al., 1997; Baquet et al., 2004). BDNF protein is transcribed from a single, highly complex gene that carries a number of promoters to generate a tissue-specific and stimulus-induced pattern of BDNF expression (Timmusk et al., 1993, 1994, 1995; Aid et al., 2007; Liu et al., 2006).

The regulation of BDNF exon II promoter is known to depend mainly on the activity of a repressor element 1/neuron-restrictive silencer element (RE1/NRSE). RE1/NRSE is a 23 bp DNA sequence that when positioned upstream of a minimal promoter, is capable of repressing transcription in an orientation- and distance-independent manner. The RE1/NRSE binding protein (REST/NRSF) interacts with RE1/NRSE sites in the nucleus and recruits co-repressors. RE1/NRSEs were subsequently found in a number of genes that are fundamental for the maintenance and terminal differentiation of neurons (Schoenherr et al., 1996), and it has been argued that the principal role of RE1/NRSE is to modulate gene expression in neurons. In line with this suggestion, high levels of REST/NRSF were found in the nuclei of embryonic stem (ES) cells, while in mature cortical neurons REST/NRSF and its co-repressors dissociate from the RE1/NRSE sites and trigger the activation of neuronal genes (Ballas et al.,2005). Expression of REST/NRSF was also observed in hippocampal stem cells but also in adult neurons, indicating the diversity of REST/NRSF actions in different populations of CNS progenitors and neurons (Sun et al., 2005).

Like the other neurotrophins, BDNF is synthesised from a large precursor protein that is proteolytically cleaved to yield the mature protein. BDNF is initially synthesised from its mRNA as a 32 kDa precursor protein (pro-BDNF) in the endoplasmic reticulum, and subsequently translocated to a series of intracellular organelles (including the Golgi complex, and secretory vesicles), where proteolytic cleavage produces the 14 kDa mature form of the protein, which is finally secreted to the extracellular space (Halban and Irminger, 1994).

Mature BDNF protein binds to specific receptors such as tyrosine receptor kinase B (TrkB) and p75 neurotrophin receptor (p75NTR) and acts in a paracrine and autocrine manner to control a

variety of brain processes, including the growth, development, differentiation and maintenance of neuronal systems, neuronal plasticity, synaptic activity and neurotransmitter-mediated activities (Chao, 2003, and Binder and Scharfman, 2004) (Fig. 10). BDNF is mainly present in neurons and it has been shown that hippocampal neurons produce BDNF and receive BDNF-mediated signals (Ivanova, et.al., 2001). BDNF can also be stored into glial cells by binding to truncated TrkB on their surface (Rubio, 1997).

The association of BDNF with neurogenesis was further demonstrated in studies where neurons generated from neural progenitors respond to BDNF with enhanced migration, maturation, and survival *in vitro* (Kirschenbaum and Goldman, 1995; Pincus et al., 1998; Lowenstein et.al., 1996). In agreement with these reports exercise, which has been demonstrated to increase neurogenesis (van Praag et.al., 1999b), was shown to increase levels of BDNF mRNA in the hippocampus, cerebellum and cortex (Cotman, et.al., 2002).

Other studies show *in vivo* generation of new neurons in response to exogenous BDNF suggesting that delivery of BDNF may be a feasible strategy for inducing neurogenesis from resident progenitor cells in the adult brain. Initially, infusion of BDNF for 12 days into the right lateral ventricle of adult rat brains resulted in a significant increase of proliferating BrdU-labelled cells in the olfactory bulbs and a 100% increase in the number of BrdU-labelled cells in the bulb that showed a neuronal phenotype (Zigova, et.al., 1998).

In further similar experiments, introduction of BDNF was achieved by infection of the adult rat ventricular lining with an adenoviral BDNF expression vector. These studies have also reported a 2.4-fold increase of newborn neurons in the olfactory bulb 3 weeks after viral administration. Additionally, they have demonstrated that injection of adenoviral BDNF was also associated with the addition of new neurons to the neostriatum, an otherwise non-neurogenic region of the adult brain (Abdellatif Benraiss et.al., 2001).

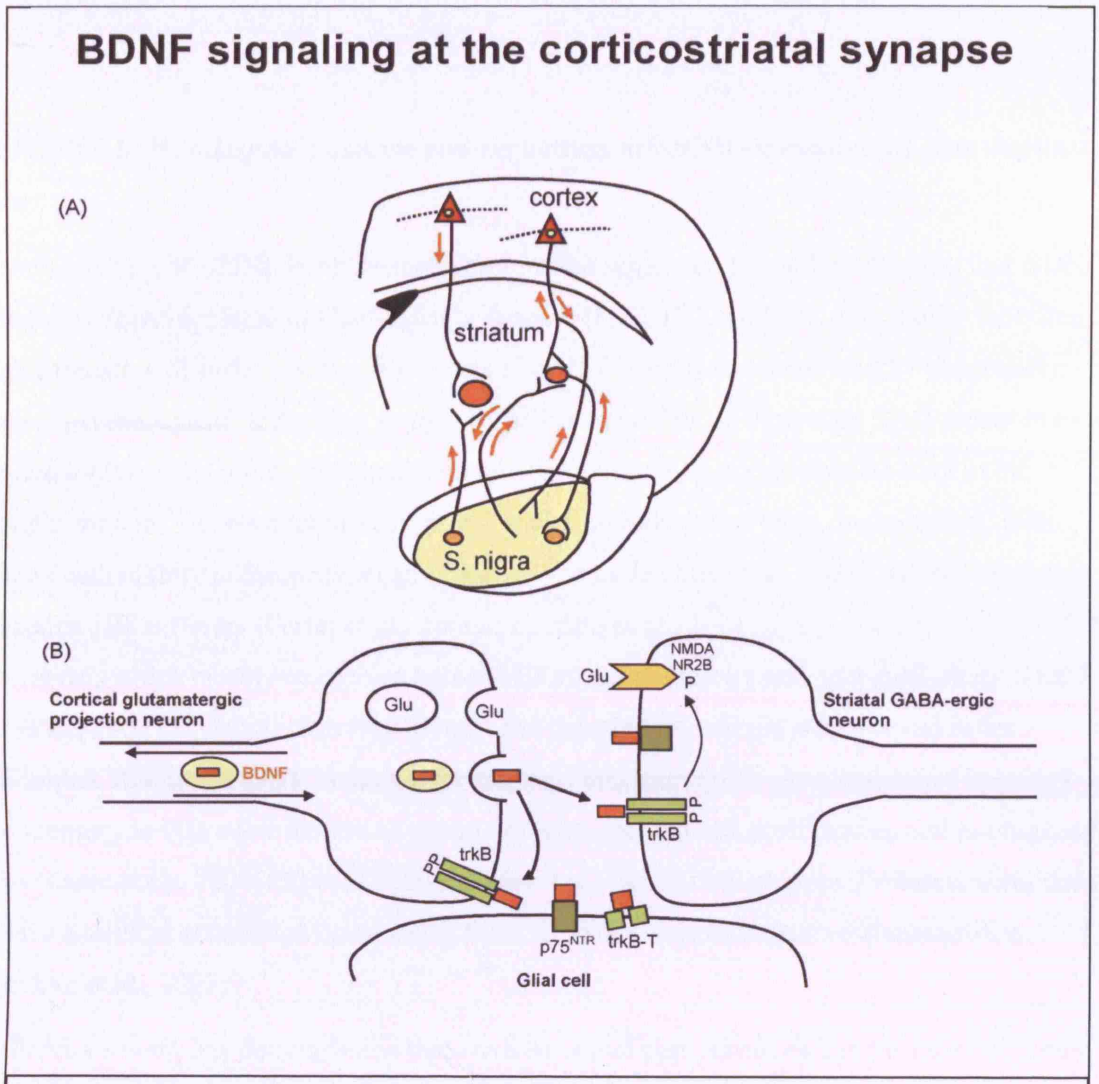

Figure 10: BDNF signalling at the corticostriatal synapse. A) BDNF is transported to the striatal neurons. Orange arrows indicate anterograde and retrograde transport. B) the scheme depiscts the axodendritic connection between cortical glutamatergic neurons and striatal GABA-ergic neurons. Following a depolarisation stimuli, BDNF is released from the presynaptic terminal (cortical neuron) and diffuses across the synaptic cleft to activate TrkB receptors located on the postsynaptic terminal (striatal neuron). Engagement of the TrkB receptor leads to protein phosphorylation, such as NR2B subunit of the NMDA receptor, determining enhanced synaptic transmission. Also, acting in an autocrine fashion, BDNF can bind to the TrkB receptor of the plasma membrane at the presynaptic terminal to increase neurotransmitter release (glutamate, Glu). Moreover, BDNF in the synaptic cleft binds to truncated TrkB and $p75^{NTR}$ receptors on glial cells to modulate glial calcium signalling. By binding to truncated TrkB, BDNF can be stored into glial cells. (Adapted from Zuccato, 2007).

1.10.1 BDNF in Huntington's disease and regulation of BDNF expression by Huntingtin protein

Involvement of BDNF in neurodegeneration was suggested by studies showing that BDNF expression is downregulated in Huntington's Disease (HD). HD is a fatal, dominantly inherited, neurodegenerative disorder that usually onsets in midlife, and is characterized by progressive cognitive, psychological, and motor symptoms and is caused by an expanded CAG repeat in exon 1 of the *Huntingtin* gene, which translates into an abnormally long polyglutamine tract in the Huntingtin protein. The neuropathology of HD includes widespread brain degeneration, with neuronal death mainly in the striatum and cerebral cortex (Reiner et al., 1988). BDNF levels are decreased in HD sufferers (Ferrer et al., 2000a; Zuccato et al., 2001) and in the transgenic R6/2 HD mouse model, which closely resembles human HD symptomatology and neuropathology (Luthi Carter et al., 2002). A decrease in BDNF has been detected in both the striatum and in the hippocampus. Reduced BDNF in the hippocampus is consistent with observations of impaired spatial memory in HD mice, as well as reports of hippocampal cell proliferation and neurogenesis deficits (Lazic et al., 2004; Gil et al., 2005; Grote et al., 2005). Although preliminary, these data may have a clinical correlation considering that HD patients show cognitive abnormalities (Schmidtke et al., 2002).

Previous work has demonstrated that environmental enrichment delays the onset of motor symptoms in this mouse model. It is interesting that re-motivation therapy also improves functioning in HD patients (Sullivan et al., 2001). More recent studies have confirmed that enrichments ameliorates motor symptoms and prevents loss of body weight in R6/ 2 HD mice and that it also causes an upregulation of BDNF in the striatum, which could explain the enhanced performance in the motor tests (Spires et.al., 2004).

Further studies revealed that wild-type Huntingtin protein regulates BDNF transcription (Zucatto et al., 2001) and suggested that the reduced BDNF transcription observed in HD may depend on the level and activity of the wild-type protein (Zuccato et al., 2003). Initially, it was reported that extra copies of wild-type huntingtin increase BDNF production in vitro and in vivo, and similarly that brain tissue and cells depleted of endogenous huntingtin are characterised by reduced BDNF levels. Moreover, neuronal inactivation of huntingtin in conditional homozygous knock-out mice (Dragatsis et al., 2000) led to a statistically significant reduction in BDNF mRNA levels. In this system, the reduced BDNF mRNA II level is responsible for the lower amount of total BDNF mRNA found in the absence of endogenous huntingtin. It was found that wild-type but

not the mutant protein activates BDNF gene transcription by inhibiting the RE1/NRSE within BDNF promoter II. The mechanism by which wild-type huntingtin protein controls BDNF expression is by retaining REST/NRSF in the cytoplasm, thus reducing the activation of the RE1/NRSE silencer element and allowing BDNF gene transcription (Zuccato et al., 2003). Subsequent reports supported this view by indicating that wild-type huntingtin and REST/NRSF co-localise (Zuccato et al., 2005). By contrast, mutated huntingtin causes the pathological entry of REST/NRSF into the nucleus where it can bind to the RE1/NRSE site and lead to BDNF repression (Zuccato et al., 2003).

1.11 Hypothesis and aims

It has been demonstrated that different forms of brain injury such as stroke/ischemia, inflammatory demyelination and seizures enhance neurogenesis in the hippocampus of the adult rodent brain (Parent et al., 1997; Scharfman et al., 2000; Nakatomi et al., 2002; Liu et al., 1998). The induction of a stem cell response following various pathological conditions raises the possibility that upregulation of neurogenesis as a result of neuronal loss and/or other neuropathological features occurs in a wider array of neurodegenerative diseases. Therefore, further studies of stem cell response under conditions of neurodegenerative disease are needed, to advance our knowledge of the basic biology of stem cells, with a view of exploiting this knowledge in the design of novel therapeutic concepts of brain repair. To this end, we will examine stem cells in the context of another neurological disorder, prion disease, which is a fatal, transmissible neurodegenerative disease marked by neuronal loss and also characterized by aggregation of the abnormal isoform of the prion protein in the brain. Profound hippocampal degeneration has been observed in a transgenic mouse model of prion disease (tg37) which therefore provides a suitable experimental model to study stem cells in this established neurogenic area. Although transplantation of stem cells or stimulation of endogenous stem cells as an option of therapy of prion diseases remains an ambitious target, the study of stem cell recruitment in prion disease will nevertheless give important clues about the pathobiology of stem cells under certain neurodegenerative conditions.

Recently a role for PrP has been described in stem cell proliferation and differentiation. We will investigate the role of prion protein in proliferation in the dentate gyrus by studying mouse lines expressing different levels of PrP. An *in vivo* study on the effect of PrP loss on neuronal differentiation in the dentate gyrus will also be included. Moreover, we will examine the role of PrP on neural stem cell growth.

Recent studies support the involvement of the neurotrophic factor BDNF in neurogenesis. *In vitro* work has shown that neurons generated from neural progenitors respond to BDNF with enhanced migration, maturation, and survival. Moreover, it has been reported that administration of exogenous BDNF into the brain promotes the generation of new neurons. In a preliminary study, we will examine whether prion infection affects BDNF expression and whether there is a correlation between the level of neurogenesis and the BDNF levels in the hippocampus of animals affected by prion disease. In addition, BDNF levels in the hippocampus will be estimated in mouse strains

expressing PrP at different levels, in order to investigate a possible connection between BDNF, which plays a role in neurogenesis, and PrP, which has already been shown to play a role in progenitor proliferation and differentiation *in vitro*.

Therefore the aims of this study are:

- We will examine the effect of prion disease on neural stem cell proliferation and differentiation in the hippocampus with a particular focus on the neurogenic area of the dentate gyrus. We will study stem cell recruitment in the dentate gyrus of mock-inoculated (inoculated with normal brain homogenate) and prion infected (inoculated with RML inoculum) mice. Proliferating (progenitor) cells will be labelled with the thymidine analogue BrdU which is incorporated into dividing cells. By immunostaining for BrdU we will assess proliferation in the dentate gyrus. Furthermore, BrdU-labelled cells will be analysed within a period of days for co-expression of neuronal or astroglial markers. We will also identify other populations of proliferating cells in the brain, such as microglial, by immunostaining for the microglial-specific marker Iba-1.

  We will estimate stem cell proliferation in prion infected FVB wild type mice which show an incubation period of approximately 18 weeks (~122 days) before symptoms appear. We will analyse stem cell proliferation at later time points during the incubation period, when neuropathology is established. Specifically, we will assess proliferation at the 110th day of incubation (16th week) and also at the onset of symptoms. Moreover, we will establish the proportion of proliferating cells exhibiting a neuronal, astroglial or microglial phenotype in the dentate gyrus of prion-infected wt mice.

- We will examine the prion-infected transgenic tg37 mice. These animals carry 3 copies of the floxed *Prnp* transgene (hemizygous). Upon RML inoculation they exhibit characteristic neuropathological changes throughout the brain with increased spongiosis and neuronal loss in the hippocampal area (Fig. 11), and they succumb to the disease by the end of the 12th week post inoculation. We will analyze stem cell proliferation at later time points during the incubation period, when neuropathology is established. In particular, we will examine the 11th and 12th weeks of incubation and compare with the earlier time point of 8th week. Stem cell differentiation will be examined at the 11th wk of incubation.

- We will study an established transgenic model of reversal of clinical prion disease, the NFH-Cre/tg37 mice which have been described in detail (chapter 1.6.6). They carry 3 copies of the floxed *Prnp* transgene (Lox-PrP, hemizygotes). PrP depletion at a late stage of incubation (11 wk

p.i.) reverses the already established spongiosis, reverses neuronal loss and rescues the mice from clinical prion disease. We will investigate the effect of PrP depletion and the subsequent reversal of the disease on stem cell proliferation and differentiation. We will study proliferation at various time points after PrP depletion, and will assess differentiation at the 13th week post-inoculation when the PrP depletion has already occurred.

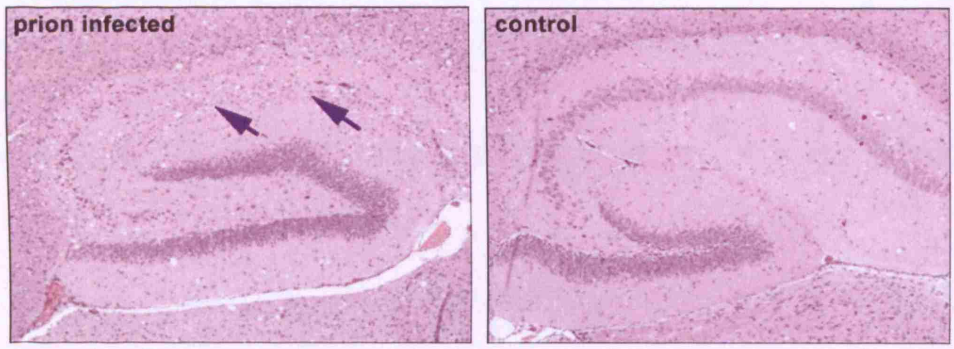

Figure 11: There is profound loss of the neuronal ribbon (arrows) and manifestation of spongiosis in the hippocampus of prion infected tg37 mice at 12-13 wk post inoculation.

- We will investigate the role of prion protein in neurogenesis in the dentate gyrus of un-inoculated (or mock-inoculated) mice. We will examine proliferation in mouse lines expressing different levels of the PrP. Specifically, we will examine wild type mice, *Prnp*$^{0/0}$ mice, transgenic mice over-expressing PrP (tg37) and transgenic mice in which the PrP gene is selectively deleted in neurons upon the expression of NFH at 8-10 weeks of age (NFH-Cre/tg37). In order to assess the role of neuronal PrP on neuronal differentiation in the dentate gyrus, we will examine the differentiation of BrdU-labelled cells in the dentate gyrus of NFH-Cre/tg37 mice before (9wk old) and after (15wk old) Cre-mediated PrP depletion in neurons.

- We will study the role of PrP on stem cell growth. For this purpose, neural stem cells will be isolated from the hippocampus of adult wild type and PrP knock-out mice and neurospheres will be grown in culture. We will include preliminary observations on the growth pattern of wt and *Prnp*$^{0/0}$ neurospheres.

- We will examine whether prion infection affects the level of BDNF expression in the hippocampus and correlate the results with the data we will obtain from the neurogenesis study. We will analyse BDNF levels in the hippocampus of mock-inoculated and RML-inoculated tg37 mice and also in also in RML-inoculated NFH-Cre/tg37 mice following the reversal of clinical prion disease.

- We will assess whether there is a correlation between PrP and BDNF expression in the hippocampus, by estimating BDNF levels in mouse strains exhibiting different levels of PrP expression. We will examine wild type mice, $Prnp^{0/0}$ mice, transgenic mice over-expressing PrP (tg37) and finally transgenic mice in which the PrP gene has been selectively deleted in neurons (NFH-Cre/tg37).

2 Materials and Methods

2.1 Animals

All animals were housed in standard conditions and all procedures including culling of animals were carried out in accordance with the Home Office regulations (Animal scientific procedures act 1986).

This study is based on 4 mouse lines which are wild type mice, tg37 transgenic mice, NFH-Cre/tg37 double transgenic mice and PrP knock-out mice (*Prnp*$^{0/0}$). All the mouse strains were raised in an FVB background. Both the tg37 and NFH-Cre/tg37 lines carry 3 copies of the Lox-PrP transgene and express PrP at 3 times wild type levels. All tg37 and NFH-Cre/tg37 mice in this study were hemizygous for the Lox-PrP transgene. The breeding schemes applied to obtain hemizygotes were:

1. Tg37 mice homozygous for the Lox-PrP transgene were crossed with *Prnp*$^{0/0}$ mice and the offsprings were screened for the Lox-PrP construct by PCR. Only the animals that were tested positive were selected (hemizygous).
2. Tg37 mice homozygous for the Lox-PrP transgene were crossed with NFH-Cre mice (tg63, raised in *Prnp*$^{0/0}$ background) to produce double transgenic NFH-Cre/tg37 mice. The offsprings (all hemizygous for *Prnp*) were screened for both NFH-Cre and Lox-PrP and the NFH-Cre/Lox-PrP double positives were selected.

2.2 Genotyping

Tg37 transgenic mice were genotyped before inoculation. The NFH-Cre/tg37 double transgenic mice used in this study were kindly offered by Giovanna Mallucci and were received genotyped.

2.2.1 Tail DNA extraction

Gloves were worn to avoid contamination of the samples. The reaction tubes (1.5 ml) were autoclaved before use. A piece of tail (approximately 0.5cm) was digested in a solution containing 0.5ml of tail lysis buffer and 3µl of 10mg/ml Proteinase K. The mix was incubated for a minimum of 2-3 hours at 55°C, shaking vigorously. The contents of the tube were centrifuged for 10 min at 13,200 rpm. The supernatant was transferred into a new tube containing 0.5 ml of isopropanol and mixed for 2 min on an Eppendorf thermomixer to precipitate DNA. The mixture was centrifuged

again for 1 min at 13,200 rpm. The supernatant was discarded and the pellet was air-dried for 5-10 min. Finally 200µl TE was added and the samples were incubated for at least 2h at 37°C shaking, and stored at 4 °C.

2.2.2 Polymerase chain reaction (PCR) and detection of PCR product

2.2.2.1 PCR conditions for amplification of Lox-PrP construct

1µl of the DNA sample was added to 24µl of PCR mixture which contained 1.5 mM $MgCl_2$, $MgCl_2$ buffer (1:10 dillution), 0.25mM dNTPs, 1 U Taq polymerase, the 4 primers (see table 1 for primer sequences) each at a 0.5 pmol/µl final concentration and distilled water.

The PCR mixture was initially heated for 2 min at 94°C to denature complex genomic DNA. The PCR cycle then started with a first denaturation step at 94°C for 30 s, a second step (annealing) at 57 °C for 45 s and a third step (extension) at 72 °C for 1 min where the enzyme taq polymerase adds bases to the primers from 5' to 3' reading the template from 3' to 5'. Bases are added complementary to the template. A total of 33 cycles were completed at maximum rampspeed (AB Applied Biosystems GeneAmp PCR System 9700). After 7 min at 72 °C for completion of partial extension products and annealing of single-stranded complementary products, the samples were cooled down to 4 °C.

2.2.2.2 Detection of PCR product by agarose gel electrophoresis

The PCR samples were separated by agarose gel electrophoresis. 1% -1.5% agarose was dissolved in 1x TAE in the microwave. 2µl of 10 mg/ml ethidium bromide was added to 500ml of 1% agarose. The liquid agarose solution was poured into the chamber. When the agarose gel was solid, the chamber was placed in the tank which was filled with sufficient 1xTAE buffer to cover the gel surface. 10µl of each PCR sample were mixed with 2 µl of 6x loading buffer. 10µl of PCR sample/loading buffer solution were loaded in each well. 7µl of 100bp ladder was loaded as a marker and the gel run at 150V for 1 hour.

Primer Sequences		
Primers for Lox-PrP PCR	**Sequence**	**Amplicon**
primer B Lox forward	5' -TTG GTT AGG GTA GCC GTA CAT- 3'	500 bp (Lox-PrP)
primer D Lox reverse	5' –ATC AGT CAT CAT GGC GAA CCT- 3'	
RB forward	5' –AAT AGA GGC ACT CCC TTC AC- 3'	300 bp (RB gene)
RB reverse	5' –GGT AAG CCC TTG ACC TAA AA- 3'	

Table 1: Sequence of primers

2.3 Prion infection

Animals were subjected to prion infection by intracerebral injection (30µl) of RML inoculum (I4096- MRC Prion unit identifier code) (experimental group). The control group was mock-inoculated with the same volume of normal brain homogenate derived from CD-1 mice (1% CD-1). Prior to injection all the animals were anaesthetized with isoflurane using Vettech Compact Anaesthesia System. The animals were checked routinely during the progression of prion disease. They were sacrificed at selected time points during incubation of prion disease with the latest being the onset of early symptoms. These included erect ears, rigid tail, piloerection, mild ataxia, abnormal breathing or mobility, aggression, hunched posture, erect penis if male, paralysis, limp clasping, agitation, pale extremities, dull eyes. The animals were culled by inhalation of CO_2 at a gradually increasing concentration.

NUMBER OF MICE INCLUDED IN INFECTIVITY STUDY			
Proliferation study (30' BrdU latency)			
Mouse strain	**Inoculation**	**Time point of BrdU injection**	**Number of mice**
FVB	Mock	96, 110, 117, 124 d p.i.	8
FVB	RML	110d p.i.	3*
FVB	RML	Onset of symptoms (124d p.i.)	3**
Tg37	Mock	8, 11, 12, 13 wk p.i.	4
Tg37	RML	8 wk p.i.	3
Tg37	RML	11 wk p.i.	3
Tg37	RML	12 wk p.i.	3
NFH-Cre/tg37	RML	12 wk p.i.	3
NFH-Cre/tg37	RML	13 wk p.i.	4
NFH-Cre/tg37	RML	37 wk p.i.	2
Differentiation study (7-8 d BrdU latency)			
Mouse strain	**Inoculation**	**Time point of BrdU injection**	**Number of mice**
FVB	RML	110d p.i.	3
Tg37	Mock	11 wk p.i.	4***
Tg37	RML	11 wk p.i.	4****
NFH-Cre/tg37	RML	13 wk p.i.	3
Differentiation study (5 d BrdU latency)			
Tg37	Mock	12 wk p.i.	2
Tg37	RML	12 wk p.i.	3
BDNF study			
Mouse strain	**Inoculation**	**Time point of sacrifice**	**Number of mice**
Tg37	Mock	12, 13 wk p.i.	3
Tg37	RML	12 wk p.i.	2
Tg37	RML	Onset of symptoms (13wk p.i.)	1
NFH-Cre/tg37	RML	12, 13, 36 wk p.i.	3
FVB	Mock	110, 117 d p.i.	3*****

* This group included 4 animals, one was found dead 4 days after RML inoculation.
** This group included 4 animals, one was found dead during the course of prion incubation
*** This group included 5 animals, one died due to adverse effects of mock-inoculation.
**** This group included 5 animals, one was found dead 5 days after RML inoculation.
***** This group consisted of 3 animals which were included in the proliferation study

Table 2: Number and details of mice included in the infectivity study

2.3.1 Working with RML infected brain

It was common procedure to decontaminate scrapie-contaminated waste (including disposed brain, consumables and solutions) by immersion into 1M NaOH for a minimum of 1 hour.

2.4 BrdU injections

To label proliferating cells, mice were given intraperitoneal (i.p.) injections of BrdU at a concentration of 50µg per g of body weight. Being a base analogue of thymidine, BrdU substitutes for thymidine during DNA synthesis and incorporates into the newly synthesized DNA. Therefore by BrdU administration, dividing (stem) cells are labelled. BrdU positive cells can be detected on brain sections by immunohistochemical techniques.

2.4.1 Proliferation of stem cells

In order to assess (stem) cell proliferation in the hippocampus of mock-inoculated and prion-infected animals, a single BrdU injection was performed at a concentration of 50µg per g of body weight and the animals were sacrificed 30 min later. For each mouse line studied, BrdU injections were carried out at specific time points during the incubation period of prion disease (table 3). For each strain, mock-inoculated animals received 30 min BrdU injections at various time points post-inoculation and the data we collected were sampled as one group (mock).

To determine the effect of *Prnp* gene inactivation on cell proliferation we performed BrdU injections in $Prnp^{0/0}$ mice and also in un-inoculated NFH-Cre/tg37 before Cre-mediated PrP deletion at 9 weeks of age and after PrP depletion at 15 and 22 weeks of age (table 4).

Mouse line	Time points of BrdU injection	BrdU latency
tg37 transgenic mice	(a) 8 wk p.i. (b) 11 wk p.i. (c) 12 wk p.i	30 min
NFH-Cre/tg37 double transgenic mice	(a) 12 wk p.i (b) 13 wk p.i (c) 37 wk p.i.	30 min
FVB wild type mice	(a) 110 d p.i. (b) Onset of symptoms (124d p.i.)	30 min

Table 3: Proliferation study. Time points of BrdU injection in RML-inoculated mice.

Mouse line	Time points of BrdU injection	BrdU latency
NFH-Cre/tg37 double transgenic mice	(a) 9 wk of age (b) 15 wk of age (c) 22 wk of age	30 min
***Prnp*$^{0/0}$ mice**	12-22 wk of age	30 min

Table 4: Proliferation study. Time points of BrdU injection in un-inoculated mice.

2.4.2 Differentiation of stem cells and characterisation of other proliferating cells

In order to determine the fate of proliferating stem cells, animals were culled within a period of days after BrdU injection and BrdU-labelled cells were analysed for expression of neuronal (β-tubulin) or astroglial (GFAP) markers. As prion disease is also characterised by microglial activation, we identified proliferating microglial cells by co-labelling BrdU-labelled cells with the microglial marker Iba-1.

For all mouse strains examined we performed BrdU injections at selected time points during the incubation of prion disease (table 5).

Mouse Strain	Time point of BrdU injection	BrdU latency
tg37 transgenic mice	11 wk p.i.	7 days
tg37 transgenic mice	12 wk p.i.	5 days
NFH-Cre/tg37 double transgenic mice	13 wk p.i.	7 days
FVB wild type mice	110 days p.i.	8 days
NFH-Cre/tg37 double transgenic mice	Un-inoculated/ 9wk old	7 days
NFH-Cre/tg37 double transgenic mice	Un-inoculated/15wk old	7 days

Table 5: Differentiation study. Time points of BrdU injection and BrdU latency in mock-inoculated, RML-inoculated and un-inoculated mice.

2.5 Histology

We obtained vibratome brain sections from all animals included in this study and performed either BrdU immunostainings to assess cell proliferation or double-labelling immuno-fluorescence to examine differentiation. For the majority of animals included in the differentiation study, we also obtained paraffin-embedded brain sections for histological analysis and verification of neuropathology of prion-infected animals.

2.5.1 Immunostaining of vibratome brain sections

2.5.1.1 Brain dissection and vibratome processing

Animals were culled and their brains were removed and preserved in 10% formalin for a maximum of 7 days until sectioned on the Vibratome.

The brains were cut on the vibratome on a sagittal plane. Initially they were removed from formalin and embedded in agarose solution. A 35mm dish was filled with warm agarose solution (3% agarose in PBS) and one hemisphere was placed with the medial side facing the bottom. The agarose was then let to solidify for at least 30 min at 4°C. The specimen was trimmed to fit the specimen holder and was glued to it with "Locktide". After adjusting a razor blade (1/2 blade) on the vibratome and setting the blade at a 30° angle, the buffer chamber was filled with PBS and the specimen holder with the specimen glued to it was placed and locked tight into the chamber. The brains were cut into 40μm sagittal sections which were collected in 24-well plates filled with PBS (0.01% sodium azide) and stored at 4 °C.

2.5.1.2 Immunostaining of vibratome brain sections with anti-BrdU antibody

Proliferating cells (30 min BrdU latency) were identified by immuno-staining for BrdU. Vibratome brain sections of 40μm thickness were washed with PBS and then incubated for 30 min at 37°C in 2N HCl. HCl denatures DNA to facilitate exposure to the anti-BrdU antibody. The sections were then rinsed for 10 min in borate buffer to neutralize hydrochloric acid and immersed in 1% H_2O_2 in PBS for 30 min to block endogenous peroxidase activity. The primary rat anti-BrdU antibody was added at a dilution of 1:500 in PBST (1h at room temperature). 0.1% BSA was also added to the antibody solution to block non-specific binding. The sections were then rinsed with PBST, with at least 3 wash changes within a period of 15 min and then incubated for 1 hour at room

temperature with the biotinylated secondary antibody (goat antiserum against rat IgG) at a dilution of 1:500 in PBST. The sections were again rinsed with PBST and incubated for 30 min with the avidin/horse radish peroxidase complex which was prepared 30 min in advance. The avidin part of the complex will bind to the biotin of the secondary antibody. The section was washed once and a small amount of the DAB (3.3 Diaminobenzidine) reagent containing 0.04% H_2O_2 was added for 5 min. DAB reacts with the horse radish peroxidase component of the complex and this reaction gives a brown reaction product which can then be examined under the light microscope.

2.5.1.3 Counterstaining and mounting of sections

The sections were immersed for 8 min in 1:4 haematoxylin and then rinsed in distilled water and immersed into acid (1% HCl in 100% ethanol) for 5-10 s to differentiate nuclear detail. They were then immersed in tap water for at least 8 min to rinse off the acid.

A drop of distilled water was placed on a slide and the section was positioned on top of it with a brush. Excess water was removed and the section was let to dry. For dehydration the section was passed through a series of solutions with gradually increasing ethanol concentration (70%-90%-100%-100% ethanol) and then immersed into xylene. The section was kept for 1 min in each solution. A drop of pertex mounting medium was added and the section was cover-slipped.

2.5.1.4 Fluorescent double immuno-staining of vibratome brain sections

BrdU labelled cells (7 or 8 days BrdU latency) were analysed by double-staining for the expression of markers specific for an early neuronal (β-tubulin), an astroglial (GFAP), or a microglial (Iba-1) phenotype.

Vibratome sections of 40μm thickness were immersed in 2N HCl for 10 min at 37°C. The sections were rinsed for 10 min in borate buffer to neutralize hydrochloric acid. They were then incubated in 1% H_2O_2 in PBS for 30 min to block endogenous peroxidase activity. The primary antibody solution was prepared in PBST (0.1% BSA) and combined two primary antibodies: the rat anti-BrdU Ab(1:1000) with either the rabbit anti-GFAP Ab (1:1000), or the rabbit anti-Iba-1 Ab (1:500). The sections were incubated in primary antibodies for 1 hour at room temperature with gently shaking and then washed in PBST, with at least 3 wash changes within a period of 15 min. The biotinylated secondary antibody (goat antiserum against rat IgG, 1:1000 in PBST) was added for 1 hour at room temperature, followed by three washes in PBST as described before. The

sections were then incubated for 20 min in TSA blocking reagent and then immersed for 20 min in the avidin/horse radish peroxidase complex which was prepared 30 min in advance. Finally TSA Cy3 was added for 5 min in the dark. The avidin part of the avidin/horse radish peroxidase complex will bind to the biotin of the secondary antibody, while horse peroxidase will react with the TSA Cy3. The sections were washed 3 times before incubated with the secondary antibody labelled with the fluorochrome Alexa 488 (anti-rabbit) that binds to either anti-GFAP (Alexa 488 dilluted 1:1000), or anti-Iba-1(Alexa 488 dilluted 1:500). Hoechst 35541, which stains cell nuclei, was also added to the secondary antibody solution at a final concentration of 250ng/ml. The sections were subsequently washed 3 times, placed on a slide and allowed to dry, before adding a drop of Dako Fluorescent mounting medium and cover sliped. They were stored at 4 °C.

Double staining for BrdU and β-tubulin was performed similarly with the exception that the two primary antibodies were added separately. As treatment with HCl prevented binding of the anti-β –tubulin antibody, the anti- β -tubulin antibody was added first in a dilution of 1:200 in PBST (0.1% BSA) and was incubated overnight at 4°C. The following morning the sections were washed 3 times with PBST and then incubated sequentially in hydrochloric acid, borate buffer and H_2O_2 as described previously. The sections were then incubated with the rat anti-BrdU antibody and the staining procedure followed as already detailed. The secondary antibody against anti-β tubulin was anti-mouse labelled with the fluorochrome Alexa 488 and it was diluted 1:200 in PBST containing 250ng/ml Hoechst.

2.5.2 Immunostaining of paraffin-embedded sections

To establish and verify the neuropathological changes in prion-infected brains, formalin-fixed brain hemispheres were decontaminated, dehydrated in graded alcohols and Xylene (tissue processor), embedded in wax , then sectioned and either stained with Haematoxylin /Eosin or immunostained. All sections were assessed for spongiosis, astrogliosis, microglial activation and deposition of abnormal prion protein. To this end, sections were immunostained with the PrP-specific antibody ICSM35, the astroglial marker GFAP and the microglial marker Iba-1.

2.5.2.1 Preparation of paraffin blocks

Brain were removed and fixed in 10% formalin. For samples suspected to contain infectious prions, decontamination with formic acid was performed within a class 1 microbiological safety

cabinet situated within an ACDP level III containment laboratory: After being encased in labelled cassettes, the samples were immersed in 98 % formic acid for 1 h. Formic acid was decanted into 2 M sodium hydroxide and the specimens were treated with approximately five volumes of 10 % buffered formal-saline for 1 h. The 10 % buffered formal-saline was exchanged at least once to ensure any excess of formic acid has been removed prior to tissue processing. The samples were removed from the ACDP level III containment laboratory and placed in the tissue processor (Peloris/ Vision Biosystems) to be treated through a series of processing stages prior to wax embedding. The stages are as follows:

1. Dehydration: the samples were taken through a series of industrial methylated spirits (IMS) (70 %; 90 %; 100 %) to remove water.
2. Clearing: the alcohol was replaced by Xylene, a fluid miscible with IMS and paraffin wax.
3. Impregnation: the Xylene was replaced with molten paraffin wax.
4. Embedding: The samples were embedded in the desired orientation in molten paraffin wax. Once the wax solidified, the samples were ready for sectioning.

2.5.2.2 Cutting sections from a paraffin block

A microtome blade was placed in the knife holder of the microtome and held in position. The paraffin block was mounted onto the Microtome chuck and the excess wax trimmed from the sample block until the whole surface of the embedded sample was exposed. The sample block was then removed from the microtome and placed on a cold plate to cool down. Once the sample block has cooled sufficiently, it was mounted back on the microtome chuck. A ribbon of serial sections of 3μm thickness were obtained and carefully removed from the blade using forceps and placed on the surface of a water bath heated to 40°C until any wrinkles on the sections have disappeared. Individual sections were separated and mounted on to labelled superfrost microscope slides and air-dried for 15 minutes. The slides were then placed in a slide holder and dried at 37°C for a minimum of 2 hours, before they were transferred in the oven (60°C) for another 2 hours.

2.5.2.3 Pre-treatment prior to immunostaining: Re-hydration and de-hydration of wax embedded sections

Wax embedded sections were re-hydrated prior to staining and then de-hydrated after staining has occurred.

The first step in the re-hydration process was the removal of wax by sequential transfer of the sections into 3 separate Xylene solutions. They were placed in the first Xylene solution for 5 minutes and into the other two for 2 minutes in each. The sections were then transferred in a solution of 100% ethanol for 2 minutes and then a further 2 minutes in each of a series of successive ethanol gradients (100%, 90% and 70%). The samples were then rinsed with tap water.

The opposite procedure was carried out for de-hydration of stained sections before mounting onto slides. More specifically, the sections were transferred for 2 minutes in each of a series of increasing ethanol solutions (70%, 90%, 100% 100%) and then placed into xylene solution for a further 2 minutes

2.5.2.4 Haematoxylin and Eosin staining

In order to observe the cellular morphology in the brains of mock-and prion-infected brains, brain sections were stained with haematoxylin and eosin. Re-hydrated sections were immersed in haematoxylin for 5 minutes and then rinsed with tap water. They were then placed into a solution of 1% acid in alcohol (1% Concentrated HCl in 100% ethanol) for 20 seconds to differentiate nuclear detail and again rinsed with cold running water for a further 20 seconds to rinse excess dye. They were immersed in eosin (0.5% aqueous solution) for 20 seconds and washed with cold running water for a further 20 seconds. The sections were de-hydrated and mounted with xylene-based mounting medium Pertex in the Cox Pro-Mounter RCM 2000.

2.5.2.5 Immunostaining with the PrP-specific antibody ICSM35

The re-hydrated brain sections were pre-treated to facilitate antigen retrieval. Initially 1xTris-EDTA citrate buffer was pre-heated to boiling point in the pressure cooker. The sections were then placed into the EDTA solution and incubated at high pressure for 5 minutes followed by low pressure for another 5 minutes. The sections were washed in tap water and immersed in formic acid (98%) for 5 minutes to promote PrP^{c} degradation, and permit detection of PrP^{Sc}. The sections were again rinsed with water to remove excess formic acid.

The automated immunostaining was carried out on the Benchmark Staining Machine from Ventana Medical Systems. The sections were incubated with protease 1 for 4 minutes to promote exposure of the PrP epitope and in Superblock for 10 minutes to reduce non-specific staining and. The sections were incubated in the primary mouse antibody (ICSM35/D-gen at 1mg/ml stock) for 32

minutes at a concentration of 1:3,000. The staining was completed by incubation with a universal biotinylated secondary antibody and its reaction with DAB which gives a brown end product that can be detected on the light microscope (IView DAB detection kit 760-091). The sections were de-hydrated and mounted with xylene-based mounting medium Pertex in the Cox Pro-Mounter RCM 2000

2.5.2.6 Immunostaining for the astroglial marker GFAP

The re-hydrated brain sections were pre-treated to facilitate antigen retrieval. The sections were placed into 1xTris-EDTA citrate solution and heated in the microwave for 25 minutes (high power) and then rinsed with tap water.
Immunostaining was performed by the Benchmark XT Staining Machine (Ventana Medical Systems). The sections were incubated in the primary rabbit a-GFAP antibody (Dako/Z0334) for 32 minutes at a concentration of 1:1,000. The staining was completed by incubation with a universal biotinylated secondary antibody and its reaction with DAB which gives a brown end product that can be detected on the light microscope (IView DAB detection kit 760-091). The sections were de-hydrated and mounted with Xylene-based mounting medium Pertex in the Cox Pro-Mounter RCM 2000

2.5.2.7 Immunostaining for the microglial marker Iba-1

Immunostaining for the microglial marker Iba-1 was performed on the Discovery machine. The brain sections were heated to 95°C for 1 h in 1xTris-EDTA citrate buffer to facilitate antigen retrieval. The sections were incubated in Superblock for 10 minutes to block non-specific binding. The rabbit anti-Iba-1 antibody (Wako/ 019-19741) was added at a concentration of 1:250 for 4 hours. The polyclonal biotinylated swine α-rabbit secondary antibody (DAKO/ E0353) was added at a concentration of 1:200. Antibody binding was detected by the brown reaction product of the reaction with DAB (DAB-MAP kit). The sections were de-hydrated and mounted with Xylene-based mounting medium Pertex in the Cox Pro-Mounter RCM 2000

2.6 Counting cells

2.6.1 Counting BrdU positive cells

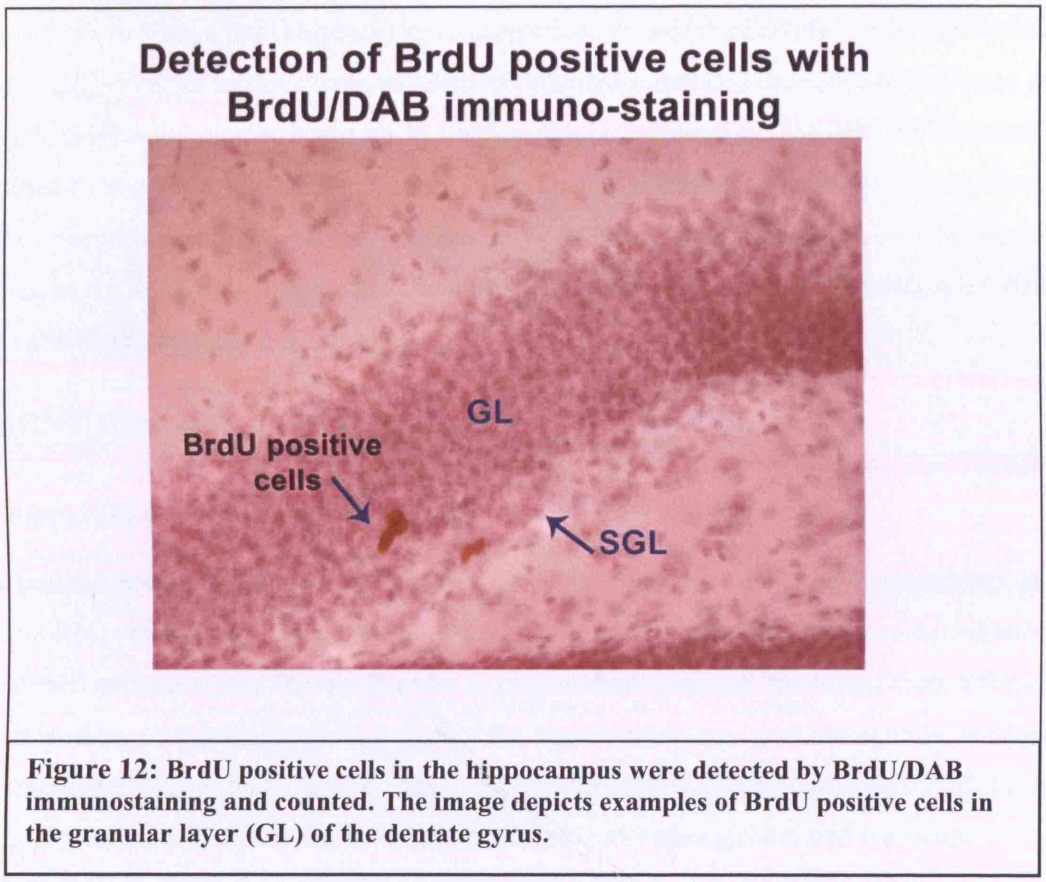

Figure 12: BrdU positive cells in the hippocampus were detected by BrdU/DAB immunostaining and counted. The image depicts examples of BrdU positive cells in the granular layer (GL) of the dentate gyrus.

To assess cell proliferation we examined animals that received a 30 min injection of BrdU. We analysed 4 sequential 40μm sagittal brain sections from each animal examined. BrdU-labelled cells in the area of the hippocampus in each section were visualized under the light microscope (Fig. 12). We counted BrdU-labelled cells in the neurogenic area of the dentate gyrus and separately in the remaining area of the hippocampus.

2.6.2 Confocal Microscopy- counting double labelled cells

Double-stained sections were examined using a Zeiss LSM 510 META laser-scanning microscope equipped with 4 lasers: Helium/Neon with wavelength of 543 nm, Helium/Neon with wavelength of 633 nm, Argon-ion with wavelengths of 458, 477, 488, and 514 nm and diode lasers

with wavelength of 405 nm. The laser compartment was attached to a Zeiss Axiovert 200 M microscope equipped with standard filter sets to visualize Rhodamine and excitable fluorochromes including DAPI, Alexa 546 and Alexa 488. The microscope was controlled via a PC operating Windows 2000 and Zeiss LSM 510 acquisition software. We obtained confocal images of BrdU-labelled cells (7 or 8 days BrdU latency) across the whole area of the dentate gyrus. The detector gain and amplifier offset settings were adjusted to optimize signal and to reduce background noise. The pinhole diaphragm diameter was set to 1 airy unit which minimized the detectable amount of fluorescence light deriving from out-of-focus areas. Scanned BrdU-labelled cells were analysed for a positive or negative phenotype for β-tubulin, GFAP or Iba-1. The phenotype of scanned cells was determined by an impartial observer and the numbers of neuronal, astroglial, or microglial BrdU-labelled cells were counted.

2.7 BDNF Elisa immunoassay

2.7.1 Preparation of hippocampus homogenates

A preliminary study was carried out to estimate the BDNF levels in the hippocampus of mock- and RML-inoculated mice and also of un-inoculated controls. The brains of culled animals were removed and were snap frozen. In order to prepare homogenates, the brains were left to thaw for approximately 15 minutes and dissection of the hippocampus was performed under the light microscope using forceps and a scalpel. The dissected hippocampi were kept on ice at all times and each was suspended in 600µl lysis buffer and homogenized with a grinder and then vortexed and centrifuged in an Eppendorf centrifuge at 1500xg (1.5 RCF) for 20 min (RT). The supernatant was collected and diluted by adding 4 volumes of DPBS. The samples were then acidified and then neutralized to maximize the yield of protein: 1 µl of 1N HCl per 50µl of diluted sample volume was added and the pH was checked to ensure that it shows a value of 3.0 or below. The samples were then mixed and incubated for 15 min at RT. They were then neutralized by addition of 1µl of 1N NaOH per 50 µl of sample volume. The pH was again measured to confirm a value of approximately 7.6. The samples were stored at -70 to -80 °C.

2.7.2 Protein determination of hippocampus homogenates (BCA method)

The protein concentration of hippocampus homogenates was calculated by the BCA method. The standard BSA (bovine serum albumin) was diluted in DBPS to produce a series of concentrations: 0, 0.2, 0.4, 0.6, 0.8, 1.0, and 1.2 mg/ml. 10µl of each of the BSA dilutions and of

each homogenate sample were loaded in wells of a 96-well plate. Both the standards and unknown samples were loaded in duplicate. The working solution was prepared by mixing reagent A with reagent B in a ratio of 50:1 respectively. 200µl of the working solution was added to each of the loaded samples and the contents of the plate were mixed vigorously on a plate shaker for 30 seconds. The lid was placed on the plate and it was transferred to 37°C for 30'-1h. BCA (Bicichoninic acid) reacts with complexes between copper ions and peptide bonds to produce a purple end product. The absorbance was measured at 570nm on a plate reader.

The concentrations and the absorbance readings for the standards were inserted into an Excel worksheet and the protein standard curve was created using the Microsoft Excel programme applications (Fig. 13). The equation for the line of the standard curve and the R^2 value were calculated. By replacing y with the absorbance value of a sample, the equation can then calculate its concentration (x). An example of a protein standard curve is depicted in figure 13.

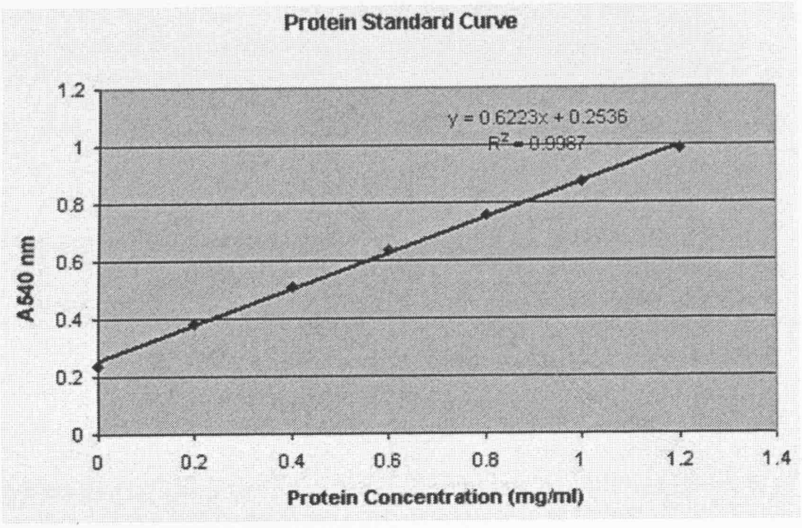

Figure 13: this is an example of a protein standard curve. The equation of the line of the standard curve can calculate the unknown protein concentration (x) of samples for a given A540 absorbance value (y). The R^2 value (=0.9987) is very close to optimal (i.e. 1).

2.7.3 BDNF Elisa protocol

The antibody solution was prepared by mixing 10µl of the anti-BDNF monoclonal antibody with 10 ml of carbonate coating buffer. 100µl of the antibody solution was added to each well of a 96-well ELISA plate, which was sealed with a plate sealer and incubated overnight at 4 ° C. The next morning the contents of the plate were discarded and the wells were washed 3 times with PBST. 200 µl of Block & Sample Buffer (1x diluted in water) was added in each well and incubated for 1h at RT. The wells were then washed 3 times with PBST. Serial dilutions of standard BDNF were produced in Block & Sample 1X buffer and 100 µl of each dilution was loaded in duplicate on the plate as shown in the representation of a 96-well ELISA plate below:

	1	2	3	4	5	6	7	8	9	10	11	12	
A											1:2,000	1:2,000	500 pg/ml
B											1:4,000	1:4,000	250 pg/ml
C											1:8,000	1:8,000	125 pg/ml
D											1:16,000	1:16,000	62.5 pg/ml
E											1:32, 000	1:32, 000	31.3 pg/ml
F											1:64,000	1:64,000	15.6 pg/ml
G											1:128,000	1:128,000	7.8 pg/ml
H											**buffer only**	**buffer only**	0

100µl of each sample (hippocampus homogenate) was added in a separate well of the 96-well plate. The samples were loaded in triplicate. The plate was sealed with a plate sealer and the samples were incubated for 2h at RT with shaking (400 rpm). The wells were then washed 5x with PBST before 100µl of anti-human BDNF antibody (1:500 in 1x block & sample buffer) was added per well and incubated for 2h at RT with shaking. The wells were rinsed 5x with PBST and 100µl of anti-IgY HRP conjugate (1:200 in 1x block & sample buffer) was added per well and incubated for 1h at RT with shaking. During this time the TMB One solution was equilibrated to RT. After another set of washes, 100µl of TMB were added in each well (RT with shaking). The reaction gave a blue end product and was stopped after 10 minutes by addition of 100µl 1N HCl in each well.

Upon acidification the blue colour changed to yellow. The absorbance was read at a wavelength of 450 nm on a plate reader.

2.7.4 Calculating the BDNF concentration standard curve in Microsoft Excel

The concentrations of standard BDNF samples and their corresponding absorbance values were inserted to adjacent columns on the excel spread sheet. To create a standard curve the following instructions were selected: chart wizard/ scatter plot/ point only sub-type. The equation of the line of the standard curve and the R^2 value were calculated. The R^2 value is a measurement of the 'goodness of fit' of the equation and predicts the accuracy by which the equation determines the BDNF concentration of samples according to their absorbance readings. The optimal value of R^2 is 1. An example of a BDNF standard curve is shown in figure 14. The BDNF concentration of each sample was calculated in pg/ml and adjusted to its corresponding total protein concentration giving a final BDNF concentration of pg per mg total protein.

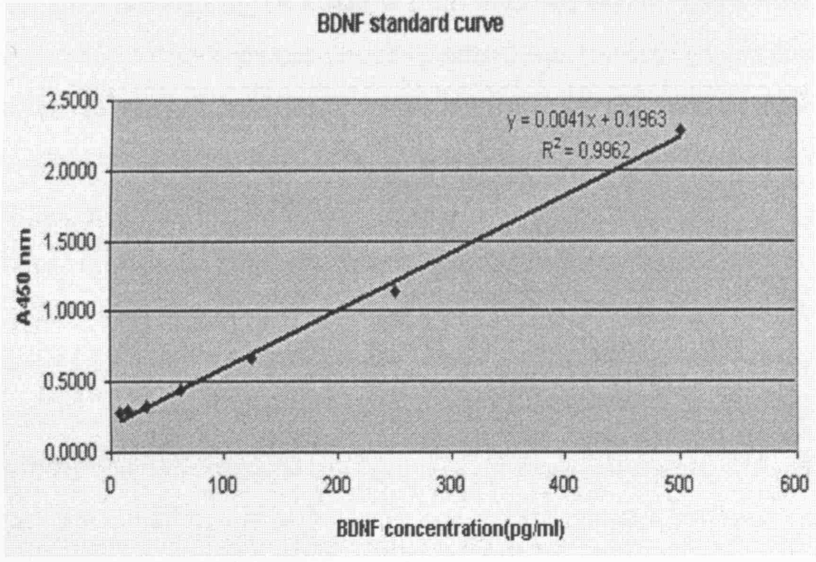

Figure 14: this is an example of a BDNF standard curve. The equation of the line of the standard curve can calculate the unknown protein concentration (x) of samples for a given A450 absorbance value (y). The R^2 value (=0.9962) is very close to optimal (i.e. 1).

2.8 Neural stem cell culture

A assay was set up to investigate the role of PrP on neural stem cell growth. For this purpose neural stem cells that were isolated from the hippocampi of wt and *Prnp*$^{-/-}$ mice were grown into culture. Mice were culled by dislocation of the neck and their brains were removed under sterile conditions and kept on ice in a Petri dish containing medium with glucose. The brains were cut in half and the hippocampus was dissected from both hemispheres. Each hemisphere was processed separately under the light microscope. The hemisphere was held into position with forceps and the hippocampus was carefully dissected using a scalpel. Dissected hippocampi obtained from 4 mice were placed in to one well of a 24-well plate and transferred in sterile laminate flow cabinet.

The excess medium was removed and the hippocampi were cut into fine pieces using sterile scissors. 1 ml of the reconstituted Papain solution was added and the plate was placed in the incubator at 37°C for 1 h. The cell suspension was passed through a needle (21G/BD) for approximately 20 times to dissociate cells. The cells were transferred to a sterile 15ml tube and centrifuged at 300g for 5 minutes at RT. The supernatant was removed with aspirator and the pellet was re-suspended in DNAse-albumin-inhibitor mixture to stop the Papain reaction. 5 ml of albumin-inhibitor solution were added in a new 15ml tube and the cell suspension was carefully layered at the top so that a discontinuous density gradient was formed. The contents of the tube were centrifuged at 70g for 6 minutes at RT so that dissociated cells pellet at the bottom. The supernatant was discarded and the cells were immediately re-suspended in 5 ml of neurosphere medium and kept in the incubator (37 °C).

The cells were allowed to grow into neurospheres within 1 week before the media was changed: the contents of the wells were collected into 15ml tubes and centrifuged at 1000 rpm for 5 minutes. The supernatant was discarded and the cells were re-suspended in the appropriate volume of neurosphere media and plated. As a standard procedure the media was changed every 3-4 days. When the neurosphere cultures reached confluence, they were dissociated and passaged: initially the neurospheres were transferred in a 15ml tube and centrifuged at 1,000 rpm for 5 minutes. The pellet was mixed with 1ml of trypsin for 5 minutes for neurospheres to dissociate into individual cells. Dissociation was assisted by pipetting and the trypsin action was inhibited with 1ml of trypsin inhibitor. The cells were then centrifuged at 1,000rpm for 5 minutes and the pellet was re-suspended in neurosphere medium.

3 Results

All parts of methodology were carried out by Kanella Prodromidou, with the exceptions of: The intracrebral inoculation of animals with either the RML inoculum or mock inoculum was performed by Julie Underwood. Stainings on paraffin-embedded sections for histological analysis (H&E, GFAP, ICSM35, Iba-1) were carried out by Kanella Prodromidou, Catherine O'Malley and Caroline Powell.

3.1 Genotyping of transgenic mice

All tg37 mice included in this study were hemizygous for the Lox-PrP transgene. Hemizygotes were obtained by crossing tg37 mice homozygous for the Lox-PrP transgene with *Prnp*$^{0/0}$ mice. The offsprings were screened for the Lox-PrP construct by PCR. Only the animals that were tested positive were selected (hemizygous). Table 6 describes the number of tg37 mice obtained by the breeding scheme applied, and confirmed positive for the Lox-PrP sequence (Fig.15).

CONFIRMATION OF TG37 GENOTYPE BY PCR			
Proliferation study (30' BrdU latency)			
Mouse strain	**Inoculation**	**Time point of BrdU injection**	**Number of mice**
Tg37	Mock	8, 11, 12, 13 wk p.i.	4
Tg37	RML	8 wk p.i.	3
Tg37	RML	11 wk p.i.	3
Tg37	RML	12 wk p.i.	3
Differentiation study (7-8 d BrdU latency)			
Mouse strain	**Inoculation**	**Time point of BrdU injection**	**Number of mice**
Tg37	Mock	11 wk p.i.	4
Tg37	RML	11 wk p.i.	4
Differentiation study (5 d BrdU latency)			
Tg37	Mock	12 wk p.i.	2
Tg37	RML	12 wk p.i.	3
BDNF study			
Mouse strain	**Inoculation**	**Time point of sacrifice**	**Number of mice**
Tg37	Mock	12, 13 wk p.i.	3
Tg37	RML	12 wk p.i.	2
Tg37	RML	Onset of symptoms	1

Table 6: Number and details of tg37 mice tested positive for the Lox-PrP sequence

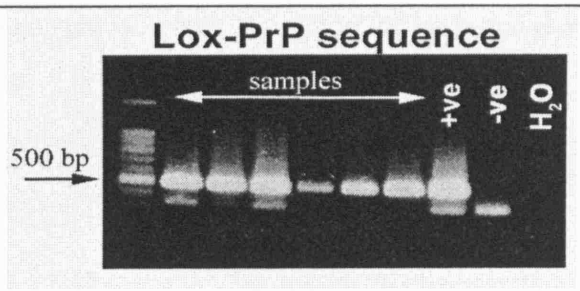

Figure 15: Examples of DNA samples (obtained from tg37 transgenic mice) screened positive for the Lox-PrP sequence. The Lox-PrP sequence is visualized at 500bp and the internal control (amplicon from retinoblastoma gene) at 300bp; the DNA ladder is shown on the first lane while the 3 last lanes represent the controls: positive, negative and H_2O.

3.2 Scoring scheme applied for histological analysis of paraffin-embedded brain sections

We performed histological analysis of prion-infected and mock-inoculated wild type and tg37 mice and also of prion-infected NFH-Cre/tg37 mice to identify prion disease-related neuropathology in the brain. Paraffin-embedded sagittal brain sections were stained for haematoxylin and eosin to assess the degree of spongiosis. Immunostainings were carried out with the astroglial marker GFAP and the microglial marker Iba-1 to detect gliosis, and also with the prion protein-specific antibody ICSM35 to examine accumulation of the abnormal form of prion protein. The hippocampus was examined in all sections and received scoring according to the intensity of staining. For scoring we adopted a scale from 0 to 3, where 0 denotes no staining and 3 characterizes intensity (Fig. 16). As expected spongiosis was not detected in control samples. In the presented series of histological analysis, little to moderate spongiosis (score1-2) was observed in prion-infected animals but we did not identify spongiosis equivalent to score 3. Accumulation of PrP^{Sc} was identified in the hippocampus by immunostaining with the PrP-specific antibody ICSM35 (Beringue et.al., 2004). Detection of PrP^{Sc} in situ requires suppression of PrP^{c} antigenicity which is achieved by formic acid treatment (Bell et.al., 1997; Van Everbroeck et.al., 1999). This method leads to denaturation of PrP^{c} but not PrP^{Sc} due to the relative resistance of the latter to degradation. Following incubation with formic acid, immunostaining with the anti-PrP antibody ICSM35 specifically recognizes PrP^{Sc}. As expected, control samples showed no staining for ICSM35. PrP^{Sc} accumulation was stronger at the later stages of prion disease. All sections examined, derived either from control or infected animals, exhibited some degree of astrogliosis and therefore a score 0 was

not applicable. Microglia are inherently present in the brain and therefore a score 0 is not applicable for microglial staining.

H&E
(spongiosis)
GFAP
(Astrocytes)
Iba-1
(Microglia)
ICSM 35
(Prion protein)
Score 0
Score 1
Score 2
Score 3
No score 3 applicable
No Score 0 applicable
No score 0 applicable
A
B
C
D
E
F
G
H
I
J
K
L
M
N
O
P

Figure 16: Scoring scheme for staining with haematoxylin and eosin and for immunostainings with the astroglial marker GFAP, the microglial marker Iba-1 and the PrP-specific antibody ICSM35. A scoring scale ranging from 0 to 3 was adopted, where 0 indicates no staining while 3 characterizes maximum intensity. A-D) Spongiosis (inset panels) in the hippocampus was detected by staining with haematoxylin and eosin. According to intensity of spongiosis sections were scored within the scale of 0-3. We did not identify spongiosis corresponding to score 3 within this series. E-H) Astrogliosis was detected in the hippocampus by immunostaining for GFAP. All sections examined presented some degree of astrogliosis and therefore a score 0 was not applicable within this series. I-L) Microglial activation was detected in the hippocampus by immunostaining for Iba-1. As microglia are inherently present in the brain, a score 0 is not applicable. M-P) Accumulation of PrP^{Sc} was identified in the hippocampus by immunostaining with the PrP-specific antibody ICSM35.

3.3 RML inoculation results in prion infection with characteristic neuropathological features

Prion-infected animals were examined to verify neuropathology of prion disease. Table 9 describes the scoring in the hippocampus of all mock- and RML-inoculated animals examined. RML-inoculation resulted in prion infection and manifestation of neuropathology characteristic of prion disease. This includes spongiosis, PrP^{Sc} accumulation, and gliosis in the form of astrocytes and microglia. As expected mock-inoculated animals did not show any spongiosis or accumulation of the abnormal form of prion protein, but some astrocytic gliosis was observed in certain samples (Fig. 28). RML-inoculated wt mice exhibited moderate spongiosis and increased gliosis and PrP^{Sc} accumulation (Fig. 20). Prion-infected tg37 mice presented variable spongiosis in the hippocampus, ranging from little (score 1) to moderate (score 2) at both 11 and 12 wk p.i. Gliosis and PrP^{Sc} accumulation were strong at 11 wk p.i. and especially profound by the 12 wk p.i. (Fig. 29, 30). Upon PrP depletion and rescue from clinical prion disease in NFH-Cre/tg37 mice, we observed an alleviation of all neuropathological features, including reversal of spongiosis and reduction of gliosis and PrP^{Sc} accumulation (Fig. 47).

Our infectivity study includes inoculation with the RML strain of mouse-adapted prions. RML-inoculation results in prion infection with neuropathology characteristic of that specific strain. For example according to unpublished studies carried out in the MRC Prion Unit, inoculation of tg37 mice with the ME7 mouse-adapted strain leads to longer incubation period. In that view, our results are mouse strain- and prion strain- restricted and will be discussed in the broader context of prion disease. Moreover, the tg37 and NFH-Cre/tg37 mouse lines included in our study show PrP over-expression. It has been reported that un-inoculated older mice carrying high copy numbers of wild-type PrP transgenes spontaneously developed neurological symptoms, such as ataxia and hindlimb

paralysis and exhibited myopathy, demyelinating polyneuropathy and focal vacuolation of the CNS (Westaway, 1994). Un-inoculated tg37 and NFH-Cre/tg37 mice have been monitored previously until they reached the age of at least 50 weeks and they do not develop spontaneous prion disease.

Numbers of mice and scoring of histological analysis in the hippocampus					
Mouse strain and inoculation	**Time point**	**Scoring**			
		H&E	**GFAP**	**ICSM35**	**Iba-1**
FVB- RML	110d p.i. (+8d Brdu latency)	1	3	3	3
FVB- RML	110d p.i. (+8d Brdu latency)	1	3	3	3
Tg37- Mock	-	0	1	0	1
Tg37- Mock	-	0	1	0	1
Tg37- Mock	-	0	2	0	1
Tg37- Mock	-	0	2	0	2
Tg37- RML	11wk p.i. (+7d Brdu latency)	2	3	3	3
Tg37- RML	11wk p.i. (+7d Brdu latency)	1	2	3	3
Tg37- RML	11wk p.i. (+7d Brdu latency)	1	2	2	2
Tg37- RML	12wk p.i. (+5d Brdu latency)	1	3	3	3
Tg37- RML	12wk p.i. (+5d Brdu latency)	1	3	3	3
Tg37- RML	12wk p.i. (+5d Brdu latency)	2	3	3	3
NFH-Cre/tg37-RML	13wk p.i. (+7d Brdu latency)	1	1	1	1
NFH-Cre/tg37-RML	13wk p.i. (+7d Brdu latency)	0	2	2	1
NFH-Cre/tg37-RML	13wk p.i. (+7d Brdu latency)	0	2	2	1

Table 7: Histological analysis and scoring of neuropathological features in the hippocampus of mock- and RML-inoculated mice. H&E staining identifies morphology/spongiosis, GFAP, ICSM35 and Iba-1 immunostainings describe astrogliosis, PrP^{Sc} accumulation and microglia activation respectively.

3.4 Neural stem cell recruitment in prion-infected wild type mice

3.4.1 Prion infection increases cell proliferation in the hippocampus but not in the dentate gyrus of wild type mice

Stem and precursor cells proliferate before they commit to a specific phenotype. We evaluated cell proliferation in the hippocampus of mock- and RML-inoculated wild type mice. Dividing cells were labelled with BrdU (30 min BrdU latency) and were detected by immunostaining of formalin fixed brain sections. For each mouse analysed we counted 4 sequential

sections of a total of 160µm thickness (Fig. 17). We determined proliferation at 110 days of incubation and at the onset of symptoms (111 and 124 days post inoculation); 3 animals were analysed for each time point and the average of cell proliferation in the hippocampus was calculated. The control group is represented by the average count of a total of 8 mice that received 30 min BrdU injection at different time points after intracerebral inoculation of normal brain homogenate (mock-inoculated). The proliferation in the neurogenic area of the dentate gyrus and the remaining area of the hippocampus was estimated separately. We found no difference in the level of proliferation in the dentate gyrus between mock- and RML-inoculated wild type mice (Fig. 18). However cell proliferation in other areas of the hippocampus is elevated at 110 days post inoculation (Fig. 19).

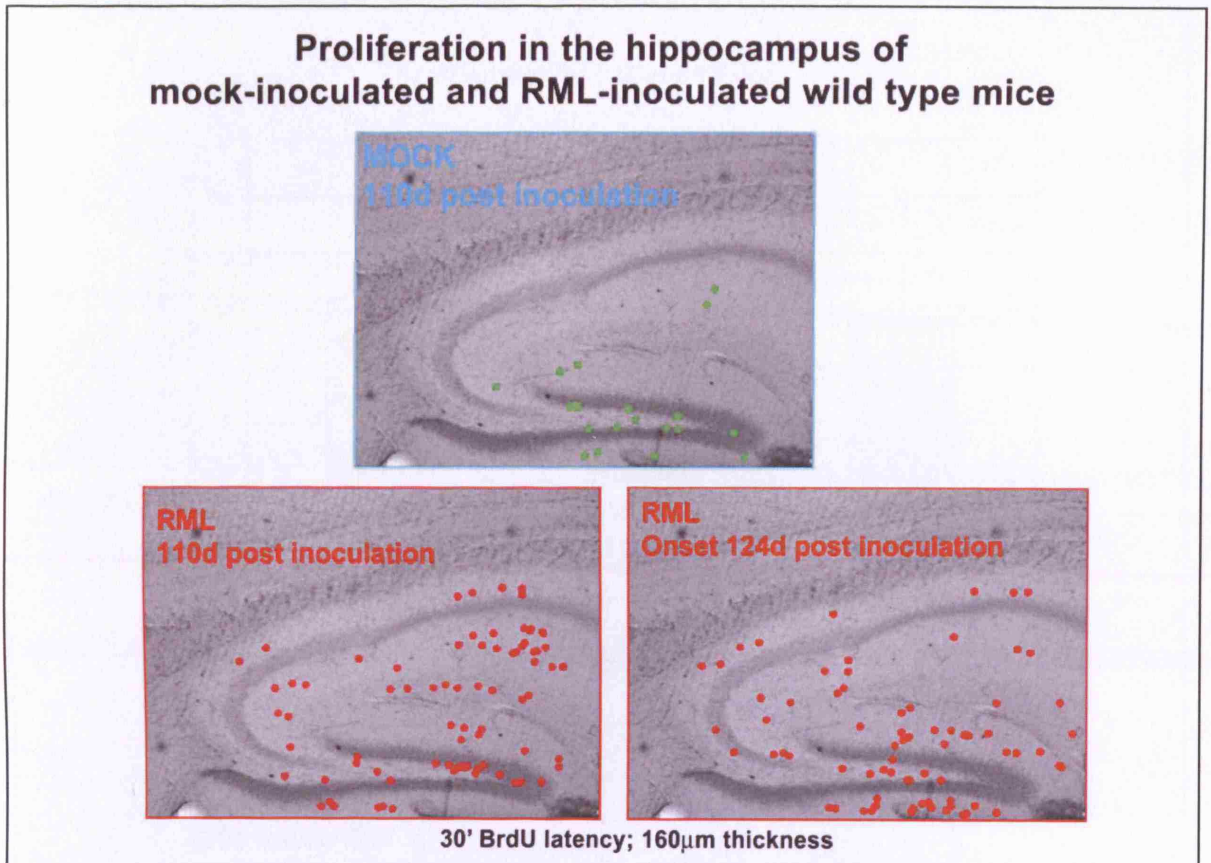

Figure 17: BrdU positive cells (dots) in the hippocampus of wild type mice were detected by BrdU/DAB immunostaining and counted. The figure depicts representative counts in a mock-inoculated mouse and RML-inoculated mice at 110d and 124d post-inoculation (30' BrdU latency; 160µm thickness). An increase in the number of BrdU-positive cells is observed in areas of the hippocampus other than the dentate gyrus in RML-inoculated wild type mice.

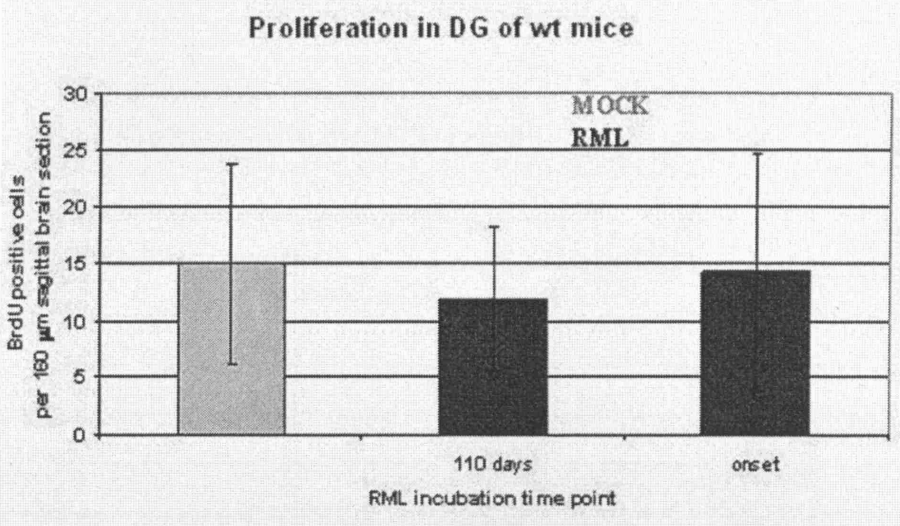

VERSUS (Unpaired t-test)	RML 110d incubation	RML onset of symptoms
mock inoculated	p=0.55	p=0.93
RML 110d incubation	--	p=0.75

Figure 18: There is no significant difference for cell proliferation in the dentate gyrus of mock- (grey bar) and RML-inoculated mice (black bars). The table summarises the statistical analysis for proliferation in the dentate gyrus of mock- and RML-inoculated mice.

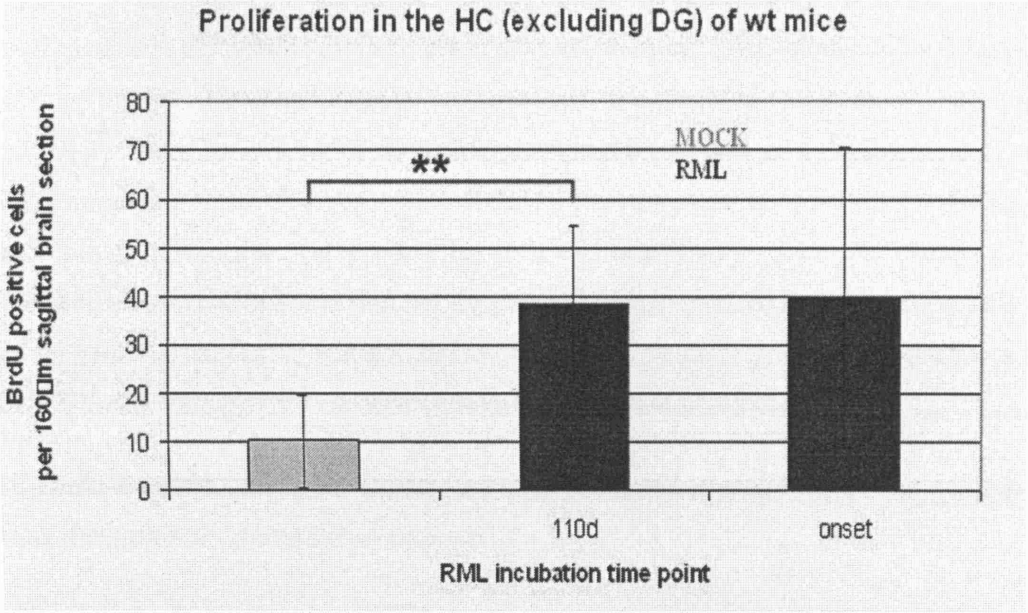

VERSUS (Unpaired t-test)	RML 110d incubation	RML onset of symptoms
Mock-inoculated	p=0.005	p=0.24
RML 110d incubation	--	p=0.95

Figure 19: Cell proliferation in the hippocampus (excluding DG) is significantly increased in RML-inoculated mice (black bars) at 110 days of incubation as compared with mock-inoculated mice (grey bar). The table summarises the statistical analysis for proliferation in the hippocampus of mock- and RML-inoculated mice. **≤ 0.05

3.4.2 Characterisation of BrdU-labelled cells in the dentate gyrus of prion-infected wild type mice

In order to determine the fate of proliferating stem cells and identify the phenotype of other proliferating cells in the dentate gyrus of prion infected wt mice, RML-inoculated wild type mice were injected i.p. with BrdU and culled eight days later. We obtained vibratome cut sagittal brain sections and also paraffin-embedded contralateral sagittal brain sections from the brain of examined animals. Neuropathological changes were verified by immunostaining of paraffin-embedded sections while the phenotype of BrdU-labelled cells was identified by double-labelling immunofluorescence of vibratome (left hemisphere). We characterised BrdU-labelled cells with markers for neuronal, astroglial and microglial phenotypes. Positive cells of all three types were identified in the dentate gyrus. Our observations are described in detail below:

3.4.2.1 BrdU-labelled cells in the dentate gyrus of prion-infected wild type mice exhibit neuronal, astroglial or microglial phenotypes

In order to establish the fate of proliferating stem cells and the identity of other proliferating cells in the dentate gyrus of prion infected mice, we performed i.p. BrdU injections at 110 days p.i. and culled the animals eight days later. Their brains were dissected and paraffin-embedded contralateral sections were examined for neuropathology characteristic of prion disease. As shown in figure 20, histological analysis revealed spongiosis, accumulation of PrP^{Sc} and astroglial and microglial activation in the dentate gyrus. The phenotype exhibited by BrdU-labelled cells was assessed by immunostaining of vibratome sections obtained from the contralateral hemisphere. 40 µm sagittal brain sections were double stained for BrdU and the neuronal marker β-tubulin to establish the number of stem cells expressing β-tubulin in the dentate gyrus. β-tubulin is expressed in post-mitotic cells and indicates differentiation into an immature neuronal phenotype. A total of five 40µm sections obtained from 3 RML-inoculated animals were analysed and the percentage of total BrdU-labelled cells in the dentate gyrus expressing β-tubulin was calculated (Fig. 21, 22). In order to determine the identity of other proliferating cells in the dentate gyrus of RML-inoculated wild type mice, BrdU-labelled cells (8 days BrdU latency) were characterised by co-labelling of either the astroglial marker GFAP or the microglial marker Iba-1. GFAP expressing cells were analysed on the confocal microscope in a total of six 40µm sections obtained from 3 RML-inoculated animals. Iba-1 expressing microglial cells were analysed on the confocal microscope in a

total of six 40µm sections obtained from 3 RML-inoculated animals. The proportion of BrdU-labelled cells expressing either of the 2 phenotypes was estimated in relation to the total number of BrdU-labelled cells we observed in the dentate gyrus at this late stage of incubation of prion disease (Fig. 21, 23, 24). In accordance with the neuropathological analysis that verified gliosis, 18.3% and 32% of proliferating cells represented activated astrocytes and microglia respectively. Moreover, a 19.5% of BrdU-labelled cells in the dentate gyrus corresponded to proliferating progenitor cells acquiring an early neuronal phenotype (Fig. 21).

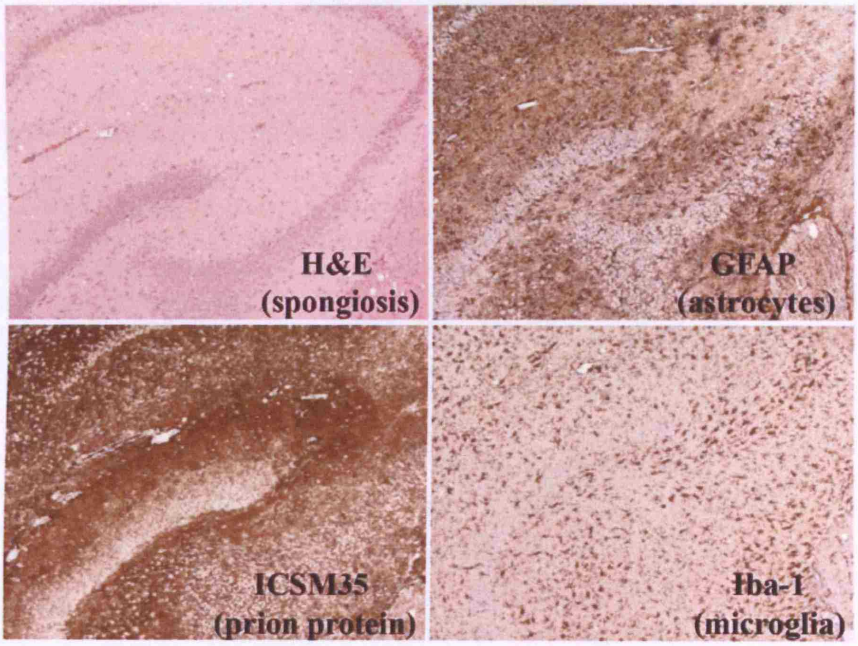

Figure 20: Contralateral sagittal sections of brains obtained from RML-inoculated FVB mice were examined for neuropathological features. For all animals we examined the analysis verified spongiosis (H&E) of low degree (score 1), and also astrogliosis (GFAP) (score 3), microglial activation (Iba-1) (score 3) and accumulation of PrP^{Sc} (ICSM35) (score 3) in the hippocampus.

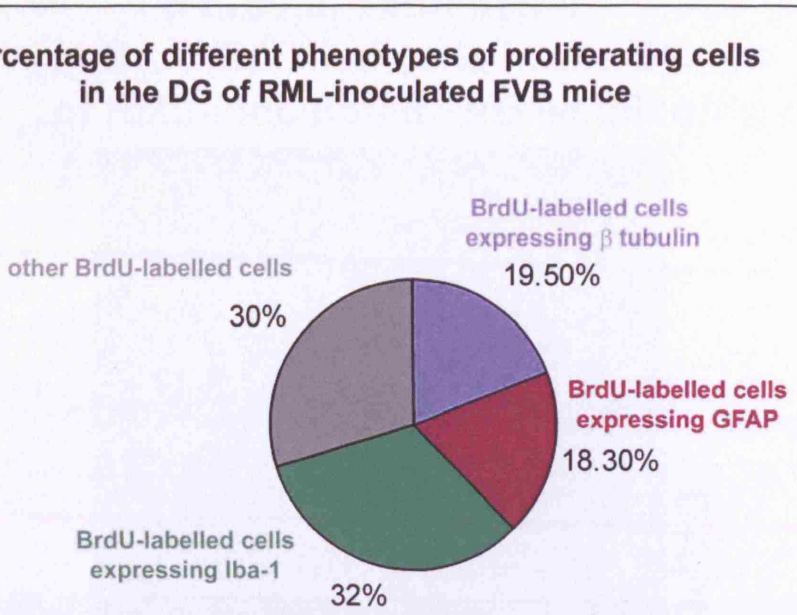

Figure 21: BrdU-labelling identifies proliferating progenitor cells, and also activated astrocytes and microglia in the dentate gyrus of RML-inoculated FVB mice (110 days p.i., 8 days BrdU latency). 19.5% of BrdU-labelled cells represent proliferating progenitor cells acquiring an early neuronal phenotype (β tubulin). 18.35% and 32% of BrdU-labelled cells correspond to proliferating astrocytes and microglia respectively, while another 30% of BrdU-labelled cells in the dentate gyrus have not been identified by the presently applied markers.

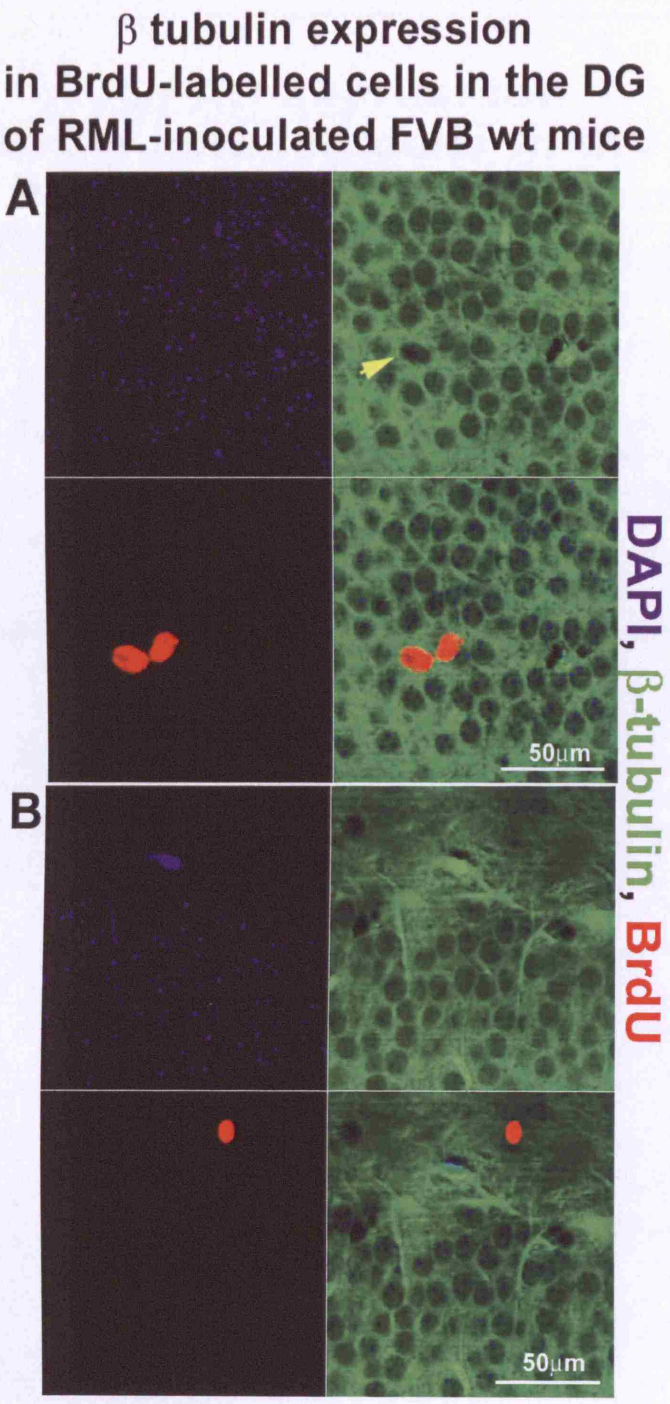

Figure 22: BrdU-labelled cells in the dentate gyrus of RML- inoculated wild type mice are positive (arrows) or negative for the early neuronal marker β-tubulin (110d incubation; 8 days BrdU latency). A) β-tubulin-positive BrdU-labelled cell in the granular layer of RML-inoculated FVB mice; B) β-tubulin negative BrdU-labelled cell in the hilus of RML-inoculated FVB mice.

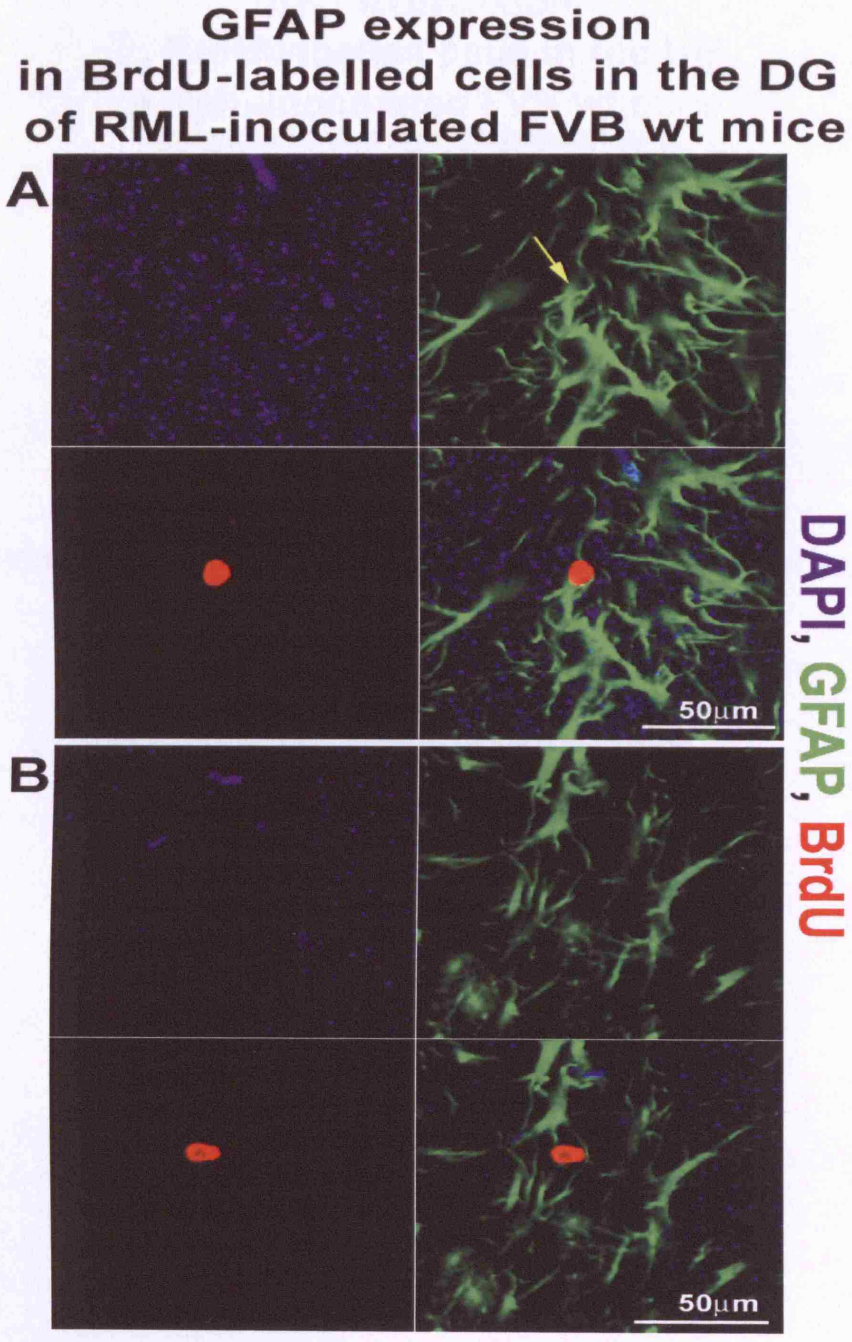

Figure 23: BrdU-labelled cells in the dentate gyrus of RML- inoculated wild type mice are positive (arrows) or negative for the astrocytic marker GFAP (110d incubation; 8 days BrdU latency). A) GFAP-positive BrdU-labelled cell in the granular layer of RML-inoculated FVB mice; B) GFAP-negative BrdU-labelled cell in the hilus of RML-inoculated FVB mice.

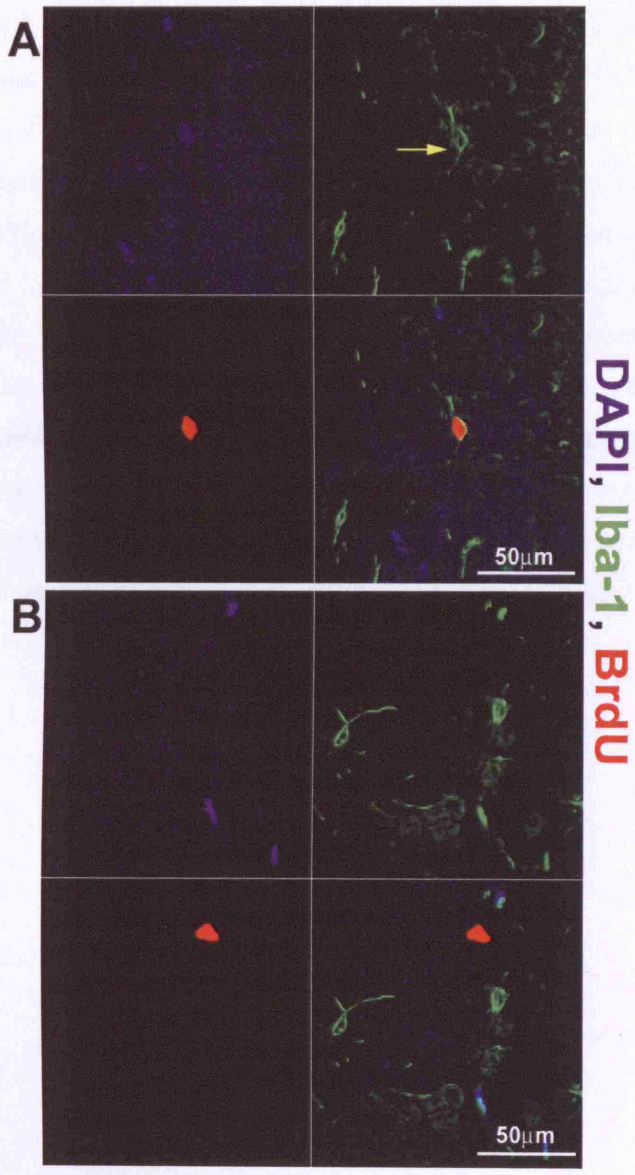

Figure 24: BrdU-labelled cells in the subgranular layer of the dentate gyrus of RML-inoculated wild type mice (110d incubation; 8 days BrdU latency) are A) positive (arrow); B) negative for the microglial marker Iba-1.

3.5 Neural stem cell recruitment in prion-infected transgenic tg37 mice

3.5.1 Cell proliferation in the hippocampus of tg37 mice increases during incubation of prion disease

Cell proliferation based on the number of BrdU positive cells in the hippocampus was also calculated for mock- and RML-inoculated tg37 mice. These mice express PrP at three times wt level and therefore show a shortened incubation period compared to wild type mice. Tg37 mice succumb to prion disease by the end of 12 weeks after RML inoculation while wild type mice succumb at 19 weeks. BrdU was injected at 3 time points during the course of the prion disease (the beginning of 8, 11 and 12 week of incubation; 30 min BrdU latency). Vibratome brain sections were immunostained for BrdU. The results for each time point are the average of 3 mice studied. The control group is represented by the average count of a total of 4 mice that received 30 min BrdU injection at different time points after intracerebral inoculation of normal brain homogenate (mock-inoculated). From each mouse of both mock and RML groups, we counted 4 sequential sections (160µm thickness). We found that prion infection results in an increase of cell proliferation throughout the area of the hippocampus including the dentate gyrus (Fig. 25, 26, 27).

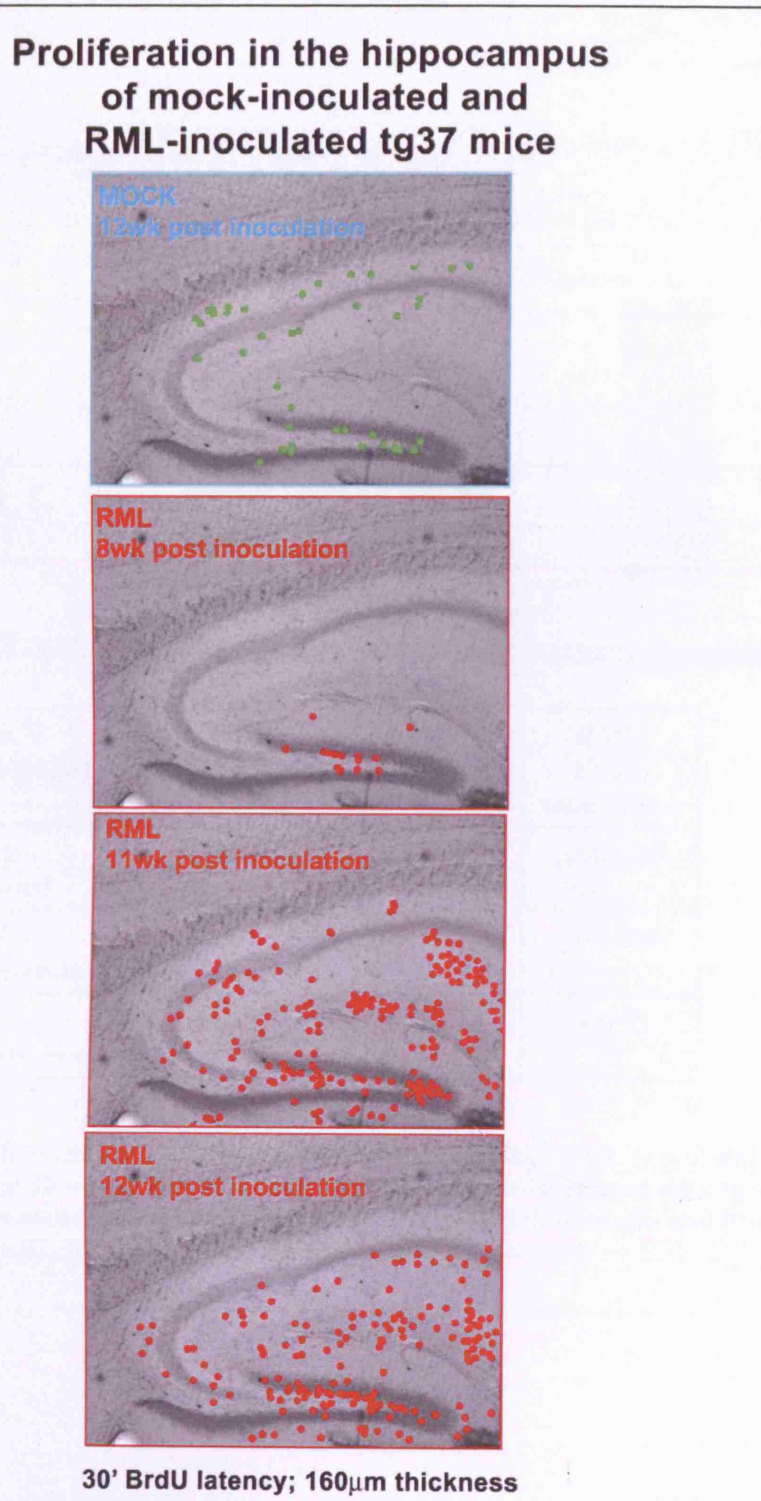

Figure 25: BrdU positive cells (dots) in the hippocampus of tg37 mice were detected by BrdU/DAB immunostaining and counted. The figure depicts representative counts in a mock-inoculated mouse and RML-inoculated mice at 8wk, 11wk and 12wk post-inoculation (30' BrdU latency; 160μm thickness). An increase in the number of BrdU-positive cells is observed in the hippocampus of RML-inoculated tg37 mice.

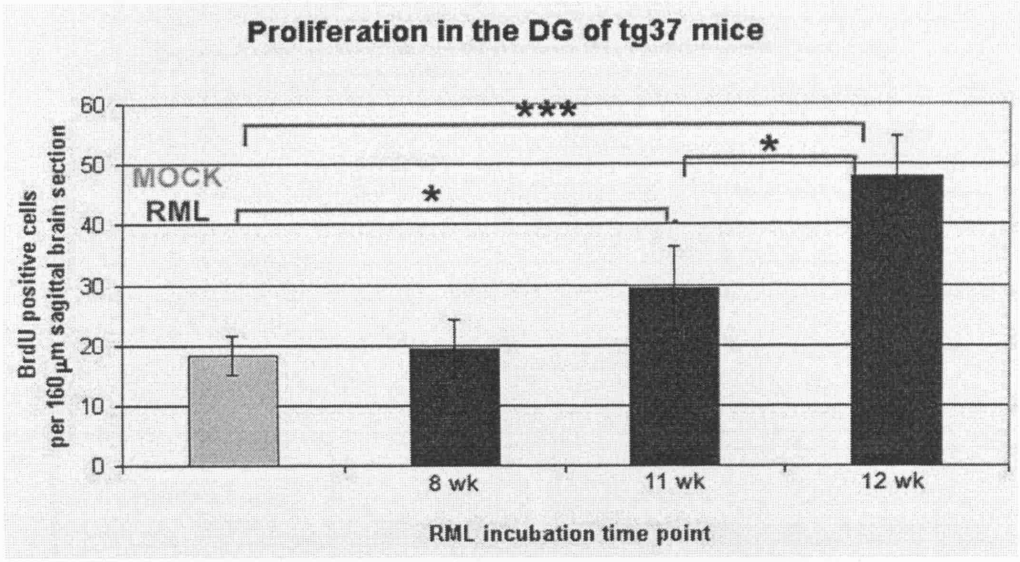

VERSUS (Unpaired t-test)	RML 8 wk incubation	RML 11 wk incubation	RML 12 wk incubation
Mock inoculated	p=0.73	p=0.03	p=0.0005
RML 8 wk incubation	--	p=0.11	p=0.004
RML 11 wk incubation	--	--	p=0.03

Figure 26: Cell proliferation in the DG is significantly increased in RML-inoculated tg37 mice (black bars) at 11 and 12 weeks of incubation compared to mock-inoculated mice (grey bar). The table summarises the statistical analysis for proliferation in the DG of mock- and RML-inoculated mice. *≤ 0.05, **≤ 0.005, *≤0.0005**

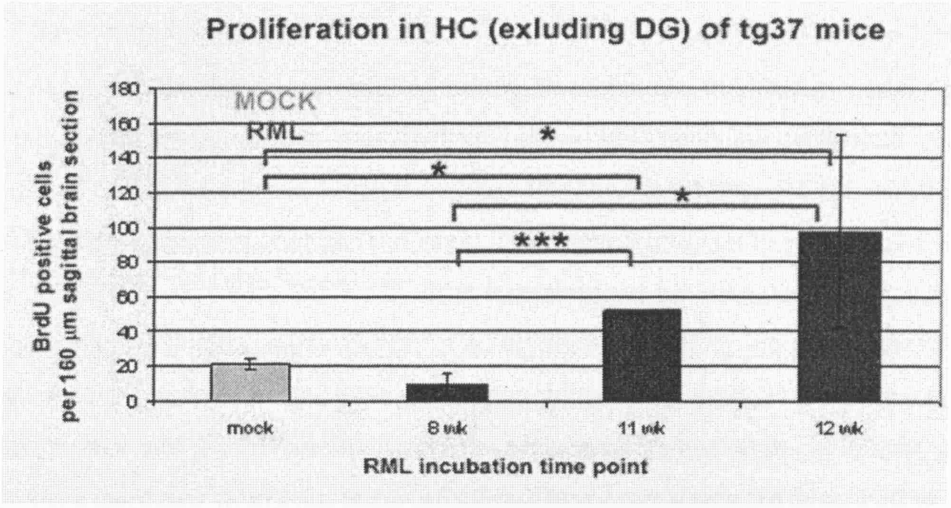

VERSUS (Unpaired t-test)	RML 8 wk incubation	RML 11 wk incubation	RML 12 wk incubation
Mock-inoculated	p=0.21	p=0.01	p=0.04
RML 8 wk incubation	--	p=0.0004	p=0.05
RML 11 wk incubation	--	--	p=0.23

Figure 27: Cell proliferation in the hippocampus (excluding DG) is significantly increased in RML-inoculated tg37 mice (black bars) at 11 and 12 weeks of incubation compared to mock-inoculated mice (grey bar) and also compared to 8wk of prion incubation. The table summarises the statistical analysis (t-test) for proliferation in the hippocampus of mock- and RML-inoculated mice. *≤ 0.05, **≤ 0.005, *≤0.0005**

3.5.2 Characterisation of BrdU-labelled cells in the dentate gyrus of prion-infected tg37 mice

To determine the fate of proliferating stem cells and assess the identity of other proliferating cells in the dentate gyrus of mock- and RML-inoculated tg37 mice, we performed i.p. BrdU injections and culled the animals seven days later. We obtained vibratome cut sagittal brain sections and also paraffin-embedded contralateral sagittal brain sections from the brains of examined animals. Neuropathology was verified by immunostaining of paraffin-embedded sections while the phenotype of BrdU-labelled cells was identified by double-labelling immunofluorescence of vibratome sections. BrdU-labelled cells were characterised with markers for neuronal, astroglial and microglial phenotypes. Positive cells of all three types were identified in the dentate gyrus and their numbers were increased following prion infection. Our observations are described in detail below:

3.5.2.1 RML-inoculated tg37mice exhibit neuropathology characteristic of prion disease

Contralateral paraffin-embedded sections from brains of mock- and RML-inoculated tg37 mice were examined by staining with haematoxylin and eosin to assess spongiosis. Gliosis was analyzed by immunostainings with the astroglial marker GFAP and the microglial marker Iba-1. PrP^{Sc} accumulation was verified in prion infected animals by immunostaining with the prion protein-specific antibody ICSM35. All mock-inoculated animals analysed did not exhibit spongiosis or PrP^{Sc} accumulation in the hippocampus. They showed variable gliosis and scored predominantly 1 and occasionally 2 for both astroglia and microglia (Fig. 28). RML-inoculated tg37 mice were examined for neuropathological changes in the hippocampus at the end of 11 and 12 weeks post inoculation. The observations were similar for both time points. Spongiosis was variable ranging from score 1 to 2, and PrP^{Sc} accumulation was strong in almost all cases (score 3). A high degree of astroglial and microglial activation was observed varying between scores 2 and 3, 3 being the score for most cases (Fig. 29, 30).

3.5.2.2 The number of BrdU-labelled cells expressing β-tubulin is increased in the dentate gyrus of prion-infected tg37 mice

In order to determine the fate of proliferating stem cells and assess the identity of other proliferating cells in the dentate gyrus of mock- and RML-inoculated tg37 mice, we performed i.p. BrdU injections and culled the animals seven days later. The phenotype exhibited by BrdU-labelled

cells was assessed by immunostaining of vibratome brain sections. BrdU-labelled cells were analysed for expression of the early neuronal marker β-tubulin to establish the number of stem cells expressing β-tubulin in the dentate gyrus. A total of seven 40μm sections obtained from 4 RML-inoculated animals and seven 40μm sections obtained from 3 mock-inoculated animals were analysed and the average number of β-tubulin expressing cells per section (i.e. 40μm) was calculated (Fig. 31-33). The number of β-tubulin expressing cells is increased in the dentate gyrus of prion infected tg37 mice. The t-test between the two groups (i.e. mock- and RML-inoculated) calculated a p-value of 0.0573, which is slightly above the 0.05 margin which reveals significance.

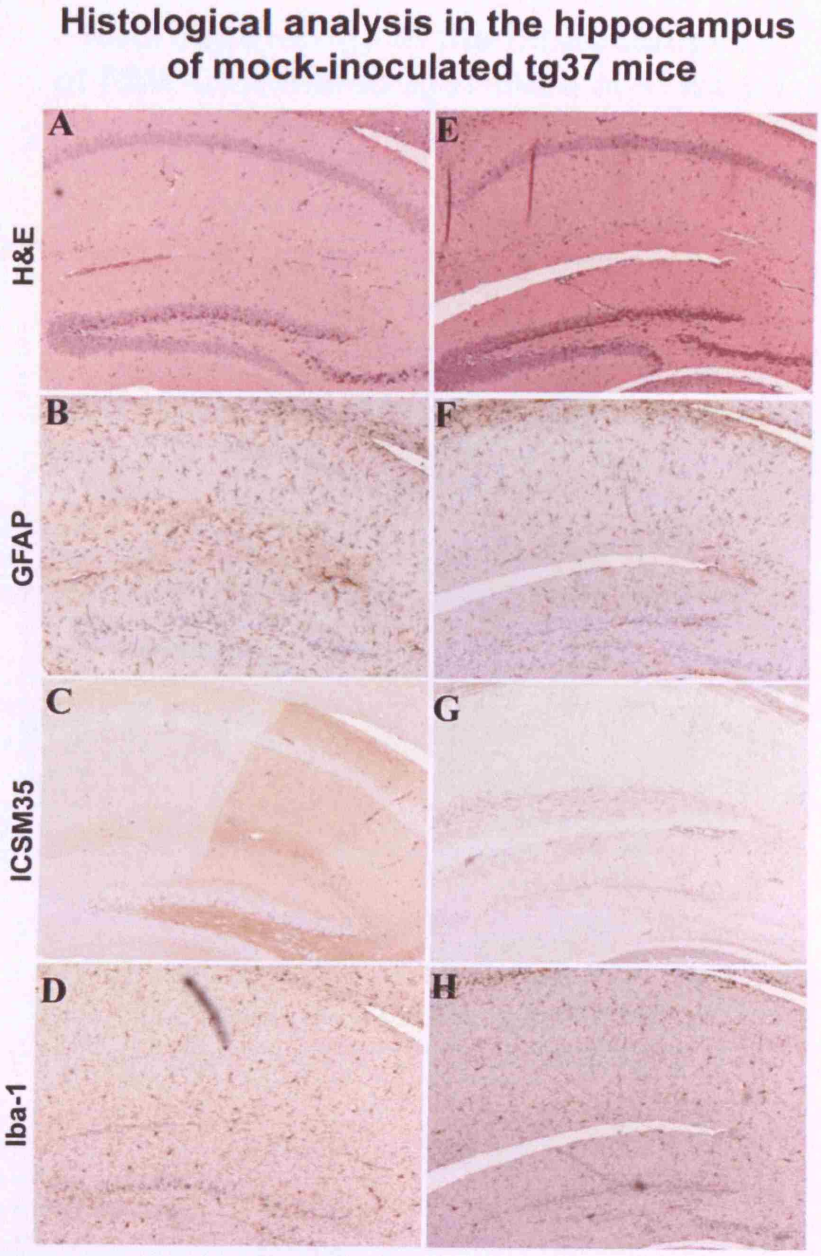

Figure 28: Contralateral sections of brains obtained from mock-inoculated tg37 mice were histologically examined. The figure shows analysis of the hippocampus of two animals: images A-D correspond to animal 1 and E-H to animal 2. Both exhibited A, E) no spongiosis (score 0), B, F) minor astrogliosis (score 1), C,G) no PrP^{Sc} accumulation (score 0) and D, H) minor microglial activation (score 1).

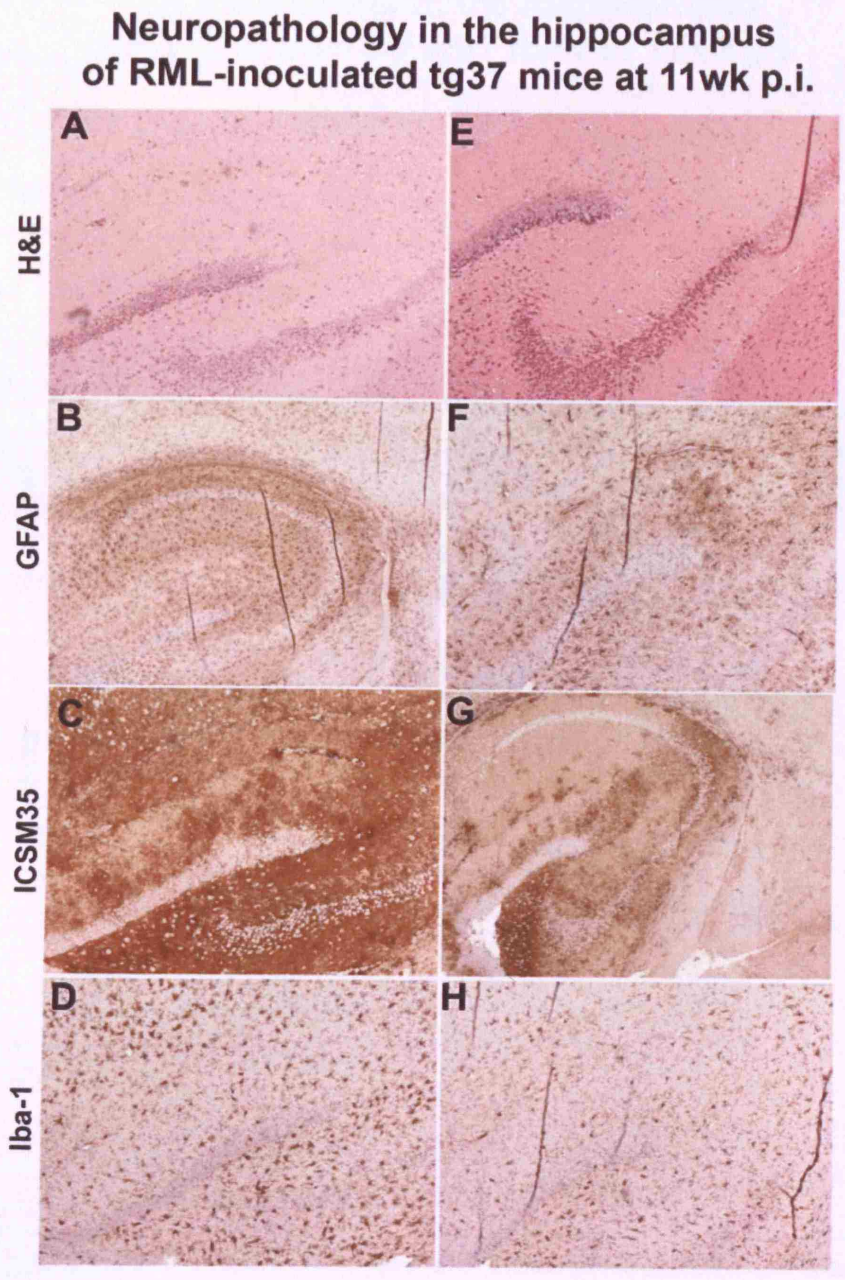

Figure 29: Contralateral sections of brains obtained from prion-infected tg37 mice were examined to verify neuropathology. The figure shows analysis of the hippocampus of two animals at the end of 11 wk post inoculation: images A-D correspond to animal 1 and E-H to animal 2. Mouse 1 exhibited A) spongiosis (score 2); B,D) high astroglial and microglial activation (score 3); and C) high PrP^{Sc} accumulation (score 3). Mouse 2 showed E) mild spongiosis (score 1); F) considerable astroglial and microglial activation (score 2); and G) PrP^{Sc} accumulation (score 2).

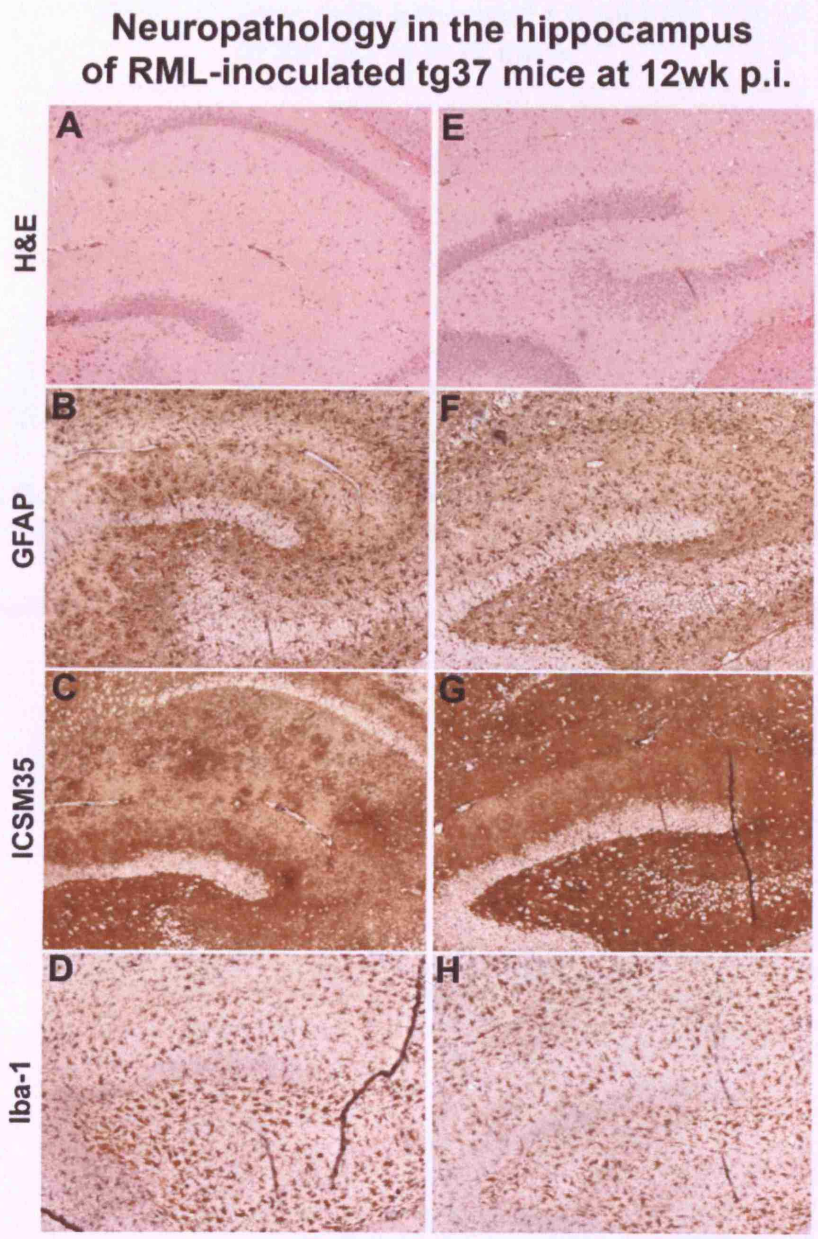

Figure 30: Contralateral sections of brains obtained from prion-infected tg37 mice were examined to verify neuropathology. The figure shows analysis of the hippocampus of two animals at the end of 12 wk post inoculation: images A-D correspond to animal 1 and E-H to animal 2. Mouse 2 exhibited A) higher spongiosis (score 2) than E) mouse 1 (score 1); Both animals showed high degree of B,F) astroglial activation (score 3) and D,H) microglial activation (score 3), and also of C,G) profound PrP^{Sc} accumulation (score 3).

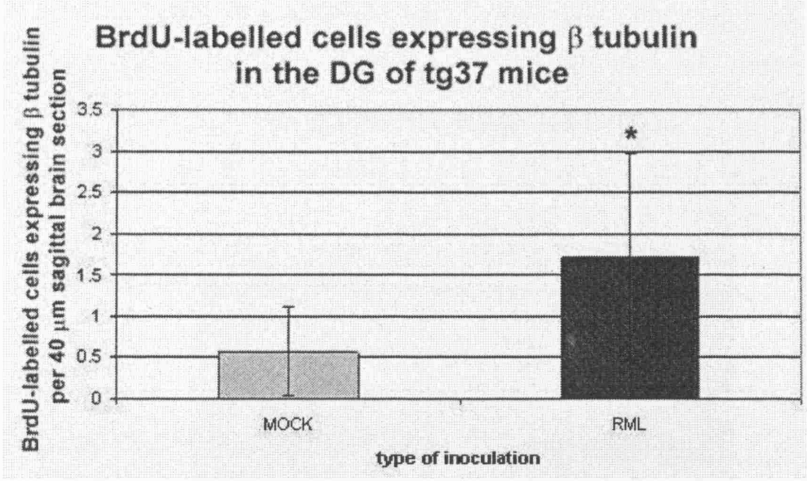

Figure 31: The number of BrdU-labelled cells expressing β-tubulin in the dentate gyrus of tg37 mice is increased at 11 week post RML inoculation (7 days BrdU latency). *≤ 0.05

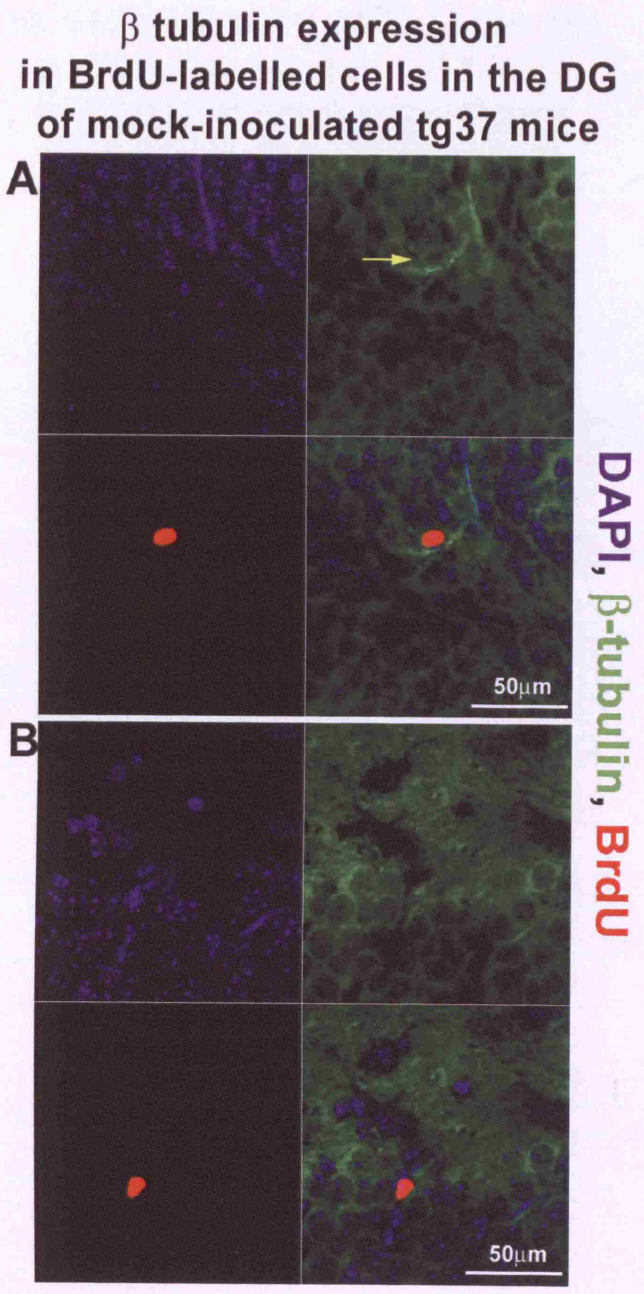

Figure 32: BrdU-labelled cells in the subgranular layer of the dentate gyrus of mock-inoculated tg37 mice are either A) positive (arrow) or B) negative for β-tubulin (7 days BrdU latency).

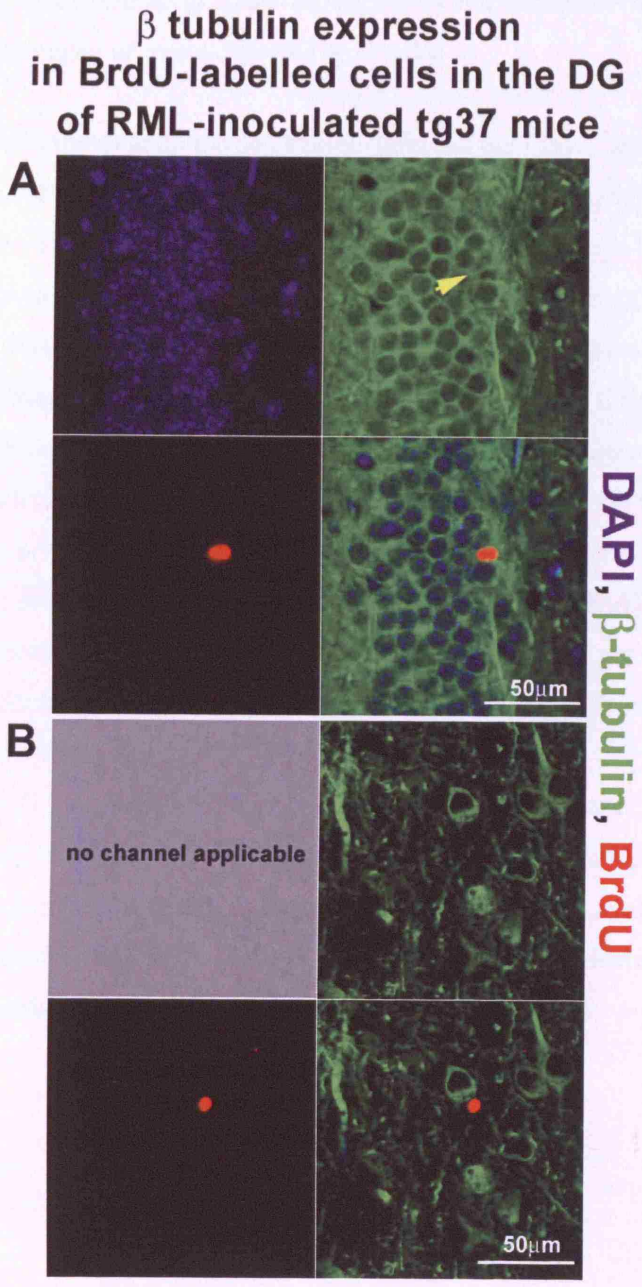

Figure 33: BrdU-labelled cells in the subgranular layer of the dentate gyrus of RML-inoculated tg37 mice are either A) positive or B) negative for β-tubulin; (11 week incubation; 7 days BrdU latency).

3.5.2.3 Identification of populations of BrdU-labelled cels exhibiting astroglial or microglial phenotypes in the dentate gyrus of prion-infected tg37 mice

BrdU-labelled cells in the dentate gyrus of prion-infected tg37 mice were characterised with markers for astroglia (GFAP) and microglia (Iba-1). We analysed BrdU-labelled cells for expression of GFAP at the 11^{th} and 12^{th} week post inoculation (7 and 5 days BrdU latency respectively). To evaluate the number of GFAP positive cells in the dentate gyrus at 11 weeks post inoculation we analysed 7 sagittal brain sections obtained from 4 RML-inoculated mice and 6 sections obtained from 4 mock-inoculated mice. To assess the number of GFAP positive cells at 12 weeks of incubation we examined 6 sections obtained from 3 RML-inoculated mice and 4 sections obtained from 2 mock-inoculated mice. The number of astroglial cells in the dentate gyrus was significantly increased in prion infected mice at 11 week post inoculation as compared to mock-inoculated mice (Fig. 34, 36-38). We also observed a higher number of GFAP-positive BrdU-labelled cells in RML-inoculated tg37 mice at 12wk p.i (3.8 GFAP/BrdU per 40 μm brain section) as compared to mock-inoculated controls where we did not identify any GFAP/BrdU double positive cell in the sections examined..

BrdU-labelled cells (11 week of incubation; 7 days BrdU latency) were also analysed for expression of Iba-1. We examined 8 sections obtained from 4 RML-inoculated animals and 7 sections obtained from 4 mock-inoculated mice and found that there was a highly significant increase in the number of microglial cells in the dentate gyrus of prion infected tg37 mice as compared to mock-inoculated controls (Fig. 35, 39, 40).

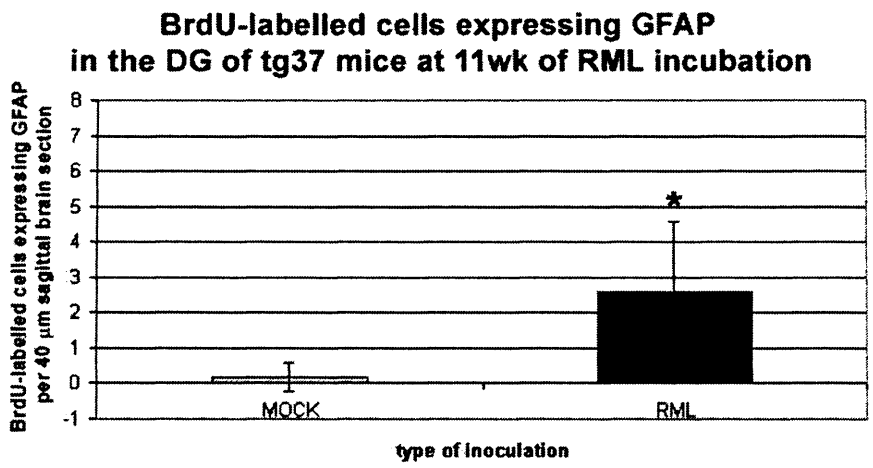

Figure 34: The number of BrdU-labelled cells expressing GFAP is increased in the DG of RML-inoculated tg37 mice at A) 11 week post inoculation, p=0.02 (7 days BrdU latency) and B) 12 week post inoculation, p=0.029 (5 days BrdU latency). *≤ 0.05

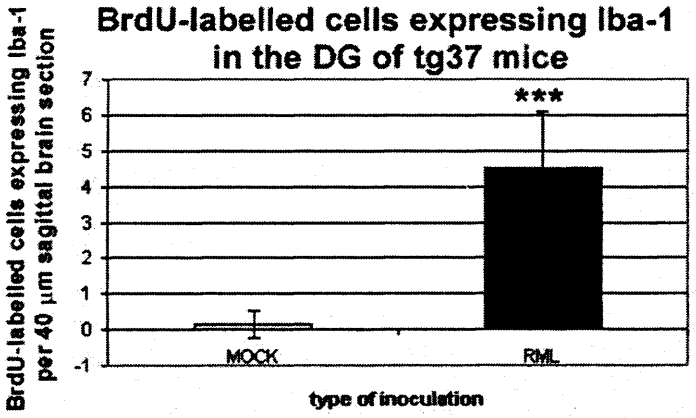

Figure 35: Increased number of BrdU-labelled cells expressing Iba-1 in the DG of RML-inoculated tg37 mice. (11 week post inoculation; 7 days BrdU latency), p=0.0001. *≤ 0.0005

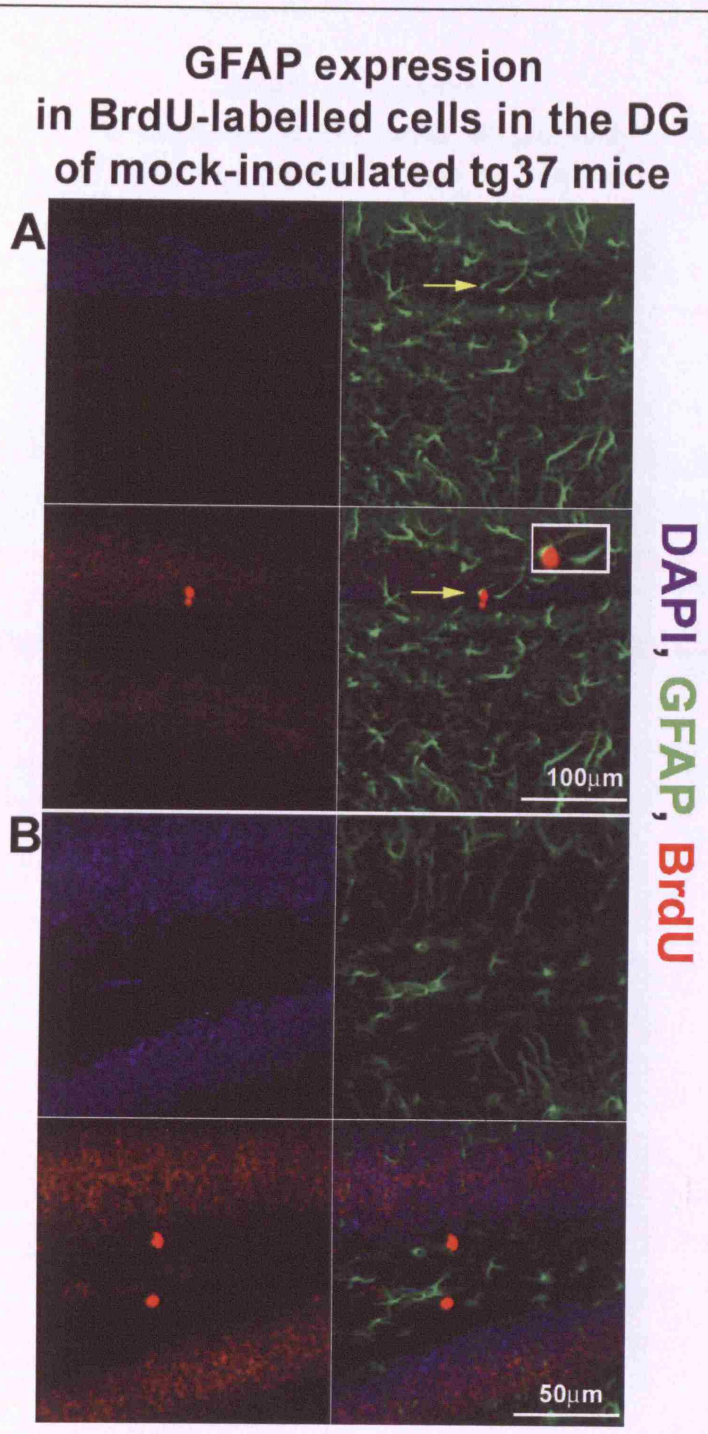

Figure 36: BrdU-labelled cells in the dentate gyrus of and mock-inoculated tg37 mice are positive (arrows) or negative for GFAP (11wk incubation; 7 days BrdU latency). A) BrdU-labelled cell in the subgranular layer is positive for GFAP; B) GFAP negative BrdU-labelled cell in the hilus.

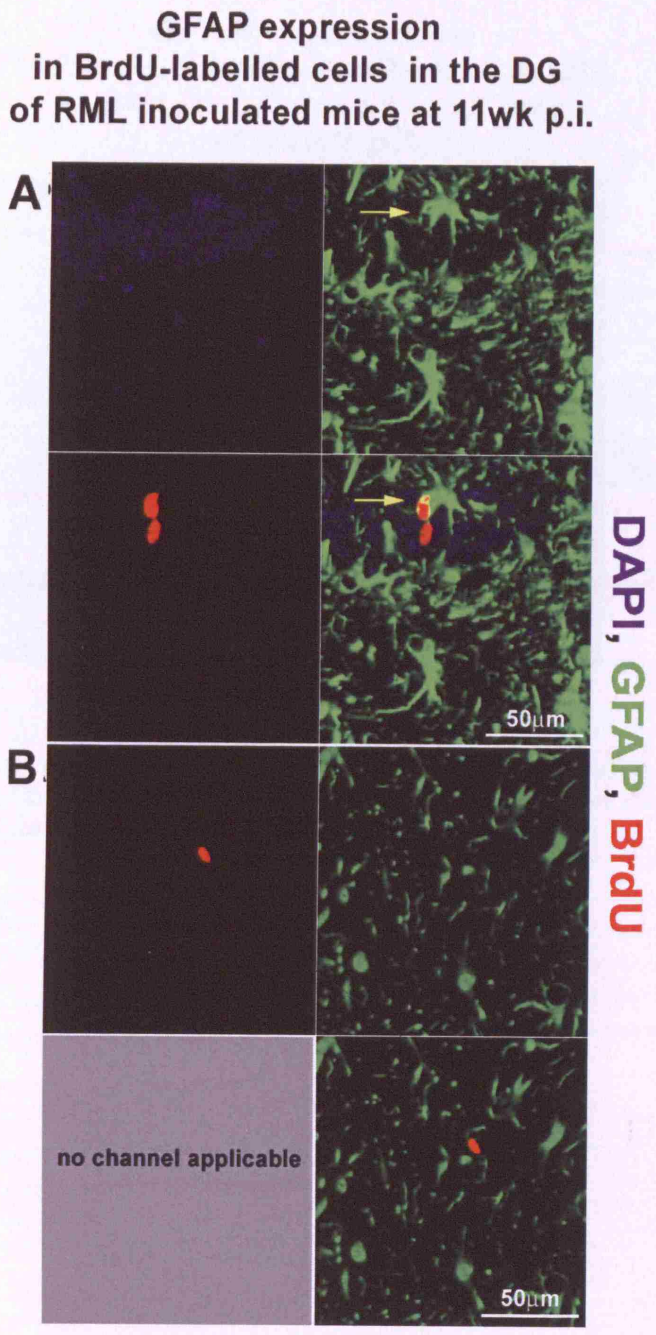

Figure 37: BrdU-labelled cells in the dentate gyrus of RML- inoculated tg37 mice are positive (arrows) or negative for GFAP (11wk incubation; 7 days BrdU latency). A) BrdU-labelled cell in the granular layer is positive for GFAP (arrow); B) example of a GFAP negative BrdU-labelled cell in the hilus.

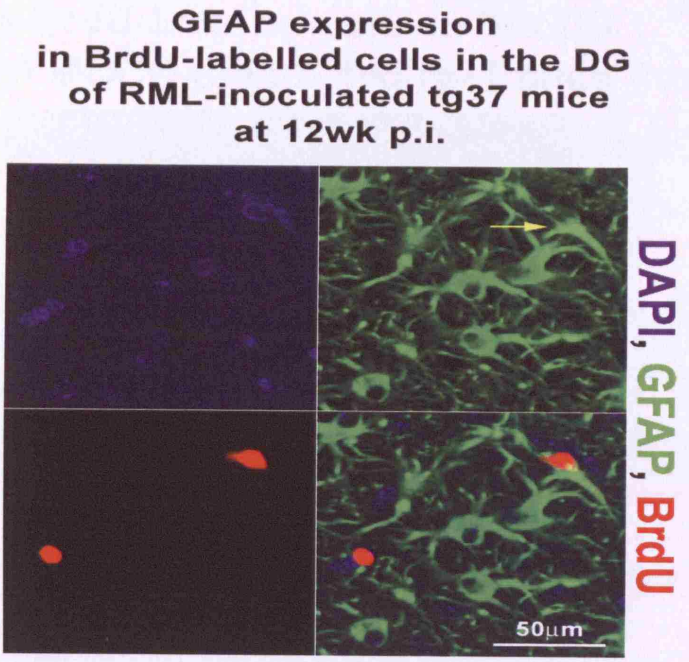

Figure 38: BrdU-labelled cells in the dentate gyrus of RML- inoculated tg37 mice are positive for GFAP (12wk incubation; 5 days BrdU latency). The figure shows a BrdU-labelled cell in the hilus which is positive for GFAP.

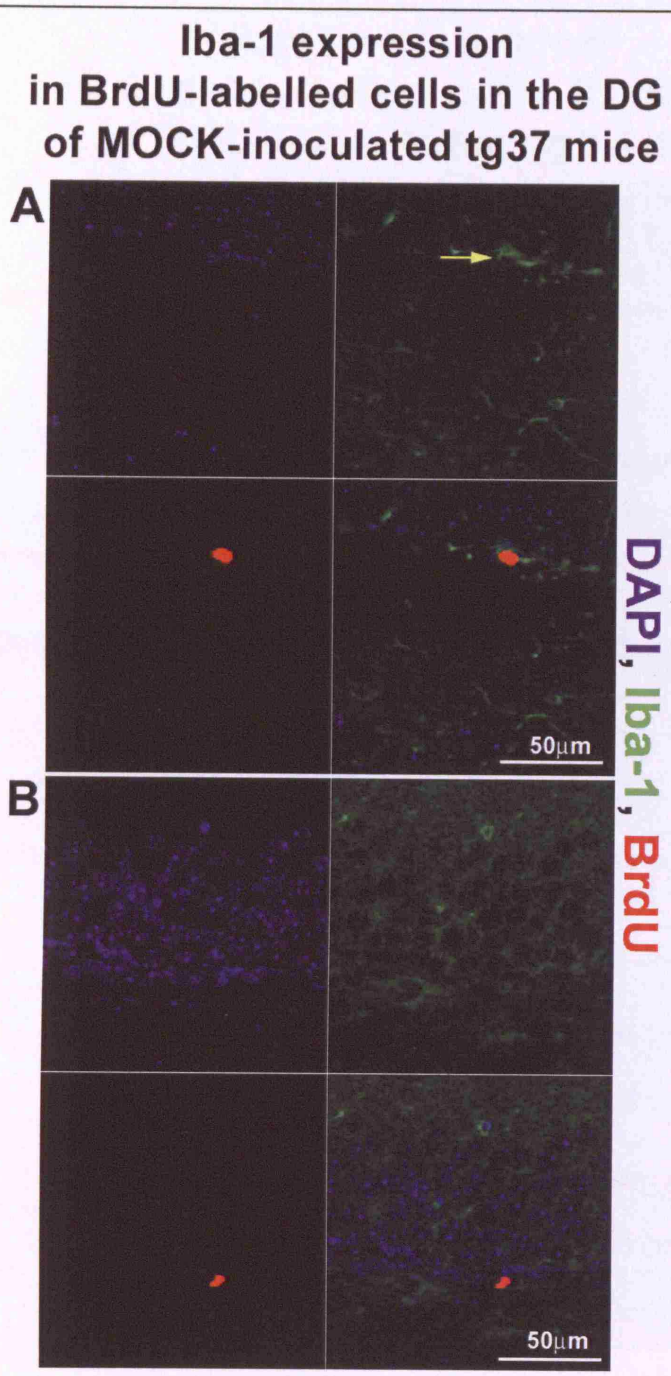

Figure 39: BrdU-labelled cells in the dentate gyrus of mock-inoculated tg37 mice are positive (arrows) or negative for Iba-1 (11 weeks of incubation; 7 days BrdU latency). A) BrdU-labelled cell in the subgranular layer is positive for Iba-1; B) Iba-1 negative BrdU-labelled cell in the subgranular layer.

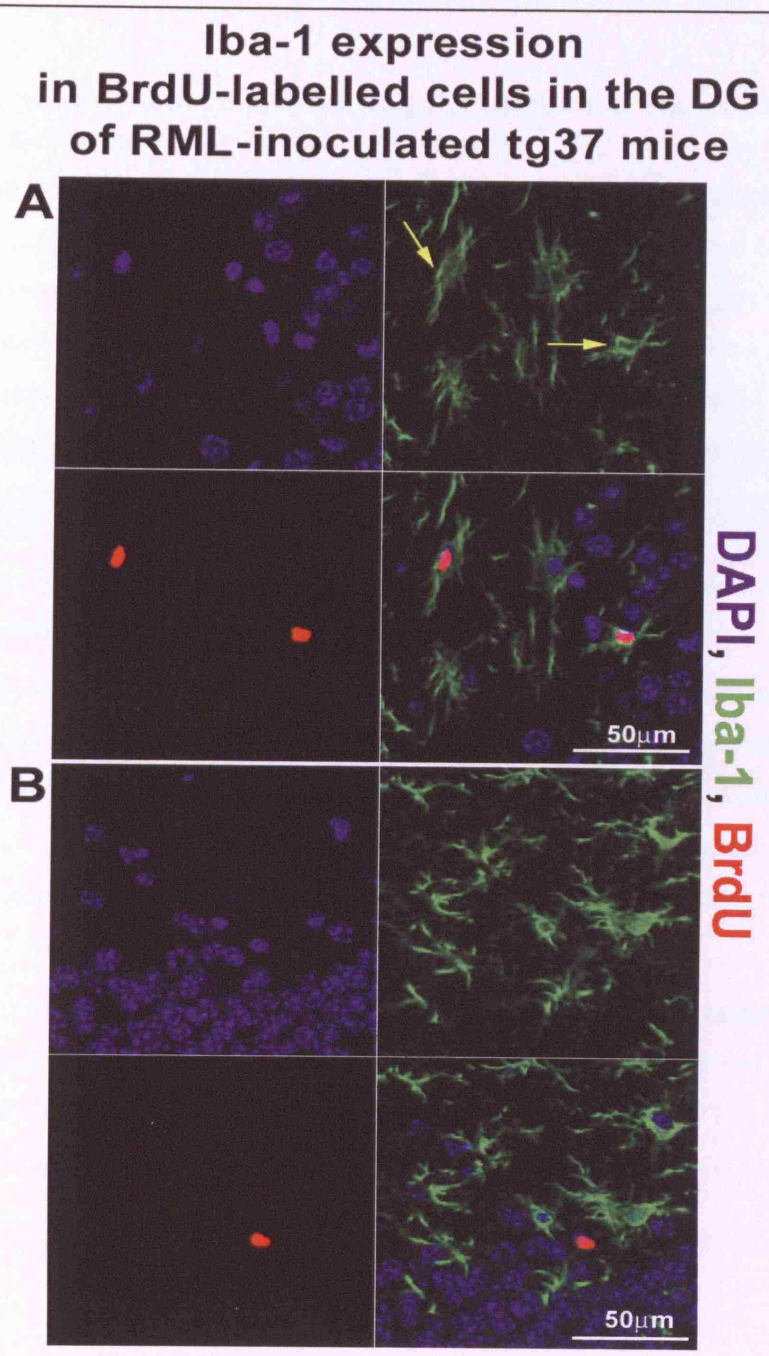

Figure 40: BrdU-labelled cells in the dentate gyrus of RML-inoculated tg37 mice are positive (arrows) or negative for Iba-1 (11 weeks of incubation; 7 days BrdU latency). A) BrdU-labelled cell in the subgranular layer is positive for Iba-1; B) Iba-1 negative BrdU-labelled cell in the subgranular layer.

3.6 Response of neural stem cells following PrP depletion and reversal of clinical prion disease

We investigated the response of neural stem cells, i.e. proliferation and differentiation, following the Cre-mediated depletion of neuronal PrP and the subsequent reversal of clinical prion disease. PrP depletion results in a decrease of cell proliferation in the hippocampus of both RML-inoculated mice and un-inoculated controls. We also found that PrP depletion does not affect the number of β-tubulin expressing cells in the dentate gyrus of prion-infected animals. However, PrP depletion results in a decrease in the numbers of proliferating astroglial and microglial cells in the dentate gyrus of the prion infected mice.

3.6.1 PrP depletion significantly decreases cell proliferation in the hippocampus of both RML-inoculated and un-inoculated mice

We studied NFH-Cre/tg37 transgenic mice. In this mouse model Cre-mediated depletion of neuronal PrP following prion infection results to reversal of neuronal loss and spongiosis, reversal of clinical prion disease and subsequent survival. We examined RML-inoculated mice after PrP depletion at 12, 13 and 37 weeks of incubation. 3 animals were analyzed for each time point except the 37 wk where 2 animals were examined. PrP depletion in RML-inoculated mice resulted in a significant decrease of proliferation in the hippocampus (Fig. 41-43).

To assess the net effect of depletion of PrP in cell proliferation we also examined un-inoculated NFH-Cre/tg37 transgenic mice before (9 weeks of age) and after (15 and 22 weeks of age) Cre-mediated PrP depletion. 3 animals were analysed for each time point. The data reveal that loss of PrP leads to a reduction of cell proliferation in the hippocampus (Fig. 44-46).

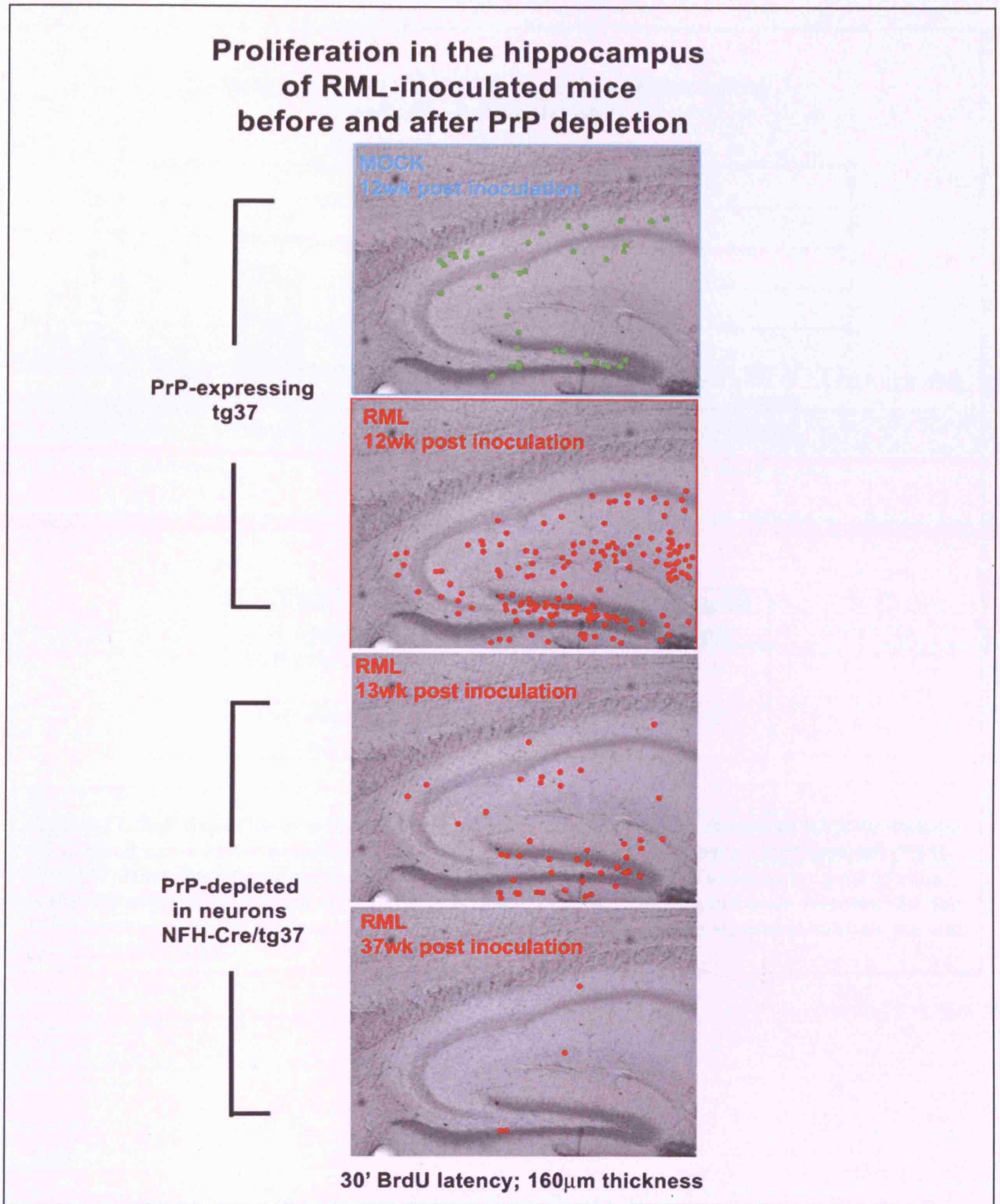

Figure 41: BrdU positive cells (dots) in the hippocampus of tg37 and NFH-Cre/tg37 mice were detected by BrdU/DAB immunostaining and counted. The figure depicts representative counts of mock-inoculated and RML-inoculated tg37 mice and also of RML-inoculated NFH-Cre/tg37 mice after PrP depletion (30' BrdU latency; 160µm thickness). A decrease in the number of BrdU-positive cells is observed in the hippocampus of RML-inoculated tg37 mice after PrP depletion.

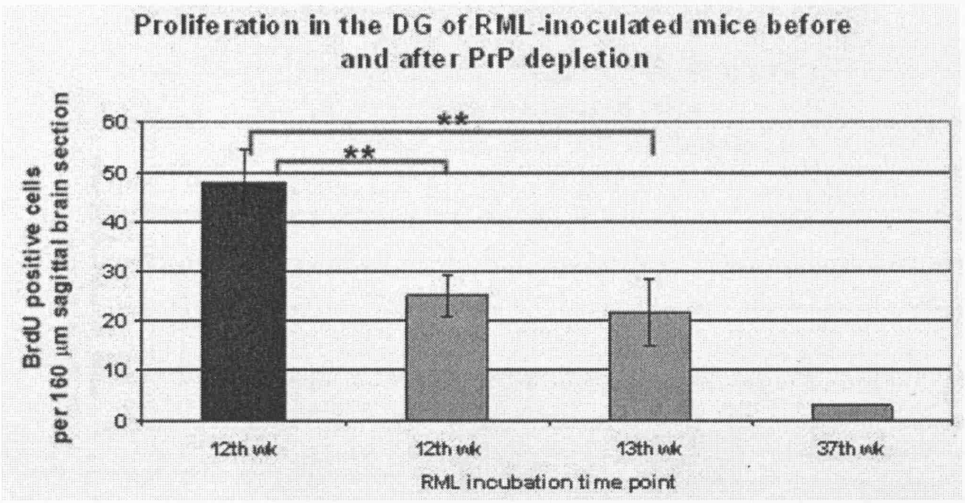

VERSUS (Unpaired)	PrP depleted 12 wk p.i.	PrP depleted 13 wk p.i.
PrP expressing	p=0.0072	p=0.0035
PrP depleted 12 wk inc	--	p=0.4760

Figure 42: PrP depletion results in a decrease of cell proliferation in the DG of RML-inoculated mice; black bar = PrP expressing (tg37) RML-inoculated mice; grey bars = PrP depleted (NFH-Cre/tg37) RML-inoculated mice; The table summarises the statistical analysis for proliferation in the DG of RML inoculated mice before and after PrP depletion. 2 mice were examined for the 37 wk time point for which standard deviation was not calculated and statistical analysis was not applicable. **≤ 0.005

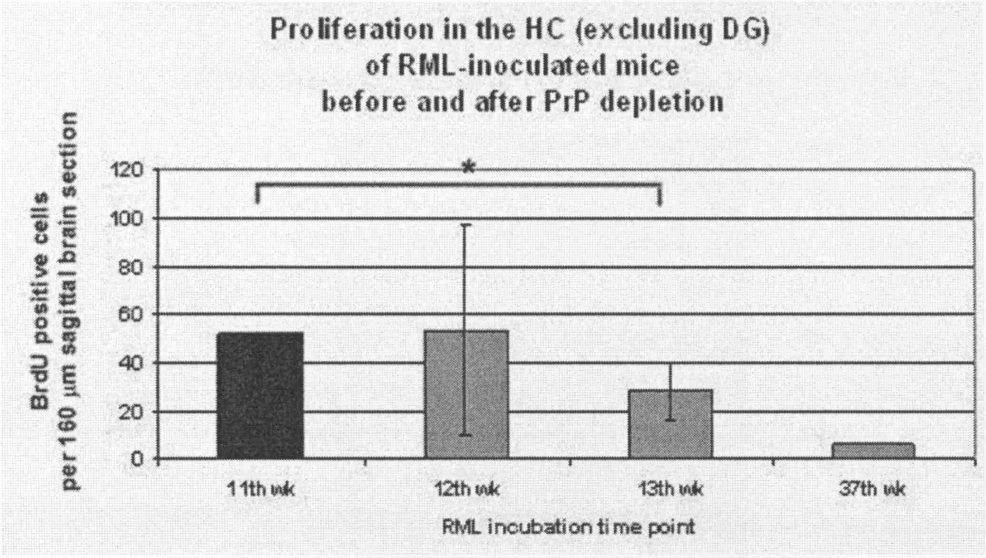

VERSUS (Unpaired)	PrP depleted 12 wk p.i.	PrP depleted 13 wk p.i.
PrP expressing 11 wk p.i.	p=0.96	p=0.03
PrP depleted 12 wk inc	--	p=0.43

Figure 43: PrP depletion results in a decrease of cell proliferation in the hippocampus (excluding DG) of RML-inoculated mice; black bar = PrP expressing (tg37) RML-inoculated mice; grey bars = PrP depleted (NFH-Cre/tg37) RML-inoculated mice; The table summarises the statistical analysis for proliferation in the hippocampus of RML inoculated mice before and after PrP depletion. 2 mice were examined for the 37 wk time point for which standard deviation was not calculated and statistical analysis was not applicable. *≤ 0.05

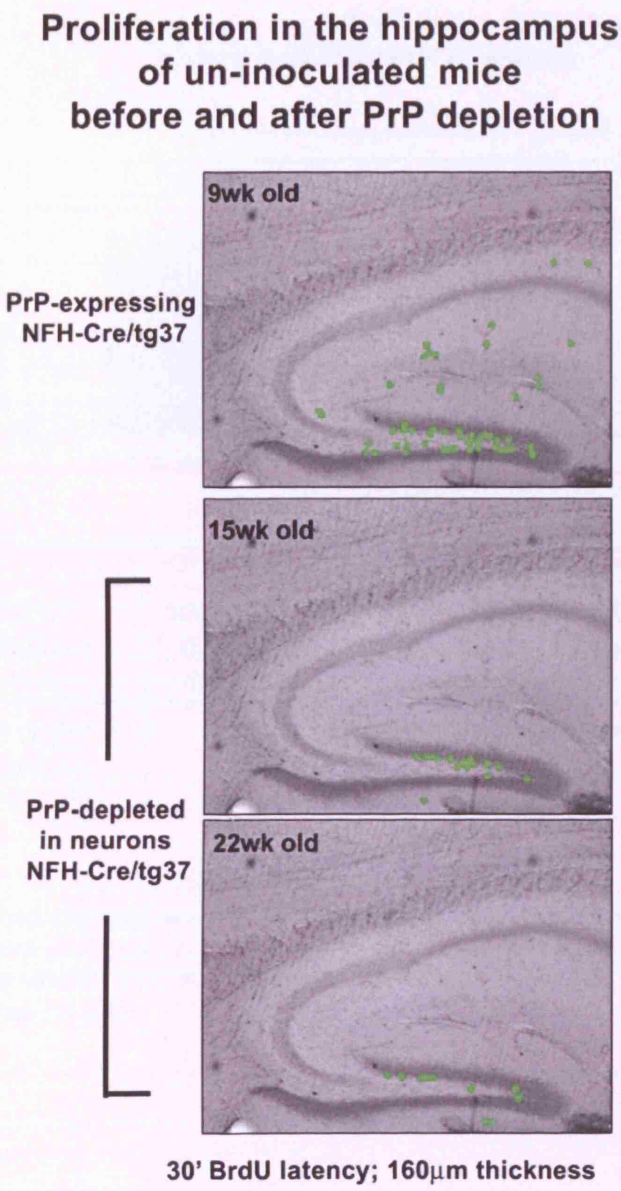

Figure 44: BrdU positive cells (dots) in the hippocampus of NFH-Cre/tg37 mice were detected by BrdU/DAB immunostaining and counted. The figure depicts representative counts of un-inoculated NFH-Cre/tg37 mice before and after PrP depletion (30' BrdU latency; 160μm thickness). A decrease in the number of BrdU-positive cells is observed in the hippocampus of un-inoculated mice after PrP depletion.

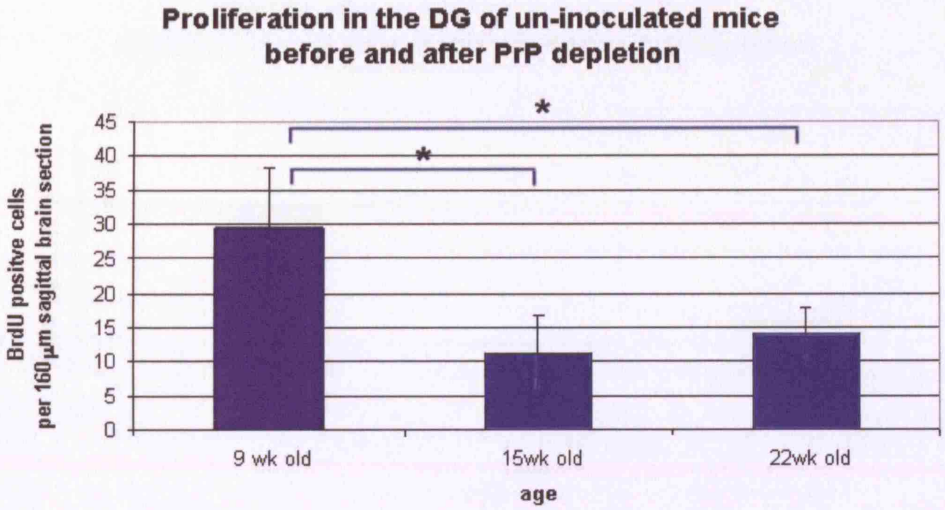

VERSUS (Unpaired t-test)	Before PrP depletion (9 week	After PrP depletion (15 week	After PrP depletion (22 week old)
Before PrP depletion (9 week old)	--	p=0.037	p=0.047

Figure 45: PrP depletion results in decrease of cell proliferation in the DG of un- inoculated NFH-Cre/tg37 mice (dark blue indicates before and light blue after PrP depletion). The table summarises the statistical analysis for proliferation in the DG of un- inoculated mice before and after PrP depletion. *≤ 0.05

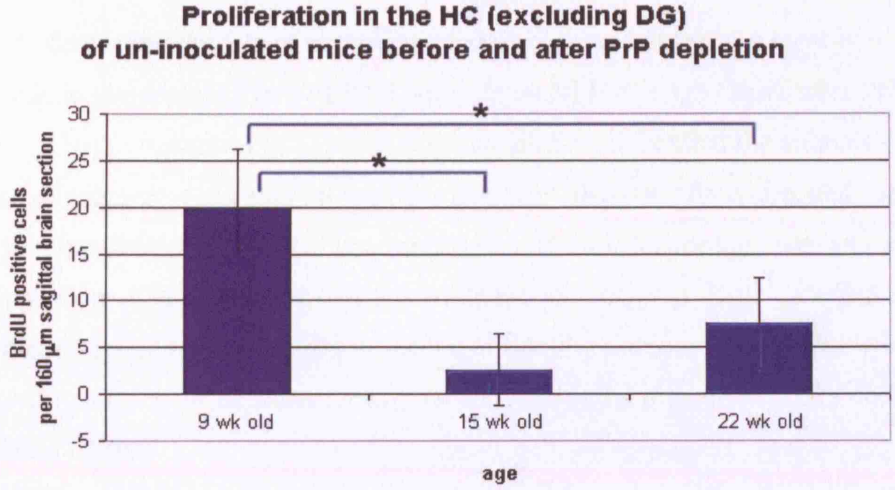

VERSUS (Unpaired ttest)	Before PrP depletion (9 week old)	After PrP depletion (15 week old)	After PrP depletion (22 week old)
Before PrP depletion (9 week old)	--	p=0.02	p=0.058

Figure 46: PrP depletion results in a decrease of cell proliferation in the hippocampus (excluding DG) of un- inoculated NFH-Cre/tg37 mice (dark blue indicates before and light blue after PrP depletion). The table summarises the statistical analysis for proliferation in the DG of un- inoculated mice before and after PrP depletion. *≤ 0.05

3.6.2 Characterisation of BrdU-labelled cells in the dentate gyrus of prion-infected NFH-Cre/tg37 mice

In order to determine the fate of proliferating stem cells and assess the identity of other proliferating cells in the dentate gyrus of RML-inoculated NFH-Cre/tg37 mice after PrP depletion, we performed i.p. BrdU injections at 13 week post inoculation and culled the animals seven days later. We obtained vibratome cut sagittal brain sections and also paraffin-embedded contralateral sagittal brain sections from the brains of examined animals. Neuropathology was assessed by immunostaining of paraffin-embedded sections while the phenotype of BrdU-labelled cells was identified by double-labelling immunofluorescence of floating sections. BrdU-labelled cells were characterised with markers for neuronal, astroglial and microglial phenotypes. Our observations are described in detail below:

3.6.2.1 Neuropathology of prion-infected mice after PrP depletion and reversal of clinical disease

We obtained contralateral paraffin-embedded sections from brains of 3 RML-inoculated NFH-Cre/tg37 mice after PrP depletion at the end of 13wk post inoculation. The sections were examined by staining with haematoxylin and eosin to assess spongiosis. Gliosis was analyzed by immunostainings with the astroglial marker GFAP and the microglial marker Iba-1. PrP^{Sc} accumulation was assessed by immunostaining with the prion protein-specific antibody ICSM35. All neuropathological features of prion disease, including spongiosis, gliosis and PrP^{Sc} accumulation were alleviated compared to prion-infected tg37 mice at 11 and 12 wk post inoculation (Fig 47 for NFH-Cre/tg37 mice and Fig. 28-30 for tg37 mice). Reversal of spongiosis in the hippocampus was verified as 2 out of 3 animals analysed did not exhibit spongiosis, in contrast to prion-infected tg37 mice which, in most cases presented spongiosis of score 2. The third NFH-Cre/tg37 animal showed decreased spongiosis and received a scoring of 1. PrP^{Sc} accumulation was variable ranging from score 1 to 2 and again decreased compared to prion-infected tg37 mice (score 3 for most cases). Microglial activation was reduced to score 1 (score 3 for tg37 mice) and astroglial activation was reduced to score 2 but still remained prominent in the hippocampus (Fig. 47) (table 9)

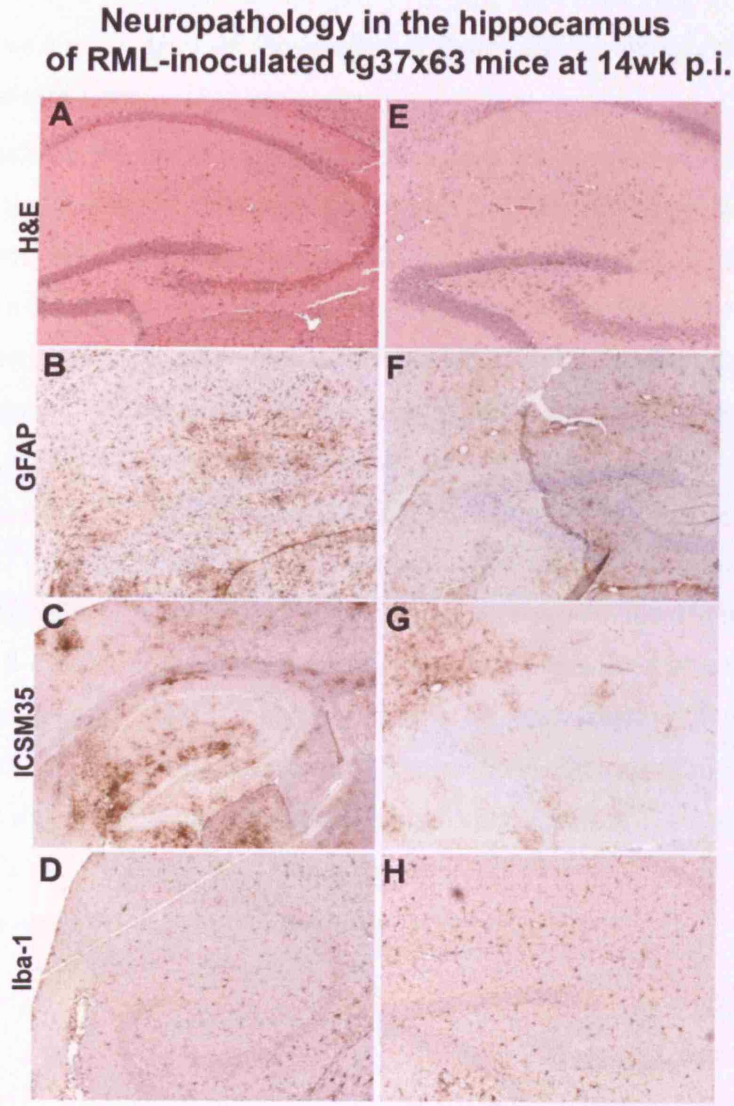

Figure 47: Histological analysis of contralateral sections of brains obtained from prion-infected NFH-Cre/tg37tg37 ater PrP depletion. The figure shows analysis of the hippocampus of two animals at the end of 13 wk post inoculation: images A-D correspond to animal 1 and E-H to animal 2. Alleviation of neuropathological features characteristic of prion disease is represented in both cases. Mouse 1 showed A) no spongiosis (score 0); B) moderate astroglial activation (score 2); C) PrP^{Sc} accumulation (score 2); and D) baseline microglial activation (score 1). Mouse 2 received a low score of 1 for all neuropathological features: E) spongiosis; F) astrogliosis; H) microglial activation; and G) PrP^{Sc} accumulation.

3.6.2.2 PrP depletion has no effect on the number of β-tubulin expressing cells in the dentate gyrus of RML-inoculated mice

In order to determine the fate of proliferating stem cells and assess the identity of other proliferating cells in the dentate gyrus of RML-inoculated NFH-Cre/tg37 mice after PrP depletion, we performed i.p. BrdU injections at 13 wk post inoculation and culled the animals seven days later. The phenotype exhibited by BrdU-labelled cells was assessed by immunostaining of vibratome brain sections. To assess the effect of PrP depletion on the number of proliferating cells expressing β-tubulin in the dentate gyrus of prion-infected mice, we examined mock-inoculated mice expressing PrP, RML-inoculated mice expressing PrP (tg37, 11^{th} week of incubation) and RML-inoculated mice after PrP depletion (NFH-Cre/tg37, 13^{th} week of incubation). We analysed BrdU-labelled cells (7 days BrdU latency) for co-expression of the early neuronal marker β-tubulin, to establish the number of proliferating stem cells or progenitor cells in the dentate gyrus differentiating into a β-tubulin-positive neuronal phenotype. We examined seven 40μm sections obtained from 4 PrP-expressing RML-inoculated animals, six 40μm sections obtained from 3 RML-inoculated animals after PrP depletion, and seven 40μm sections obtained from 3 mock-inoculated animals. The average number of β-tubulin expressing cells per section (i.e. 40μm) was calculated (Fig. 48, 49). The data show that PrP depletion does not affect the number of β-tubulin expressing cells in the dentate gyrus of prion-infected tg37 mice ($p=0.6495$).

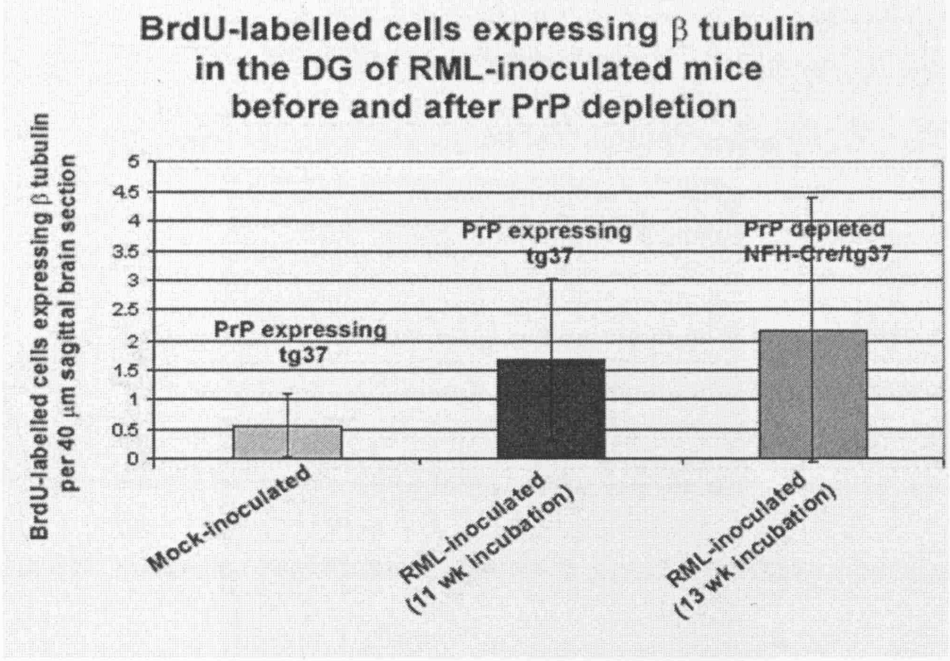

Figure 48: The number of BrdU-labelled cells (7 days BrdU latency) expressing β-tubulin in the dentate gyrus of RML-inoculated mice is not affected by PrP depletion. RML tg37 vs RML NFH-Cre/tg37: p=0.6495; mock tg37 vs RML NFH-Cre/tg37: p=0.09

3.6.2.3 PrP depletion results in a decrease in the number of astrocytes and microglia in the dentate gyrus of RML-inoculated mice

We further assessed the effect of PrP depletion on the number of proliferating cells expressing either GFAP or Iba-1 in the dentate gyrus of RML-inoculated mice. We analysed BrdU-labelled cells (7 days BrdU latency) in 3 groups of mice:

1. In RML-inoculated mice expressing PrP (tg37, 11 week of incubation),
2. In RML-inoculated mice after PrP depletion (NFH-Cre/tg37, 13 week of incubation), and
3. In mock-inoculated mice expressing PrP (tg37).

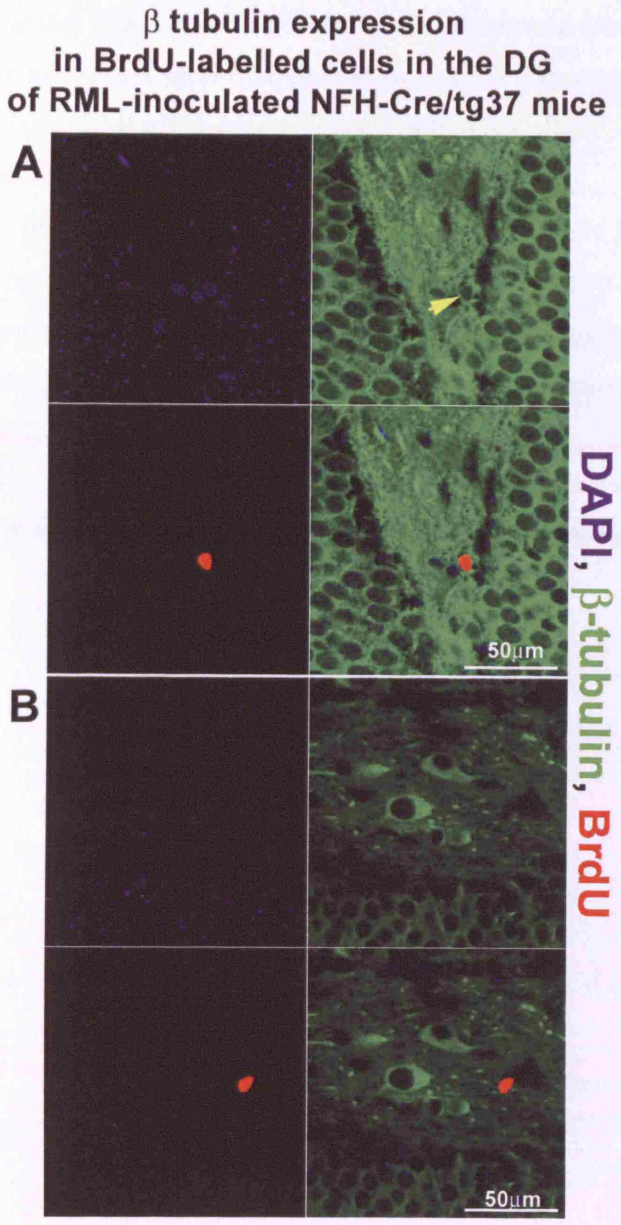

Figure 49: Examples of BrdU-labelled cells in the dentate gyrus of RML-inoculated NFH-Cre/tg37 mice after PrP depletion at 13 week of incubation (7 days BrdU latency). A) a BrdU-labelled cell in the subgranular showing a positive phenotype for β tubulin expression and B) a BrdU-labelled cell in the hilus showing a negative phenotype for β tubulin expression.

We performed BrdU/GFAP double staining on seven sagittal brain sections obtained from 4 PrP expressing RML-inoculated animals, on six 40µm sections obtained from 3 RML-inoculated animals after PrP depletion and on six sections obtained from 4 PrP expressing mock-inoculated mice. The average number of GFAP expressing cells per section (i.e. 40µm) was calculated for each of the three groups (Fig. 50, 51).

We performed BrdU/Iba-1 double staining on eight sections obtained from 4 PrP expressing RML-inoculated animals, on six 40µm sections obtained from 3 RML-inoculated animals after PrP depletion and on seven sections obtained from 4 PrP expressing mock-inoculated animals. The average number of Iba-1 expressing cells per section (i.e. 40µm) was again calculated for each of the three groups (Fig. 52, 53).

The data show that PrP depletion results in a significant decrease in the number of proliferating astrocytes and microglia in the dentate gyrus of prion-infected mice (Fig. 50-53).

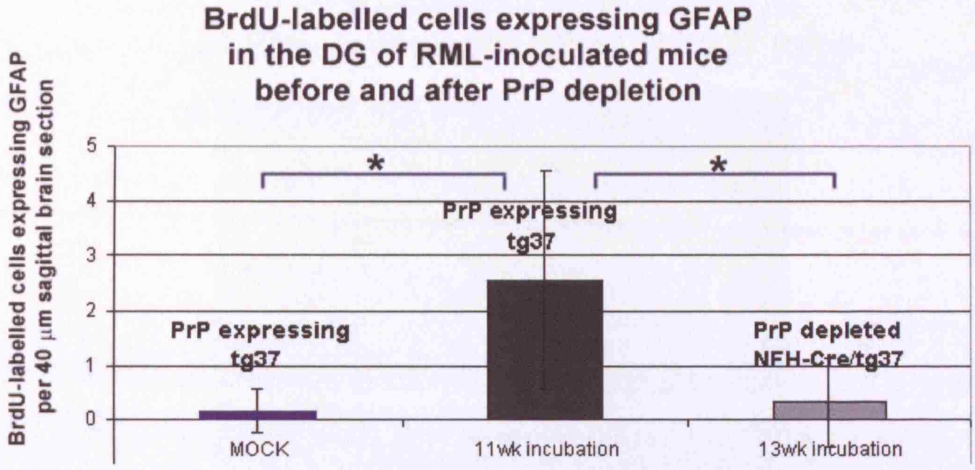

Figure 50: The number of BrdU-labelled cells (7 days BrdU latency) expressing GFAP in the dentate gyrus of RML-inoculated mice is significantly decreased as a result of PrP depletion (P=0.0261). The number of BrdU-labelled cells expressing GFAP is similar for RML-inoculated mice after PrP depletion and PrP expressing mock-inoculated mice (p=0.6643). *≤ 0.05

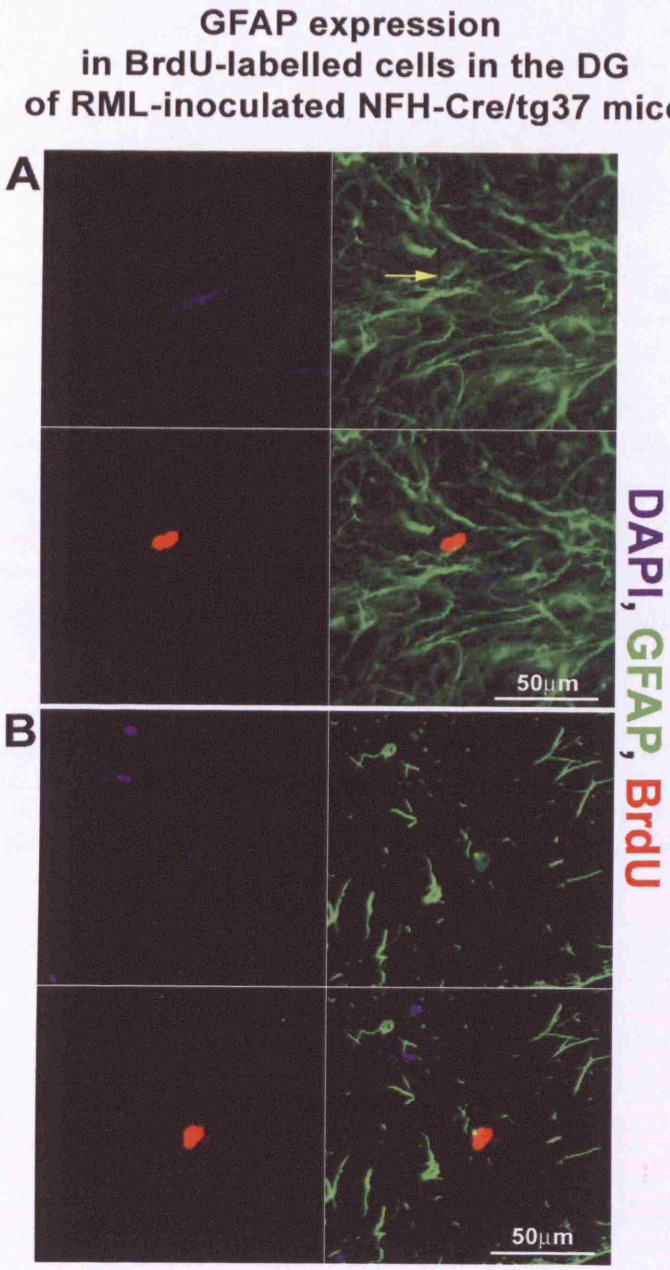

Figure 51: Examples of BrdU-labelled cells in the subgranular layer of the dentate gyrus of RML-inoculated NFH-Cre/tg37 mice after PrP depletion at 13 week of incubation (7 days BrdU latency). A) a BrdU-labelled cell showing a negative phenotype for GFAP expression and B) a BrdU-labelled cell showing a positive phenotype for GFAP expression.

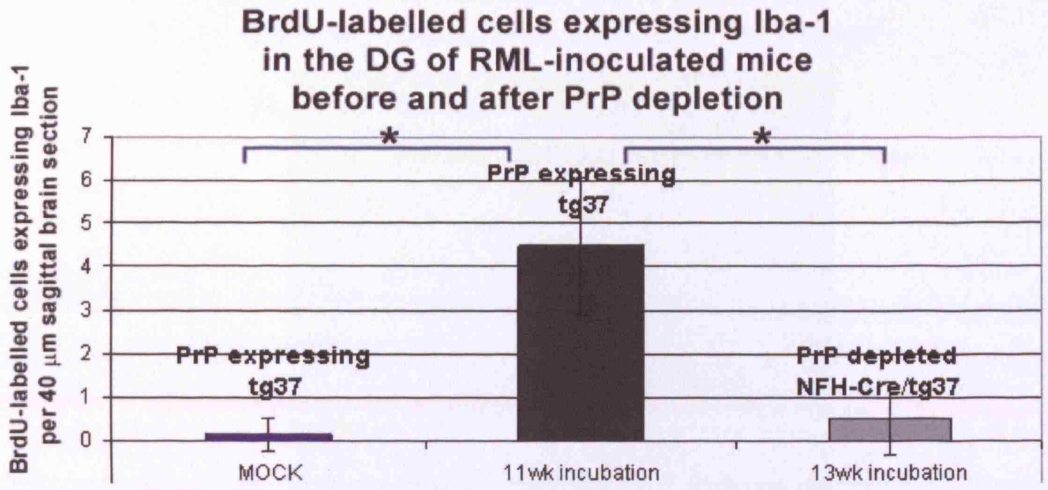

Figure 52: The number of BrdU-labelled cells (7 days BrdU latency) expressing Iba-1 in the dentate gyrus of RML-inoculated mice is significantly decreased as a result of PrP depletion (P=0.0001). The number of BrdU-labelled cells expressing Iba-1 is similar for RML-inoculated mice after PrP depletion and PrP-expressing mock-inoculated mice (p=0.3720). *≤ 0.05

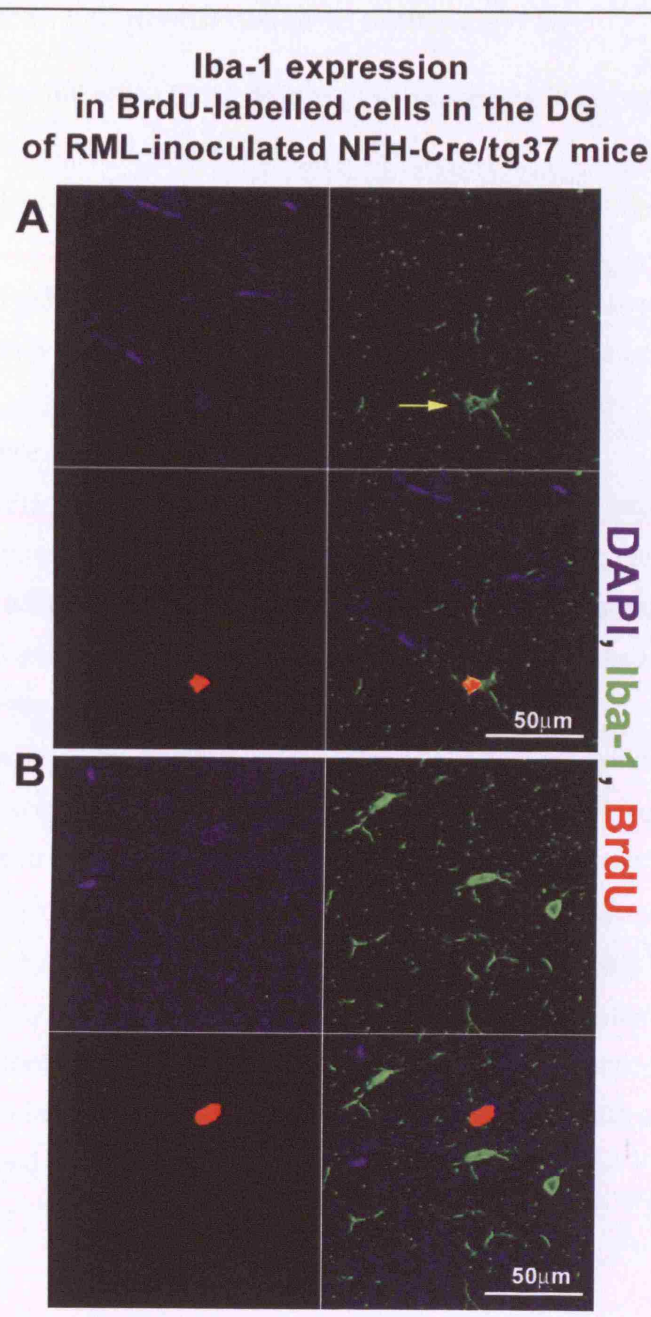

Figure 53: Examples of BrdU-labelled cells in the dentate gyrus of RML-inoculated NFH-Cre/tg37 mice after PrP depletion at 13 week of incubation (7 days BrdU latency). A) one BrdU-labelled cell in the hilus showing a negative phenotype for Iba-1 expression and B) one BrdU-labelled cell in the granular layer showing a positive phenotype for Iba-1 expression.

3.7 The role of PrP in cell proliferation in dentate gyrus

We compared cell proliferation in the dentate gyrus of 4 mouse lines with different expression levels for PrP (all lines were raised in an FVB background):

1. Mock-inoculated wild type mice (single copy of the PrP gene). We examined 8 animals of this group.
2. Mock-inoculated tg37 transgenic mice raised on a PrP null background and which express PrP at 3 times wt level (3 copies of the PrP gene; hemizygous). We examined 4 animals of this group.
3. PrP knock-out mice. We examined 6 animals of this group.
4. Un-inoculated NFH-Cre/tg37 transgenic mice raised on a PrP null background which express PrP at 3 times wt levels (3 copies of the PrP gene; hemizygous). NFH/Cre-mediated depletion of PrP occurs at ~12wk of age. We examined animals before PrP depletion at 9 weeks of age and after PrP depletion at 15 and 22 weeks of age. 3 animals were analyzed from each age group.

For each mouse analysed we counted BrdU positive cells on 4 sequential brain sections (160µm thickness). The average number of BrdU positive cells per 160µm sagittal brain section was determined in the dentate gyrus in each mouse line. We found a decrease in cell proliferation in the absence of PrP expression. However, the statistical analysis of the data reveals that cell proliferation in the dentate gyrus does not significantly differ between mouse lines. Still, cell proliferation is significantly increased in NFH-Cre/tg37 mice over-expressing PrP compared to wild type mice ($p=0.0356$). Moreover in NFH-Cre/tg37 mice there is a significant decrease in cell proliferation after PrP depletion at 15 weeks of age (compared with 9 weeks of age: $p=0.0371$) and 22 weeks of age (compared with 9 weeks of age: $p=0.0476$) [Fig. 54].

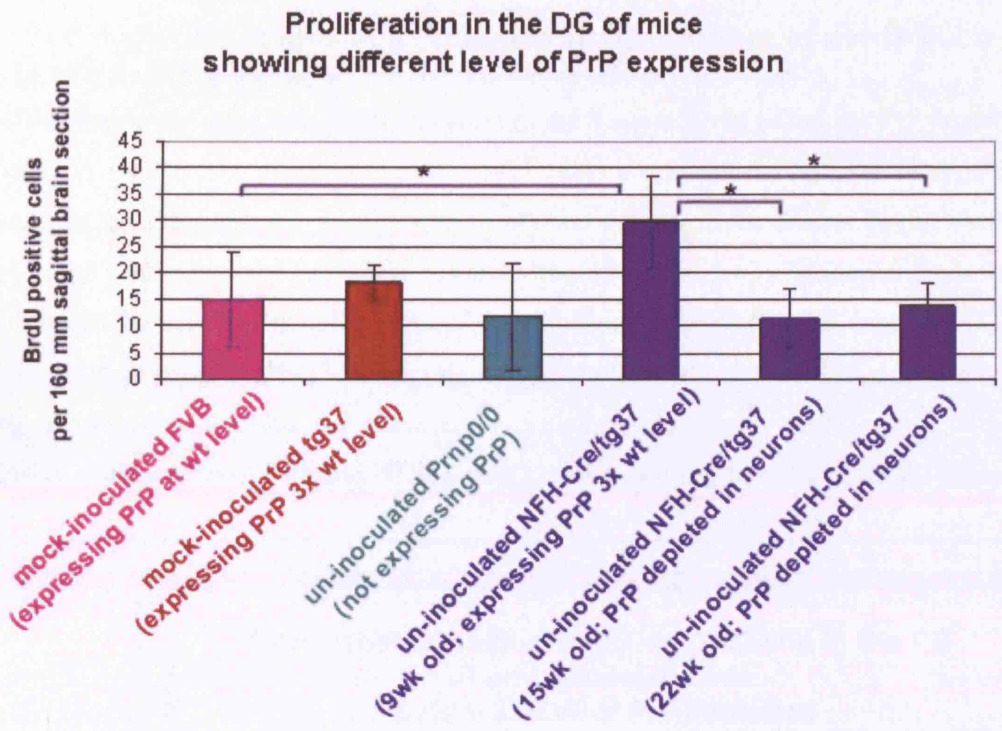

Figure 54: Depletion of PrP in NFH-Cre/tg37 mice results in a significant decrease in cell proliferation in the dentate gyrus. The analysis of different mouse strains reveals a tendency for reduced cell proliferation in the dentate gyrus in the absence of the PrP gene although the statistical analysis does not reveal significance;

- **mock-inoculated wt mice;**
- **mock-inoculated tg37 mice;**
- **un-inoculated PrP knock out mice;**
- **un-inoculated NFH-Cre/tg37 mice at 9, 15 and 22 wk of age in the order they appear on the graph. *≤ 0.05**

3.8 PrP depletion results in a reduction in the number of newly born neurons in the dentate gyrus

We observed a reduction in proliferation in the dentate gyrus following PrP depletion in neurons (Fig. 44-46, 54), which suggests that PrP plays a role in stem cell proliferation *in vivo*. To explore whether PrP depletion affects the rate of neurogenesis in the dentate gyrus, we examined NFH-Cre/tg37 mice before (9wk old, n=2) and after (15wk old, n=3) PrP depletion in neurons. In accordance to the decrease in cell proliferation we observed following PrP depletion (Fig. 44-46), there is a drop in BrdU-labelled cells expressing β tubulin in the dentate gyrus (Fig. 55-57.). This finding suggests that neuronal PrP plays a role in neurogenesis in the dentate gyrus, which is not conclusive as the group of 9wk old NFH-Cre/tg37 we examined consists of only 2 animals.

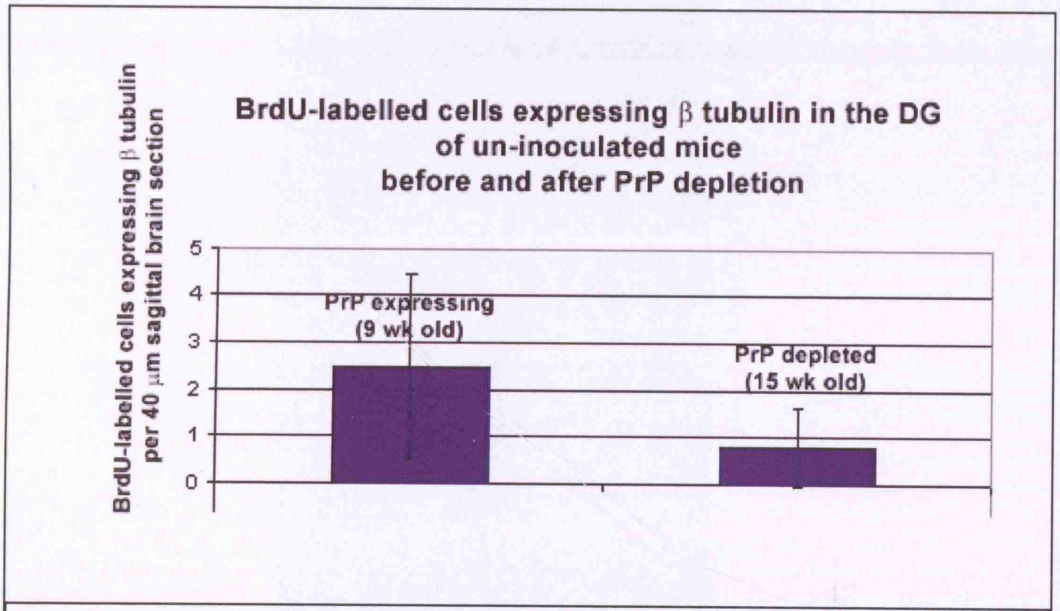

Figure 55: The number of BrdU-labelled cells (7 days BrdU latency) expressing β tubulin in the dentate gyrus is decreased by 65% after PrP depletion in neurons. NFH-Cre/tg37, 9wk old, n=2; NFH-Cre/tg37, 15wk old, n=3).

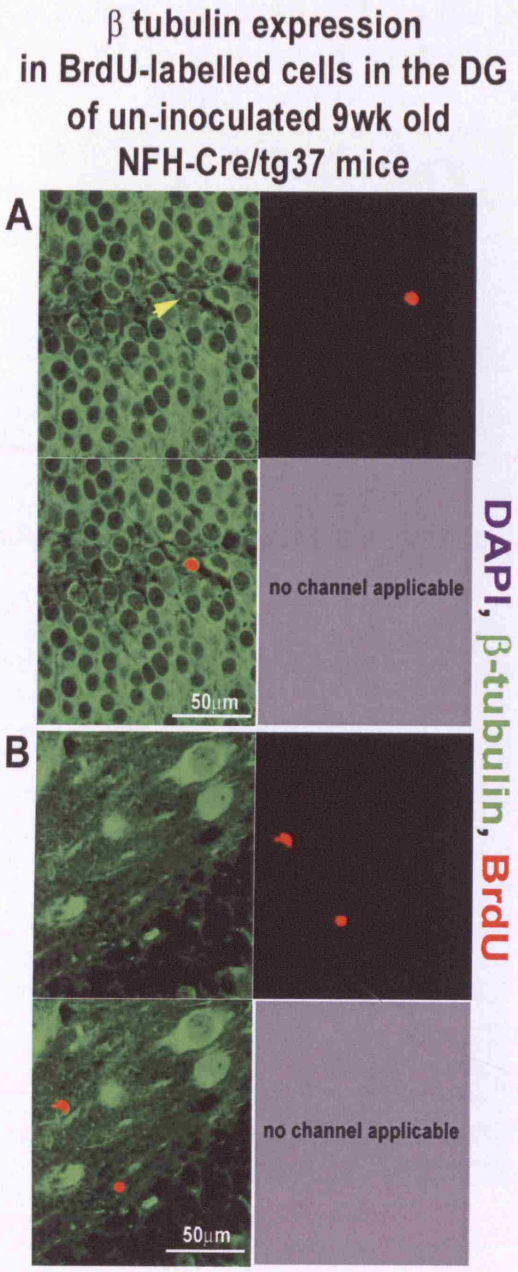

Figure 56: BrdU-labelled cells in the dentate gyrus of un-inoculated 9wk old NFH-Cre/tg37 mice are positive (arrow) or negative for the neuronal marker β-tubulin (9wk old, before PrP depletion; 7 days BrdU latency); A) A BrdU-labelled cell in the granular layer of un-inoculated NFH-Cre/tg37 mice is positive for β-tubulin; B) β-tubulin-negative BrdU-labelled cells in the hilus of un-inoculated NFH-Cre/tg37 mice.

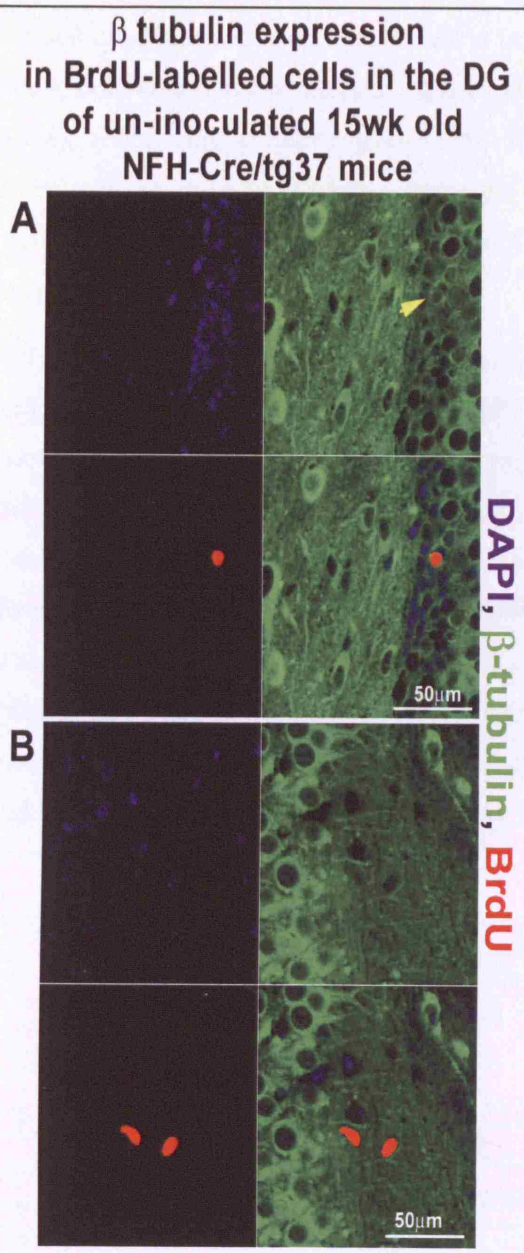

Figure 57: BrdU-labelled cells in the dentate gyrus of un-inoculated 15wk old NFH-Cre/tg37 mice are positive (arrow) or negative for the neuronal marker β-tubulin (15wk old, after PrP depletion; 7 days BrdU latency); A) A BrdU-labelled cell in the subgranular layer of un-inoculated NFH-Cre/tg37 mice is positive for β-tubulin; B) β-tubulin-negative BrdU-labelled cells in the hilus of un-inoculated NFH-Cre/tg37 mice.

3.9 A preliminary study on the role of PrP on stem cell growth

The *in vivo* data we obtained examining stem cell proliferation in the dentate gyrus of NFH-Cre/tg37 mice, showed that the loss of neuronal PrP leads to significant reduction in proliferation in the dentate gyrus (Fig. 44-46, 54). This finding further suggests that PrP plays a role in progenitor proliferation, at least in the dentate gyrus. In order to further assess the role of PrP on stem cell growth *in vitro*, we isolated neural precursors from the hippocampus of wt and $Prnp^{0/0}$ mice and allowed them to grow in culture.

Hippocampi were dissected from 4 mice for each mouse strain. The animals in both groups were of the same sex (females) and age-matched (around 8 weeks old). The isolated cells were initially re-suspended in the same amount of media and growth factors, and subsequently re-suspended in fresh media simultaneously every 3-4 days. 2 weeks after the neurosphere cultures were set up, the cells were passaged: The plate containing the wt cells showed a greater number of neurospheres and therefore its content was split in 2 new wells. By contrast, the $Prnp^{0/0}$ culture contained a lesser number of neurospheres, which were transferred in a new single well. 4 days after passaging, the wt culture exhibited an increased number of neurospheres and cluster of cells compared to the $Prnp^{0/0}$ culture (Fig. 58). Moreover, although the wt culture kept expanding, the $Prnp^{0/0}$ neurospheres remained low in number throughout the study.

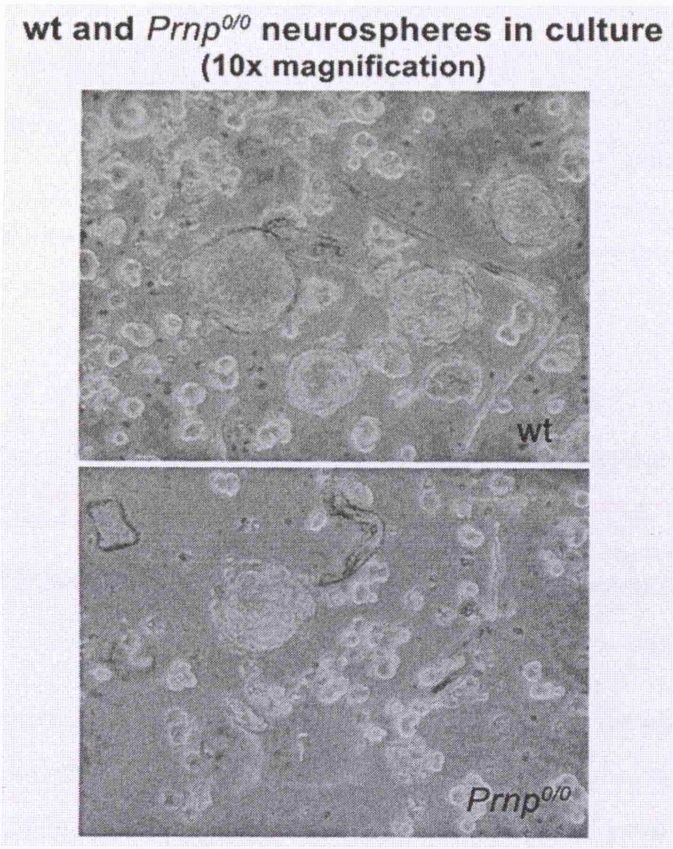

Figure 58: A greater number of neurospheres and cluster of cells is observed throughout the area of the wt stem cell cuture as compared with the *Prnp*$^{0/0}$ culture. The images show a 10x magnified area of the stem cell culture for each mouse strain.

3.10 Prion infection does not result in a significant change in BDNF levels in the hippocampus

Various groups have reported a role for BDNF in neurogenesis. We set up a study to assess whether the stem cell response we observed in the DG of prion-infected tg37 mice was associated with a change in BDNF expression in the hippocampus and whether PrP depletion and reversal of disease (RML-inoculated NFH-Cre/tg37) had an effect in BDNF levels. A preliminary study was carried out to estimate the BDNF levels in the hippocampus of mock- and RML-inoculated mice and also of RML-inoculated NFH-Cre/tg37 mice after PrP depletion. The number and details of mice included in this study are described in the table below:

Group	Mouse strain	Inoculation	Time point	Number of mice examined
Mock-inoculated Tg37	Tg37	mock-inoculated	-	3
RML-inoculated Tg37	Tg37	RML-inoculated	12wk p.i	2
RML-inoculated Tg37	Tg37	RML-inoculated	onset of symptoms	1
RML-inoculated NFH-Cre/tg37	NFH-Cre/tg37	RML-inoculated	after PrP depletion	3

Table 8: Number and treatment of inoculated mice included in the BDNF study.

Each sample was run in triplicate on the BDNF elisa assay and the standard deviation was calculated. For the purpose of this study and for the comparison between mock- and RML-inoculated mice, the value we obtained from a tg37 mouse at onset of symptoms was sampled in the same group as the values from two tg37 mice at 12wk p.i. However, the value of the sample representing onset of symptoms (Fig. 59) is particularly higher than the other values of the same or any other group. In that respect, it would be interesting to investigate further on a possible increase of BDNF at the onset of symptoms, by examining a greater number of samples. As depicted in the graph, the distribution of BDNF values we obtained does not reveal significant differences between the 3 groups (Fig. 59).

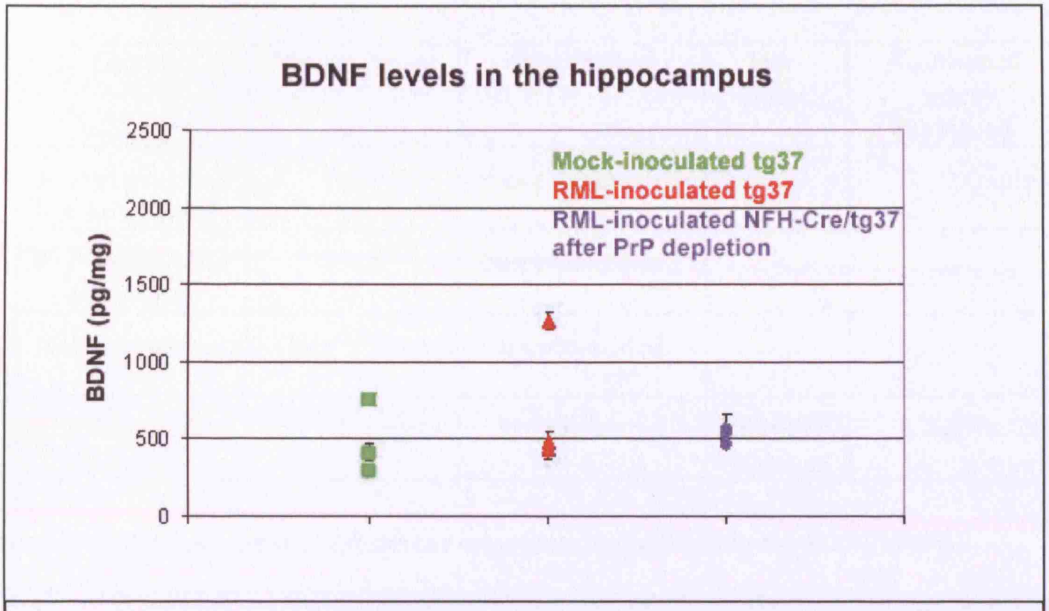

Figure 59: There is no change in BDNF levels as a result of prion infection or upon reversal of clinical prion disease. The BDNF values of mock-, RML-inoculated tg37 mice, and RML-inoculated NFH-Cre/tg37 mice after PrP depletion do not show significant differences.

3.11 Reduced expression of PrP results in decreased BDNF levels in the hippocampus.

Recent reports implicate the prion protein in stem cell proliferation and differentiation, while other studies have highlighted the role of BDNF in neurogenesis. In order to assess whether there is a correlation between BDNF and PrP expression in the neurogenic area of the hippocampus, we examined and compared BDNF expression in mouse strains showing different levels of PrP expression. The mouse strains and numbers we analyzed are detailed in the table below:

Group	Mouse strain	Inoculation	Time point	Number of mice examined
PrP expressing at 3x wt level	Tg37	mock-inoculated	-	3
PrP expressing at wt level	FVB	mock-inoculated	-	3
Not expressing PrP	*Prnp*$^{0/0}$ mice	un-inoculated	-	2
PrP depleted in neurons	NFH-Cre/tg37	un-inoculated	after PrP depletion	2

Table 9: Number and details of different mouse strains included in the BDNF study.

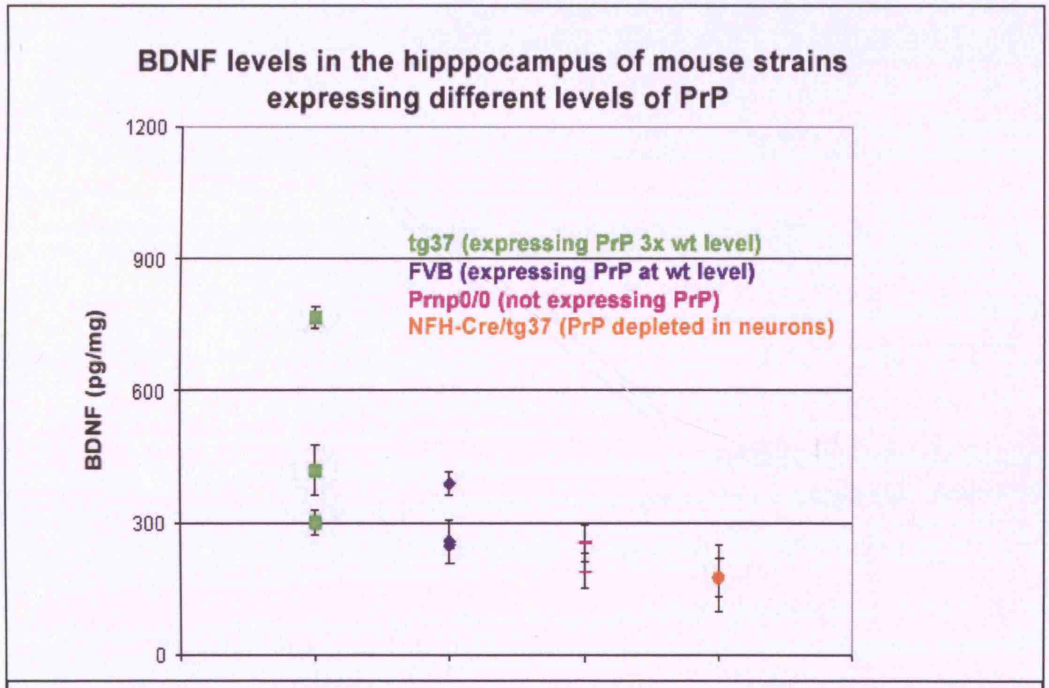

Figure 60: BDNF values drop as PrP expression is decreased. Greater BDNF values are observed in the hippocampus of mice over-expressing PrP and they decrease in PrP knock out mice.

- **Mock-inoculated tg37 mice (expressing PrP 3x wt level);**
- **Mock-inoculated wt FVB mice (expressing PrP at wt level);**
- **Un-inoculated *Prnp*$^{0/0}$ mice;**
- **Un-inoculated NFH-Cre/tg37 mice after neuronal PrP depletion.**

Our data do not show significant differences between different strains. Moreover, as some groups consisted of observations on 2 animals, it was not feasible to calculate a t-test value for significance. However, as illustrated on the graph, a trend was revealed that shows a correlation between PrP and BDNF expression in the hippocampus (Fig. 60). There is a higher level of BDNF expression in mice over-expressing PrP, as compared with PrP knock-out mice (*Prnp*$^{0/0}$), or mice where PrP is depleted in neuronal cells (NFH-Cre/tg37).

4 Discussion

Recent studies show that neural stem cells can be stimulated in response to brain injury. An increase in proliferating stem cells and a subsequent increase in newly formed neurons have been demonstrated in animal models of a wide range of pathological conditions such as stroke/ischemia, epilepsy and demyelination. These observations raise the possibility that neuropathological features, such as neuronal loss, may be involved in mediating a stem cell response, which could occur in a wider range of neurodegenerative disorders. Under this spectrum, we examined stem cell recruitment in prion disease, which is a transmissible, fatal neurodegenerative disease characterised by accumulation of the abnormal form of PrP, by neuronal loss, spongiosis and both astroglial and microglial activation.

The neural stem cell response was assessed by determining cell proliferation and differentiation into neuronal or glial phenotypes. Cell proliferation was determined by BrdU labelling and BrdU immunostaining. To assess differentiation, BrdU positive cells traced within a period of days were co-labelled with markers specific for immature neurons (β-tubulin) and astrocytes (GFAP). Proliferating microglia was identified by the expression of Iba-1 (ionized calcium binding adaptor molecule 1) in BrdU positive cells.

We verified the neuropathology of prion-infected animals, and analysed neural stem cells in prion disease with a particular focus on the dentate gyrus, which is one of the established areas in the adult rodent brain where proliferating stem cells reside. The effect of prion disease on proliferation and differentiation of stem cells was examined in wild type mice and PrP-transgenic tg37 mice that over-express PrP and show shortened incubation period as well as profound hippocampal degeneration. Also, the effect of both Cre-mediated depletion of neuronal PrP and the subsequent reversal of clinical prion disease on stem cell proliferation and differentiation was investigated.

Several studies described a role for PrP in stem cell proliferation and differentiation. In order to study the role of PrP in cell proliferation in the dentate gyrus we studied various mouse strains showing different levels of expression for PrP. Specifically, we examined wild type mice, *Prnp*$^{0/0}$ mice, mice over-expressing PrP and a mouse model of Cre-mediated depletion of neuronal PrP. We further investigated the role of neuronal PrP depletion in differentiation in the dentate gyrus. Finally, we conducted a preliminary *in vitro* study to assess the role of PrP on stem cell growth.

BDNF, a member of the neurotrophic family, is involved in neurogenesis and is downregulated in Huntington's disease. We estimated BDNF expression in prion-infected animals

and correlated our findings with the data we obtained from the study on stem cell proliferation and differentiation. Moreover, we examined BDNF expression in mouse lines expressing different levels of PrP, to assess for a possible association between PrP and BDNF, as both proteins have been shown to play a role in differentiation and/or survival of newly born neurons. Description and interpretation of our data are discussed in detail below.

4.1 Discussion of general parameters related to the design of the study

It has been reported that neurogenesis is influenced by genetic factors (Kempermann et al., 1997) and therefore for the purpose of comparison, all mouse strains included in this study are of identical genetic background. We examined the following mouse strains: wild type FVB, tg37, NFH-Cre/tg37 and $Prnp^{0/0}$. All transgenic mouse lines have been generated in an FVB background and were maintained by serial backcrossing. These mouse strains were more than 10 generations backcrossed as presented in relevant publications (Collinge et.al., 1994; Mallucci et.al., 2002; Mallucci et.al., 2003). All mice used in this study were progeny from these published lines and are at an estimated 30 generations backcrossed against FVB background. Moreover, PrP expression in mouse lines over-expressing PrP (tg37 and NFH-Cre/tg37) has been estimated at 3 times wt level as documented in the relevant references (Mallucci et.al., 2002; Mallucci et.al., 2003). PrP depletion in the majority of neuronal cells of NFH-Cre/tg37 mice has been demonstrated and published (Mallucci et.al., 2002; Mallucci et.al., 2003).

Cell proliferation (including stem cell proliferation) was estimated in the dentate gyrus and separately in the remaining area of the hippocampus. We examined both stem cell proliferation and differentiation in the dentate gyrus which is an established neurogenic niche in the adult brain. However, as proliferating astrocytes and microglia are present in the brain during incubation of prion disease, we analyzed cell proliferation in other areas of the hippocampus as well. Stem cell proliferation was examined by BrdU immunostaining of 4 sequential 40 μm sections for each animal analysed. All groups consisted of at least 3 animals, which is the minimum number that can provide a statistically valid result. For stem cell differentiation, each group included 3-4 animals, from which we obtained and examined by double-labelling immuno-fluorescence a total of 6-8 sections. Our conclusions are drawn from data where statistical analysis was feasible. All other observations are treated and discussed as indications.

Variability was observed within groups in some cases. Although the animals included in the study are age-matched, some groups were of mixed sex and therefore variation may reflect the influence of sex on cell proliferation and/or neurogenesis in the hippocampus. However, great variation was observed in FVB groups which always consisted exclusively of female mice but this cannot be attributed to methodology as the results for tg37 mice did not always present such a variation.

4.2 Prion infection and hippocampal degeneration increases proliferation in the dentate gyrus of mice over-expressing PrP.

A stem cell is defined as a cell capable of proliferation and life-long self-renewal. Stem cells are multipotent i.e. they can give rise to different cell types. Neural stem cells can generate the main classes of neural cell types i.e. astrocytes, oligodendrocytes and neurons. Stem cells can undergo symmetric, proliferative divisions that generate two daughter stem cells or asymmetric, divisions which generate a daughter stem cell plus a more differentiated cell such as progenitor cell or a neuron. Progenitor cells have a more restricted fate and would typically undergo symmetric differentiating divisions to generate two neuroblasts which then give rise to mature neurons, which are terminally differentiated and post-mitotic cells (Chenn and McConnell, 1995; Mione et al., 1997; Miyata et al., 2001; Miyata et al., 2004; Noctor et al., 2001). Proliferating stem cells have been found in specific regions of the adult rodent brain and particularly in the subventricular zone (SVZ) (Luskin, 1993; Quinones-Hinojosa et al., 2006; Lois and Alvarez-Buylla, 1993; Curtis, 2007) and in the subgranular layer (SGL) of the dentate gyrus (Markakis and Gage, 1999; van Praag et al., 2002; Kempermann et al., 2003)

BrdU has been used extensively as a marker for cell proliferation in areas of the brain inhabited by stem cells. Being a thymidine analogue, BrdU becomes incorporated into cells where DNA synthesis occurs and therefore labels not only for proliferation but also of DNA repair and apoptosis. However, quantification of cellular proliferation by BrdU labelling is similar to Ki-67 immuno-staining, another method of detecting dividing cells (Eadie et al., 2005). Ki-67 is expressed in all phases of the cell cycle except the resting phase and is not detectable during DNA repair processes, providing a clear view of cell division. Therefore data that show BrdU to produce patterns of detection similar to Ki-67, support its use as a marker of cell proliferation. Moreover, time course experiments involving co-labelling with immature and mature neuronal markers, reveal

the sequential and progressive maturation of BrdU-labelled cells from neural progenitor cells to terminally differentiated neurons (Brown et al., 2003; Cameron et al., 1993; Kempermann et al., 2003; Lendahl et al., 1990; Palmer et al., 2000; van Praag et al., 2002). These studies represent a strong argument in favor of the use of BrdU for labelling of stem cells and the study of neurogenesis.

Recent studies employing detection with BrdU, have demonstrated stimulation of neural stem cells in response to injury. Labelling with BrdU has revealed an increase in proliferating cells in the SVZ after stroke. Anti-mitotic treatment with the drug cytosine-β-D-arabinofuranoside (Ara-C) reduced this increase of BrdU positive cells (Arvidsson et al., 2002). In addition, it has been shown that seizures cause a dramatic and prolonged increase in cell proliferation in the SGL of the dentate gyrus as assessed again by BrdU labelling and also by immuno-staining for PCNA, a G1 and S-phase cell cycle marker (Parent et al., 1997).

The aim of this project was to examine stem cell proliferation and differentiation in the context of prion disease, a transmissible, neurodegenerative disease featuring gliosis, microglial activation and spongiform degeneration of neurons at a variable degree. We analysed cell proliferation during the incubation of prion disease in the neurogenic area of the hippocampus in both wild type mice and mice over-expressing PrP (tg37 mice). Tg37 mice show a shortened incubation period and profound degeneration in the hippocampal area. We labelled proliferating cells by i.p. administration of BrdU (30 min BrdU latency) at different time points during the incubation of prion disease. At each time point we injected a single dose of 50mg/kg of body weight. BrdU is available for labelling in the adult brain for approximately a 2h period after i.p. injection (Hayes and Nowakowski, 2000). A single dose of BrdU would be sufficient to label cells that are dividing. Neural stem cells are slowly dividing cells and by asymmetric divisions give rise to progenitor cells that divide rapidly but for a limited number of cycles (Morshead et al., 1998). A single BrdU injection is therefore more likely to label proliferating progenitor cells which show a fast turnover rate rather than the relatively quiescent stem cells.

Our data reveal that prion disease affects cell proliferation in the hippocampus differently in wild type and in tg37 transgenic mice. Prion disease results in increased cell proliferation in the dentate gyrus only in tg37 mice but not in wild type mice (Fig. 17, 18, 25, 26). Increased proliferation was observed in other areas of the hippocampus in both mouse strains (Fig. 17, 19, 25, 27). The increase in cell proliferation in the hippocampus probably reflects the increase in the population of activated astrocytes and microglial cells which is a characteristic feature of prion disease (Williams et al., 1997). BrdU-labelled proliferating cells in the dentate gyrus of wt mice

acquired a neuronal phenotype within 8 days (Fig. 21-22), thus confirming that BrdU labelling identifies proliferating progenitor cells, and further that the cell proliferation we estimated in the dentate gyrus partly represents proliferation of neural precursors. The proliferating cells (30 min BrdU latency) that were found to be increased in the dentate gyrus of RML-inoculated tg37 mice could again represent populations of glial cells, as supported by the increase in the number of BrdU positive cells in this area identified as astrocytes and microglia 7 days after labelling with BrdU (Fig. 34-40). Furthermore, the increase in cell proliferation in the neurogenic area of the dentate gyrus suggests an increase in proliferating progenitor cells (neuroblasts) which is strengthened by the finding that the number of newly formed neurons is also increased following prion infection in tg37 mice (Fig. 31-33).

4.3 Prion infection stimulates a stem cell response in the dentate gyrus of PrP-over-expressing tg37 mice

Several studies have demonstrated increase in stem cell-derived neurons in response to brain injury. It has been shown that stroke results in enhanced proliferation of stem cells in the SVZ, followed by the migration of neuroblasts to the site of injury in the striatum where they differentiate into mature neurons within a period of 4 weeks as assessed by the expression of the neuronal marker NeuN (Arvidsson et al., 2002). Furthermore, rodent models of ischemia in the hippocampus have revealed that neurogenesis is increased in the affected areas of the hippocampus. Most studies agree on the time required for BrdU-labelled cells to acquire a mature neuronal phenotype: after the induction of an ischemic insult and within 26-28 days, BrdU-labelled cells in the hippocampus express NeuN, a marker specific of a mature neuronal phenotype (Liu et al., 1998; Nakatomi et al., 2002).

Another type of brain injury associated with increased neurogenesis in the hippocampus is epilepsy. Pilocarpine-induced status epilepticus causes a dramatic and prolonged increase of cell proliferation in the subgranular layer at 3, 6 and 13 days after seizure. BrdU-labelled cells in the granular layer expressed the early neuronal marker β-tubulin within a period of 7 days while within 28 days they showed a more mature neuronal phenotype with the expression of MAP-2 (Parent et al., 1997).

We examined the response of neural stem cells during the progression of prion disease in tg37 mice. Proliferating progenitor cells were labelled with BrdU at a later stage of the disease. In order to assess possible neuronal differentiation within a period of 7 days, BrdU-labelled cells were analysed for the expression of the early neuronal marker β-tubulin.

In keeping with the increase in cell proliferation in prion infected tg37 mice, we observed in the dentate gyrus an increase in the number of proliferating cells acquiring an early neuronal phenotype as identified by β-tubulin expression (Fig. 31-33). Therefore prion disease and the subsequent spongiosis and neuronal loss in tg37 mice seem to elicit a stem cell response towards increased generation of new neurons. These findings suggest that the factors that contribute towards the increase of neurogenesis in the dentate gyrus in the context of prion disease are multiple copies of the PrP gene and /or distinct neurodegeneration in the area of the hippocampus (tg37 mice).

These data imply a neuroprotective role for PrP which has already been proposed by other studies: For example Chiarini and colleagues (Chiarini et al., 2002) have shown that engagement of

retinal neuronal cells by anti-PrP peptide is followed by an increase in intracellular concentration of cAMP and similarly in protein kinase A activity which leads to protection against apoptosis. This effect was not observed in *Prnp*$^{-/-}$ explants incubated with the peptide. The authors emphasized on the neuroprotective effect of antibodies that increase the intracellular concentration of cAMP, which further argues for the role of PrP as a signalling molecule with neuroprotective properties. To this end, a recent study demonstrated that over-expression of PrP^C by adenovirus mediated gene targeting into ischemic rat brain reduced the volume of cerebral infarction (Shyu et al., 2005). Furthermore it has been shown that *Prnp*$^{0/0}$ mice are more susceptible to traumatic brain injury than wild-type animals, by manifesting a significantly larger lesion volume compared to their wt littermates upon injury (Hoshino et al., 2003).

The neuroprotective role of PrP^c has been attributed to the activation of neuroprotective signal transduction pathways and particularly to a direct anti-bax function (Chen et al., 2003; Chiarini et al., 2002). Bax is a member of the Bcl-2 family of proteins that displays pro-apoptotic properties and promotes cell death. The process of apoptosis mediated by Bax involves the release of cytochrome *c,* and other mitochondrial events, such as the breakdown of the mitochondrial membrane potential and the release of pro-apoptotic factors (Daniel et al., 2003). It has further been demonstrated that not only the presence but also over-expression of PrP^c in human primary neurons protects against Bax-mediated apoptosis (Roucou et al., 2004).

Conditions that increase neurogenesis in the adult rodent brain		
Stimulus	*Area of the brain studied*	*Reference*
Environmental enrichment	Hippocampus (*neurogenesis*)	Kempermann, 1997, Nature
Exercise (running)	Dentate gyrus (*neurogenesis*)	Van Praag, 1999, PNAS USA and Nat Neurosci
EAE (Experimental Autoimmune Encephalitis)	SVZ (*cell proliferation*), olfactory Bulb (*neurogenesis*), white matter (*generation of astrocytes and oligodendrocytes*)	Picard-Riera, 2002, PNAS USA
Stroke	SVZ (cell *proliferation*), striatum (*neurogenesis*)	Arvidsson, 2002, Nat Med
Stroke	Dentate gyrus (*neurogenesis*)	Liu, 1998, J Neurosci
Ischemia	Cerebral cortex, striatum (*neurogenesis*)	Jin, 2003, Mol Cell Neurosci
Ischemia	Hippocampus (*neurogenesis*)	Nakatomi, 2002, Cell
Seizures	Dentate gyrus (*neurogenesis*)	Parent, 1997, J Neurosci

Table 10: **Neurogenesis in the adult brain is increased in response to various physiological and pathological stimuli.**

When considering therapeutic approaches, it has to be determined whether the stem cell response observed in prion-infected tg37 mice contributes to brain repair and whether a therapeutic approach for prion disease involving stem cell stimulation may be explored. Firstly, the time necessary under physiological conditions for neuronal differentiation and functional integration of new neurons is 4 weeks while it takes several more months before they differentiate into morphologically mature granule cells (van Praag et al., 2002). It was further demonstrated that the newly formed neurons remained stable in number and in their relative position in the granule cell layer for at least 11 months (Kempermann et al., 2003).

Several studies have shown that under pathological conditions, such as ischemia, neurons are generated within 4 weeks and survive for a period of 6-7 months (Liu et al., 1998; Nakatomi et al., 2002). However although the newly formed neurons were able of receiving synaptic inputs they

have remained immature in morphology and exhibited altered electrophysiological properties even within a period of 3 months after their generation (Nakatomi et al., 2002).

Integration of regenerated neurons is a prerequisite for restoration of brain functions. As the progression of prion disease in tg37 mice is relatively rapid and enhanced stem cell response was only observed at the late stage of the disease, approximately 2-3 weeks before the onset of symptoms, there is probably limited time for the newborn neurons to fully mature and integrate into the circuitry.

Moreover, although not many cell models exist that support prion propagation, it has been shown recently that neural precursors undergoing differentiation were able to replicate prions. Both fetal-derived and adult neural progenitors were kept under conditions that promote differentiation. Their infection with a mouse-adapted prion strain (RML) resulted in de novo production of PrP^{Sc}. Addition of lysates prepared from infected cells to non-infected cultures lead to production of PrP^{Sc} (propagation) by these cells. As differentiated neural precursors were able to propagate prions in vitro (Milhavet et al., 2006), it is possible that adult neural stem cells act as a reservoir for infection and that migration/differentiation of these cells actually contributes to the development of the disease rather than providing brain repair. In that respect transplantation of stem cells in prion disease can prove problematic. However, it has been demonstrated that transplantation of embryonic stem cells derived from PrP-deficient mice at a late stage of incubation resulted in 50% recovery of neuronal loss in the hippocampus. This strategy prevented transplanted cells from becoming infected and showed a remarkable prolongation of neuronal survival without, however, affecting the course of clinical disease or the final outcome as the animals finally succumbed to prion disease. Stem cell transplantation and/or stimulation of endogenous progenitor cells are the subject of intensive research towards the therapy of many neurodegenerative conditions, and may also prove promising for cell replacement in prion disease.

Moreover, the contribution of different cell types in prion propagation can provide insight into the mechanism of prion replication and aggregation and as neural precursor cells have been shown to propagate prions *in vitro* they are an interesting candidate for studying their involvement in the process *in vivo*. For example, the role of stem cells in prion propagation *in vivo* could be explored by selectively inactivating prion protein expression in these cells.

4.4 The double life of an astrocyte

Proliferating cells in the dentate gyrus of both prion- and mock-inoculated mice were labelled with BrdU and analyzed within 7-8 days for the expression of the astrocytic marker GFAP. The presence of activated astrocytes in the brain is a characteristic neuropathological feature of prion disease (Budka et al., 1995). Therefore, the increased cell proliferation in the hippocampus of both prion-infected wild type and tg37 transgenic mice (Fig. 17, 19, 25-27) may partly reflect an increase in proliferating astrocytes. In the dentate gyrus we found proliferating astrocytes (7 days BrdU latency) to be increased in the transgenic tg37 model of prion infection (Fig. 34). We also observed a fraction of BrdU-labelled cells to exhibit an astrocytic phenotype in RML-inoculated wt mice. These BrdU-labelled cells showing an astrocytic phenotype may again demonstrate reactive gliosis. Astrogliosis is a hallmark of prion diseases and occurs early in the course of the disease (DeArmond et al., 1987; Diedrich et al., 1991; Jendroska et al., 1991). As it has been shown that activated astrocytes co-localize with PrP^{Sc} in the brain, it has been proposed that the proliferation of astrocytes may occur in response to PrP^{Sc} rather than in response to neuronal cell death (DeArmond et al., 1987; Mackenzie, 1983; Manuelidis et al., 1987). To investigate the effect of PrP^{Sc} on astrocyte proliferation, in vitro studies examined the response of astrocytes upon addition of the neurotoxic prion protein peptide PrP 106-126. (Hafiz and Brown, 2000; Thellung et al., 2000). This peptide corresponds to the residues 106-126 of the PrP sequence, shows a high tendency to form amyloid fibrils *in vitro*, is partially resistant to proteolysis and induces apoptotic neuronal death in primary cultures of cortical, hippocampal and cerebellar neurons (De Gioia et al., 1994; Forloni et al., 1993; Tagliavini et al., 1993; Jobling et al., 1999; Thellung et al., 2000; Thellung et al., 2002). It has been reported that addition of the PrP 106-126 fragment to astrocyte cultures induces proliferation (Thellung et al., 2000),while other studies claimed that the synergistic action of the PrP106-126 peptide and PrP106-126-induced microglia is necessary for astrocytes to proliferate (Hafiz and Brown, 2000).

Also, BrdU-labelled cells with a GFAP-positive phenotype in the dentate gyrus of prion-infected tg37 mice may otherwise represent progenitor cells restricted to an astroglial fate. Alternatively according to recent data, astrocytes may act themselves as progenitor cells and their increase may signify an increase in neuronal precursors. Astrocytes identified by the expression of GFAP in the brain have been the subject of extensive study towards identifying their neurogenic

potential although their frequent division was initially ascribed to a process of ongoing gliogenesis (Cameron et al., 1993; Palmer et al., 2000).

Several studies have described GFAP-expressing astrocytes as primary progenitors in both the SVZ and the dentate gyrus. These studies were based on anti-mitotic treatments that destroy the rapidly dividing cells including the transient precursors from which neuroblasts originate (Doetsch et al., 1999; Seri et al., 2001). Following the anti-mitotic treatment the number of the remaining proliferating cells identified as astrocytes (B cells) decreased over time to give rise to cells morphologically described as transient precursors (D cells in the SGL of the dentate gyrus and C cells in the SVZ). These data provide evidence that astrocytes act as primary progenitors (B cells) from which transient secondary precursors originate (D cells) (Fig. 61). Secondary precursor D cells were detected in the SGL just after astrocytes divided and before new neurons appeared. The transient precursors of SVZ (C cells) share morphological characteristics with those in the SGL (D cells). They both show dark cytoplasm in contrast to the light cytoplasm of astrocytes and they have dense nuclei. However the D cells observed in the SGL were small compared to SVZ C cells and divided less frequently than C cells which were highly mitotic.

Some SGL astrocytes remained labelled with thymidine analogues after prolonged periods of time which suggested that precursor astrocytes may divide asymmetrically with one daughter cell remaining an astrocyte/precursor while the other committing to a neuronal progeny (Doetsch et al., 1999; Seri et al., 2001).

Astrocytes are considered differentiated cells belonging to the glial lineage and it is therefore intriguing that they may display stem cell properties. Astrocytes provide important structural, metabolic and trophic support to neurons. They interact with endothelial cells to form the blood-brain barrier, absorb neurotransmitters and secrete growth factors and cytokines. They are further involved in the formation and stabilization of synapses and the modulation of synaptic efficacy. As astrocytes contain multiple processes with intermediate filaments rich in GFAP, they are usually detected by the expression of this protein. It may be that a distinct, much less abundant population of GFAP-expressing cells exist, which behave as neural stem cells and co-exist with astrocytes in the germinal zones of the post-natal and adult brain. However, astrocytes in the mitotic studies described above were defined as astrocytes based not only on their GFAP expression but also in their morphology and characteristic astrocytic ultrastructure, including glycogen granules, thick bundles of intermediate filaments (9-10 nm in diameter) and gap junctions. Moreover, recent *in vitro* studies have demonstrated the conversion of mature astrocytes into neural progenitors upon treatment with TGFα. Exposure to TGFα lead to morphological alterations of astrocytes,

reminiscent of the bipolar shape of radial glia, a population of neural progenitors. Moreover, in contrast to un-treated controls, TGFα-treated astrocytes exhibited a strong Olig-2 immunoreactive signal, which is downregulated in mature astrocytes as it inhibits astroglial conversion of neural precursors (Sharif et al., 2006). During development astrocytes are deriving from radial glia, which have neural stem cells properties. It has been proposed that astrocytes may maintain their neurogenic potential because of their derivation from radial glia (Doetsch et al., 1999). In fact, astrocytes are heterogeneous in structure, morphology and function and better markers are required to distinguish the different classes of astrocytes in the adult brain in particular those that can function as stem cells.

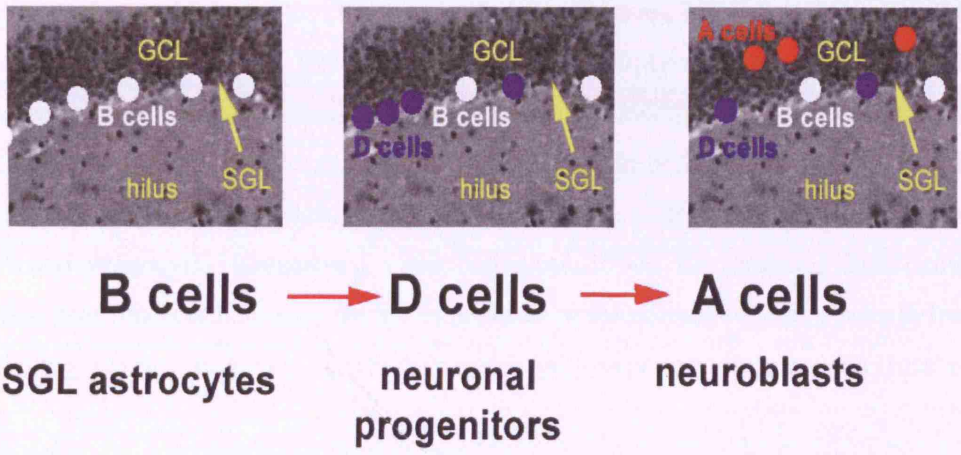

Figure 61: GFAP-expressing astrocytes act as primary progenitors in the subgranular cell layer (SCL) of the dentate gyrus.

The scheme describes the series of events where SGL astrocytes (B cells depicted with white colour) act as slowly dividing primary progenitors that give rise to secondary precursors (D cells depicted with blue colour) which in turn give rise to neuroblasts (A cells depicted with red colour) in the granular cell layer (GCL). (figure design based on Seri et.al., 2001)

Finally, studies have shown that GFAP-positive hippocampal astrocytes facilitate the neuronal fate commitment of adult stem cells (Song et al., 2002), providing the appropriate environment for adult neurogenesis. There was an increase in β-tubulin expressing cells in prion-infected tg37 mice. The abundance of astrocytes in the dentate gyrus of prion-infetced tg37 mice may have played a role in this generation of neurons.

4.5 The role of microglia activation in prion disease remains unclear

The presence of activated microglia as part of an early inflammatory response in prion disease has been reported in various studies (Brown, 2001; Marella et al., 2005; Szpak et al., 2006; Williams et al., 1997; Aoki et al., 1999; Betmouni et al., 1996; Giese et al., 1998; Guiroy et al., 1994; Miyazono et al., 1991). Microglia are derived from monocytes in the bloodstream that enter the brain during embryonic development and differentiate into tissue-resident microglia. Microglia become activated in response to various pathological stimuli, exhibit changes in shape and become locomotive and phagocytic (Kreutzberg, 1996; Nakajima, 1993). We analysed BrdU-labelled cells in mock- and prion-infected animals for the expression of the calcium-binding protein Iba1 (ionized calcium binding adaptor molecule 1), which is restrictedly expressed in microglia (Imai et al., 1996).

We found that prion disease significantly increases proliferating microglial cells in the dentate gyrus of tg37 mice, albeit at an advanced stage of the disease (Fig. 35, 39-40). Proliferating microglia was also detected in the dentate gyrus of RML-inoculated wt mice (Fig. 21, 24). The role of microglia in prion disease has been studied extensively. However our knowledge on the role of microglia in mediating neurodegeneration in prion disease remains limited.

Most reports on human prion diseases show evidence that microglia may be associated with PrP^{Sc} plaques (Betmouni, 1996; Guiroy, 1994; Miyazono, 1991). Animal models of prion disease have provided a clearer picture. Similar to our results, mice infected with scrapie show significant activation of microglia (Betmouni et al., 1996). There is evidence that in mouse models of prion disease microglia activation precedes apoptosis and neuronal death and also precedes clinical manifestation (Betmouni et al., 1996; Giese et al., 1998).

Other studies in mice have shown that following prion infection, PrP deposition was first detected after 30 days and microglial activation after 60 days while apoptosis was present from 75

days post-inoculation (d.p.i.) and peaked in terminally ill animals with almost complete loss of CA1 pyramidal neurons (Williams, 1997). These data suggested that PrP^{Sc} accumulation rather than neuronal loss is responsible for recruitment of microglial cells in prion disease. Further, microglia recruitment was observed in the retina following direct injection of PrP^{Sc} -containing homogenate prepared from prion-infected neuroblastoma line. In the same study they have shown that in culture microglia migrate in response to signals from prion infected neurons and astrocytes. It has been suggested that chemokines released by prion-infected neurons and astrocytes lead the migration of microglia to the vicinity of PrP^{Sc} where they may exert a neurotoxic effect (Marella and Chabry, 2004).

An active role for microglia in removing prion-infected neurons has been demonstrated in tissue culture studies where the extent of neuronal death caused by prions was greatly increased in the presence of microglia (Bate et al., 2001; Brown et al., 1996). In support of these observations large numbers of microglial cells in the brain have been reported in a study of autopsy material from sCJD patients. Microglial cells were identified to be in a homing activation stage. In this stage microglia cells discriminate between degenerating and surviving neurons, and selectively respond to signals from damaged neurons and eliminate them (Szpak et al., 2006).

Moreover, in vitro data provide evidence that soluble factors released by microglia have an effect on neural stem cell migration and further induce the differentiation of both adult and embryonic neural precursors towards a neuronal phenotype (Aarum et al., 2003). Therefore the activated microglia we detected in the dentate gyrus of prion infected tg37 mice may play a role in the generation of new neurons. Indeed, the number of β-tubulin expressing cells is also increased in the tg37 model of prion disease. It has been argued that microglial activation as a common feature of pathological processes may play an important role in directing the replacement of damaged cells in the CNS (Aarum et al., 2003).

4.6 Depletion of neuronal PrP decreases cell proliferation in the hippocampus

Previous studies have shown that depletion of neuronal PrP at a late stage of prion disease rescues neurons and reverses spongiosis and clinical prion disease (Mallucci et al., 2003). We have examined this mouse model to assess the effect of PrP depletion on cell proliferation and differentiation. PrP depletion in this model system occurs between the 8^{th} and 10^{th} week p.i. due to NFH-Cre-mediated recombination. We assessed cell proliferation at 13 weeks post inoculation

(p.i.). To establish the net effect of removal of neuronal PrP on proliferation, we also analyzed cell proliferation in the dentate gyrus of un-inoculated controls before (9 weeks of age) and after (15 and 22 weeks of age) PrP depletion. We have observed that PrP depletion reduces cell proliferation in the hippocampus of both prion-infected mice and controls (Fig. 41-46). However cell proliferation in the hippocampus after PrP depletion remained significantly higher in prion-infected mice compared to un-inoculated controls (inoculated versus un-inoculated mice after PrP depletion: $p=0.02$). These data indicate a role for neuronal PrP in cell proliferation (Chiarini et al., 2002; Kuwahara et al., 1999; Bounhar et al., 2001).

Furthermore, PrP depletion and reversal of clinical disease resulted in a decrease of proliferating astrocytes and microglia in the dentate gyrus (figures 50-53). This reduction in proliferation of astrocytes and microglia may be related to the reduced production of PrP^{Sc} by neurons. Additionally, BrdU-labelled cells (7 days BrdU latency) identified as GFAP-positive astrocytes may act as neural progenitors or may be the product of neural stem cell differentiation. Under this spectrum a decrease of astrocytes may alternatively reflect a decrease in progenitor cells and/or a drop in the number of stem cells directed to an astroglial fate.

Finally, PrP depletion and reversal of neuronal loss did not alter the number of β-tubulin expressing cells in the dentate gyrus (compared to RML-inoculated PrP expressing animals at a late time point during incubation) (Fig. 48-49). It is possible that the time window after PrP depletion was too short for neuronal differentiation to have been affected and examination of later time points would be useful to explore this hypothesis.

4.7 Is there a role for neuronal PrP on cell proliferation in the dentate gyrus?

Recent studies showed that PrP^{c} plays a role on cellular proliferation in the adult DG, indicated by the reduced proliferation in the DG of *Prnp*$^{0/0}$ mice compared to wild type mice and mice over-expressing PrP (Steele et al., 2006). We obtained similar data although the mouse lines included in our work are different from the ones described in the above study. We examined tg37 transgenic mice which express PrP at 3 times wild type levels. Our data suggest reduced cell proliferation in the dentate gyrus in the absence of PrP. More specifically the average proliferation in wt mice is 15 (BrdU positive cells/160μm) and is increased by 22% in PrP-over-expressing tg37 mice while it is reduced by 21% in *Prnp*$^{0/0}$ mice (Fig. 54). However we have observed great variability among samples within the same group and therefore the statistical analysis did not reveal significant differences between groups. However, when we studied NFH-Cre/tg37 mice, which

express PrP at 3 times wt level, we found that cell proliferation in the dentate gyrus was significantly increased by 50% compared to wild type mice (p=0.03) (Fig. 54).

Finally, Cre-mediated neuronal PrP depletion in NFH-Cre/tg37 mice resulted in a significant decrease in cell proliferation in the dentate gyrus by 50-60% (Fig. 44-46, 54). This finding shows that the loss of neuronal PrP reduces cell proliferation in the dentate gyrus and further suggests that neurons, being post-mitotic cells themselves, may be involved in a PrP-dependent mechanism that controls the proliferation of other cell types. Moreover, PrP depletion mediated by NFH expression may also occur in stem cells during their neuronal maturation. In that respect, PrP in stem cells may also play a role in cell proliferation.

4.8 Is there a role for neuronal PrP in neurogenesis in the dentate gyrus?

Our data on cell proliferation revealed a reduction in proliferation in the dentate gyrus in response to neuronal PrP depletion. This finding further suggests that PrP depletion results in a decrease in progenitor proliferation in the known neurogenic area of the dentate gyrus. We next investigated on the effect of neuronal PrP depletion on neuronal differentiation in the dentate gyrus. We estimated the number of BrdU-labelled cells acquiring a neuronal, β tubulin-positive phenotype in the dentate gyrus of NFH-Cre/tg37 mice before (9 wk old) and after (15 wk old) PrP depletion. Although not conclusive, because of the lack of sufficient number of mice examined, the data we collected indicate that depletion of neuronal PrP results in reduction of newly formed neurons in the dentate gyrus (Fig. 55-57). Our findings contradict recently published data that failed to demonstrate an involvement of cellular PrP on neurogenesis in the dentate gyrus when comparing wt mice with $Prnp^{0/0}$ mice (Steele, 2006). However, we studied a transgenic model of neuronal PrP depletion rather than $Prnp^{0/0}$ mice where PrP is constitutively knocked-out. Our data, therefore, suggest that neuronal PrP in specific may promote neuronal differentiation as its loss results in inhibition of neurogenesis. Moreover, PrP depletion mediated by NFH expression may also occur in stem cells during their neuronal maturation. Depletion of PrP upon NFH expression results in a decrease in the rate of neurogenesis, suggesting that stem cell PrP may also be involved in the differentiation process. To this end, recent studies demonstrated an increase in the expression of PrP in differentiated neurons (Steele, 2006).

Furthermore, the physiological role of PrP remains elusive as PrP knock out mice develop physiologically, and only mild abnormalities have been reported in mice without PrP expression. It may be that in the absence of prion protein another molecule/mechanism acts as a substitute. A

system, such as NFH-Cre/tg37 mice, where prion protein expression is disrupted may uncover more about its physiological function, by revealing the effects of its abrupt loss. Finally, as we studied conditional PrP depletion in mice over-expressing PrP, we have to consider the possibility that the loss of over-expression of PrP may have an exaggerated effect on neurogenesis.

4.9 A preliminary study provides indication that PrP plays a role in stem cell growth

In follow up of our finding that PrP depletion in neurons results in reduced proliferation in the dentate gyrus (Fig. 39), suggesting that PrP plays a role in progenitor proliferation, we set up a preliminary study to examine the role of PrP on stem cell growth. We established neurosphere cultures of wt and *Prnp*$^{0/0}$ hippocampal neural precursor cells. Our observation that wt precursor cells produce a greater number of neurospheres compared to *Prnp*$^{0/0}$ cells when cultured under the same conditions cannot be conclusive as is derived from a single experiment and does not include any quantification of cell growth (Fig. 58). Moreover, one could argue that the difference in growth rate is due to different number of stem cells been initially isolated from the dissected hippocampi. However, a low number of cells initially isolated from the hippocampus could not explain the sustained inability of *Prnp*$^{0/0}$ cells to grow in culture as the number of neurospheres they produced remained low throughout the 2 months of culture. Although this observation does not provide sufficient justification for the role of PrP on stem cell growth, it indicates that formation of neurospheres and possibly stem cell proliferation is reduced in the absence of PrP. In line with this, recent studies have demonstrated a role of PrP in stem cell proliferation and differentiation. It has been shown that PrP^{c} is expressed in multipotent neural precursors as well as in mature neurons and its expression increases in fully differentiated mature neurons both *in vitro* and *in vivo* (Steele et al., 2006). Also, the rate of differentiation of multipotent neural precursors was increased in mice over-expressing PrP compared to wt or *Prnp*$^{0/0}$ mice. In other experiments, transplantation of HSCs from *Prnp*$^{0/0}$ bone marrow exhibited impaired self-renewal in serial transplantation (Zhang et al., 2006). Finally, NGF (nerve growth factor) which induces differentiation has been shown *in vitro* to activate the *Prnp* promoter. After addition of NGF to PC12 cells, activation of the *Prnp* promoter was analysed using the luciferase reporter system. NGF induces activation of the *Prnp* promoter and subsequently leads to up-regulation of PrP expression through a pathway that involves MEK1 kinase. MEK 1 is an important component of the mitogen-activated protein kinase (MAPK)

signalling pathway, which is the common mechanism regulating cellular processes such as proliferation, differentiation and apoptosis (Zawlik, 2006).

4.10 BDNF levels are not affected by prion infection

Brain-derived neurotrophic factor (BDNF) is a member of the nerve growth factor family of neurotrophins. The involvement of BDNF in neurogenesis has been supported by several studies (Kirschenbaum and Goldman, 1995; Pincus et al., 1998; Lowenstein D.H. et.al., 1996; Carl.W. Cotman, 2002). Moreover, a role for BDNF in neurodegeneration was suggested when it was shown that its expression is downregulated in Huntington's Disease (HD), a fatal neurodegenerative disorder characterized by neuronal loss, and progressive cognitive, psychological, and motor symptoms (Ferrer et al., 2000a; Zuccato et al., 2001; Luthi Carter et al., 2002).

We conducted a study to assess whether the stem cell response we observed in the DG of prion-infected tg37 mice was associated with a change in the BDNF expression in the hippocampus. We estimated BDNF levels in prion-infected and non-infected tg37 mice and also in prion-infected, PrP-depleted NFH-Cre/tg37 mice, where neuronal loss and clinical symptoms are reversed. We did not observe significant differences in BDNF levels between infected and non-infected mice (Fig. 59). To this end, a study that reported on the BDNF levels in the cerebrospinal fluid (CSF) of CJD patients and healthy controls revealed no significant differences (Albrecht et.al., 2006). Moreover, it was found that BDNF expression is regulated by wild type huntingtin protein, which activates BDNF gene transcription by inhibiting the RE1/NRSE silencer element within BDNF promoter II. The mechanism by which wild-type huntingtin protein controls BDNF expression is by retaining the RE1/NRSE-binding protein (REST/NRSF) in the cytoplasm, thus reducing its binding to and activation of the RE1/NRSE silencer element and therefore allowing BDNF gene transcription (Zuccato et al., 2003). There is no evidence of obstruction of this regulation in prion disease and therefore it is reasonable that BDNF levels would not be altered as a result of prion infection.

The variation we observed among samples of the same group (Fig. 53) may be attributed to sex as a factor that determines BDNF expression in the hippocampus. For example, it is well documented that estrogen synthesis and expression of estrogen receptors is sexual dimorphic in the postnatal hippocampus (Davis, A.M. et.al., 1999; Madeira, M.D. et.al., 1991). To this end, all groups of tg37 mice (mock- and RML-inoculated) and the group of RML-inoculated tg37x63 mice consisted of both male and female mice.

4.11 Is there a correlation between BDNF and PrP expression in the hippocampus?

Our data revealed a tendency for reduced proliferation in the DG in the absence of PrP expression (Fig. 54), which is also supported by recent data (Steele et al., 2006). The reduced proliferation in the neurogenic area of the DG may reflect a drop in the proliferation of neuronal precursors. Taking into account that BDNF plays a role in neurogenesis (Kirschenbaum and Goldman, 1995; Pincus et al., 1998; Lowenstein et.al., 1996; Zigova, et.al., 1998; Abdellatif Benraiss et.al., 2001), we assessed whether there is a correlation between PrP and BDNF expression. Therefore, we examined BDNF expression in mouse strains expressing different levels of PrP. We analyzed wt mice, mock-inoculated tg37 mice, which express PrP at 3 times wt levels, and also un-inoculated *Prnp*$^{0/0}$ mice and NFH-Cre/tg37 mice, where PrP is depleted in neurons.

The unpaired t-test was calculated where possible. For example it was not feasible to compare the data of un-inoculated *Prnp*$^{0/0}$ and NFH-Cre/tg37 mice, since both groups consist of two animals. We did not find a significant difference between wt and over-expressing tg37 mice. However, a trend was revealed that showed a correlation between PrP and BDNF expression in the hippocampus (Fig. 60): BDNF expression is increased in mice over-expressing PrP and conversely reduced in PrP knock out mice. Although not conclusive, this observation suggests that the regulation of PrP and BDNF expression in the hippocampus may be interconnected.

5 Conclusions

We have shown that late-stage scrapie stimulates a stem cell response in the dentate gyrus of transgenic mice that over-express the prion protein and exhibit distinct hippocampal degeneration (tg37 mice).

We verified neuropathology in the hippocampus of prion-infected mice, which included little to moderate spongiosis, gliosis and PrP^{Sc} accumulation. We assessed stem cell response in the dentate gyrus by determining cell proliferation and differentiation of stem cells into neuronal and glial phenotypes. There was an increase in proliferating cells in the dentate gyrus of prion infected tg37 mice. Proliferating cells were identified as astrocytes and microglia which may represent reactive gliosis, a characteristic neuropathological feature of prion disease. Alternatively, the detected GFAP-positive astrocytes may be derived from progenitor cells with a pro-astroglial fate. Moreover, the increase in GFAP-expressing cells may reflect an increase in neural precursors as several studies suggest that GFAP-positive cells can function as neuronal precursors in vivo.

We detected a significant increase in β-tubulin expressing cells in the dentate gyrus of tg37 transgenic mice during the progression of prion disease. However, whether the newly formed neurons in prion disease have restorative potential remains to be elucidated. It is noteworthy that the time required for the complete maturation and integration of newborn neurons is several months and the short period of scrapie incubation in the mouse model studied would not permit neurogenesis to be completed.

Finally, our data suggest a role for neuronal PrP in cell proliferation in the dentate gyrus. More specifically, inactivation of PrP expression in neuronal cells during scrapie incubation period and in non-inoculated controls significantly decreases cell proliferation in the dentate gyrus. The reduction in cell proliferation in the dentate gyrus of prion-infected mice following depletion of neuronal PrP is partly reflected by a reduction in the numbers of proliferating astroglial and microglial cells. However, the number of proliferating cells acquiring a neuronal phenotype is unaffected by PrP depletion (and reversal of clinical prion disease) at least at an early time point following PrP depletion.

6 References

Neuropathology. 2000. David Ellison, Seth Love, Harcourt Publishers Limited

Aarum, J., Sandberg, K., Haeberlein, S. L., and Persson, M. A. (2003). Migration and differentiation of neural precursor cells can be directed by microglia. Proc Natl Acad Sci U S A *100*, 15983-15988.

Abdellatif B., Chmielnicki E., Lerner K., Roh D., and Goldman S.A. (2001). Adenoviral Brain-Derived Neurotrophic Factor Induces Both Neostriatal and Olfactory Neuronal Recruitment from Endogenous Progenitor Cells in the Adult Forebrain. The Journal of Neuroscience 21(17): 6718–6731.

Aguzzi, A., and Weissmann, C. (1997). Prion research: the next frontiers. Nature *389*, 795-798.

Aid, T., Kazantseva, A., Piirsoo, M., Palm, K., Timmusk, T. (2007). Mouse and rat BDNF gene structure and expression revisited. J. Neurosci. Res. 85, 525–535.

Altar, C.A., Cai, N., Bliven, T., Juhasz, M., Conner, J.M., Acheson, A.L., Lindsay, R.M.,Wiegand, S.J. (1997). Anterograde transport of brain-derived neurotrophic factor and its role in the brain. Nature 389, 856–860.

Altman, J., and Das, G. D. (1965). Autoradiographic and histological evidence of postnatal hippocampal neurogenesis in rats. J Comp Neurol *124*, 319-335.

Amoureux, M. C., Cunningham, B. A., Edelman, G. M., and Crossin, K. L. (2000). N-CAM binding inhibits the proliferation of hippocampal progenitor cells and promotes their differentiation to a neuronal phenotype. J Neurosci *20*, 3631-3640.

Anderson, R. M., Donnelly, C. A., Ferguson, N. M., Woolhouse, M. E., Watt, C. J., Udy, H. J., MaWhinney, S., Dunstan, S. P., Southwood, T. R., Wilesmith, J. W., *et al.* (1996). Transmission dynamics and epidemiology of BSE in British cattle. Nature *382*, 779-788.

Aoki, T., Kobayashi, K., and Isaki, K. (1999). Microglial and astrocytic change in brains of Creutzfeldt-Jakob disease: an immunocytochemical and quantitative study. Clin Neuropathol *18*, 51-60.

Arvidsson, A., Collin, T., Kirik, D., Kokaia, Z., and Lindvall, O. (2002). Neuronal replacement from endogenous precursors in the adult brain after stroke. Nat Med *8*, 963-970.

Asante, E. A., Linehan, J. M., Desbruslais, M., Joiner, S., Gowland, I., Wood, A. L., Welch, J., Hill, A. F., Lloyd, S. E., Wadsworth, J. D., and Collinge, J. (2002). BSE prions propagate as either variant CJD-like or sporadic CJD-like prion strains in transgenic mice expressing human prion protein. Embo J *21*, 6358-6366.

Ballas, N., Grunseich, C., Lu, D.D., Speh, J.C., Mandel, G. (2005). RESTand its corepressors mediate plasticity of neuronal gene chromatin throughout neurogenesis. Cell 121, 645–657.

Baquet, Z.C., Gorski, J.A., Jones, K.R. (2004). Early striatal dendrite deficits followed by neuron loss with advanced age in the absence of anterograde cortical brain-derived neurotrophic factor. J. Neurosci. 24, 4250–4258.

Barnea, A., and Nottebohm, F. (1994). Seasonal recruitment of hippocampal neurons in adult free-ranging black-capped chickadees. Proc Natl Acad Sci U S A *91*, 11217-11221.

Basler, K., Oesch, B., Scott, M., Westaway, D., Walchli, M., Groth, D. F., McKinley, M. P., Prusiner, S. B., and Weissmann, C. (1986). Scrapie and cellular PrP isoforms are encoded by the same chromosomal gene. Cell *46*, 417-428.

Bate, C., Reid, S., and Williams, A. (2001). Killing of prion-damaged neurones by microglia. Neuroreport *12*, 2589-2594.

Bell JE, Gentleman SM, Ironside JW, McCardle L, Lantos PL, Doey L, Lowe J, Ferguson J, Luthert P, McQuaid S, Allen IV. (1997) Prion protein immunocytochemistry-UK five centre consensus report. Neuropathol Appli Neurobiol 23(1):26-35

Bellinger-Kawahara, C., Cleaver, J. E., Diener, T. O., and Prusiner, S. B. (1987a). Purified scrapie prions resist inactivation by UV irradiation. J Virol *61*, 159-166.

Bellinger-Kawahara, C., Diener, T. O., McKinley, M. P., Groth, D. F., Smith, D. R., and Prusiner, S. B. (1987b). Purified scrapie prions resist inactivation by procedures that hydrolyze, modify, or shear nucleic acids. Virology *160*, 271-274.

Beringue V., Vilette D., Mallinson G., Archer F., Kaisar M., Tayebi M., Jackson G.S., Clarke A.R., Laude H., Collinge J. and Hawke S. (2004). PrP^{Sc} binding antibodies are potent inhibitors of prion replication in cell lines. J. Biol. Chem. 279 (38): 39671–39676

Bernoulli, C., Siegfried, J., Baumgartner, G., Regli, F., Rabinowicz, T., Gajdusek, D. C., and Gibbs, C. J., Jr. (1977). Danger of accidental person-to-person transmission of Creutzfeldt-Jakob disease by surgery. Lancet *1*, 478-479.

Betmouni, S., Perry, V. H., and Gordon, J. L. (1996). Evidence for an early inflammatory response in the central nervous system of mice with scrapie. Neuroscience *74*, 1-5.

Biebl, M., Cooper, C. M., Winkler, J., and Kuhn, H. G. (2000). Analysis of neurogenesis and programmed cell death reveals a self-renewing capacity in the adult rat brain. Neurosci Lett *291*, 17-20.

Binder, D.K., Scharfman, H.E. (2004). Brain-derived neurotrophic factor. Growth Factors 22, 123–131.

Bounhar, Y., Zhang, Y., Goodyer, C. G., and LeBlanc, A. (2001). Prion protein protects human neurons against Bax-mediated apoptosis. J Biol Chem *276*, 39145-39149.

Brown, D. R. (2001). Microglia and prion disease. Microsc Res Tech *54*, 71-80.

Brown, D. R., Schmidt, B., and Kretzschmar, H. A. (1996). Role of microglia and host prion protein in neurotoxicity of a prion protein fragment. Nature *380*, 345-347.

Brown, J. P., Couillard-Despres, S., Cooper-Kuhn, C. M., Winkler, J., Aigner, L., and Kuhn, H. G. (2003). Transient expression of doublecortin during adult neurogenesis. J Comp Neurol *467*, 1-10.

Brown, P., Gibbs, C. J., Jr., Rodgers-Johnson, P., Asher, D. M., Sulima, M. P., Bacote, A., Goldfarb, L. G., and Gajdusek, D. C. (1994). Human spongiform encephalopathy: the National Institutes of Health series of 300 cases of experimentally transmitted disease. Ann Neurol *35*, 513-529.

Bruce, M., Chree, A., McConnell, I., Foster, J., Pearson, G., and Fraser, H. (1994). Transmission of bovine spongiform encephalopathy and scrapie to mice: strain variation and the species barrier. Philos Trans R Soc Lond B Biol Sci *343*, 405-411.

Bruce, M. E., McConnell, I., Fraser, H., and Dickinson, A. G. (1991). The disease characteristics of different strains of scrapie in Sinc congenic mouse lines: implications for the nature of the agent and host control of pathogenesis. J Gen Virol *72 (Pt 3)*, 595-603.

Bruce, M. E., Will, R. G., Ironside, J. W., McConnell, I., Drummond, D., Suttie, A., McCardle, L., Chree, A., Hope, J., Birkett, C., *et al.* (1997). Transmissions to mice indicate that 'new variant' CJD is caused by the BSE agent. Nature *389*, 498-501.

Budka, H., Aguzzi, A., Brown, P., Brucher, J. M., Bugiani, O., Gullotta, F., Haltia, M., Hauw, J. J., Ironside, J. W., Jellinger, K., and et al. (1995). Neuropathological diagnostic criteria for Creutzfeldt-Jakob disease (CJD) and other human spongiform encephalopathies (prion diseases). Brain Pathol *5*, 459-466.

Bueler, H., Aguzzi, A., Sailer, A., Greiner, R. A., Autenried, P., Aguet, M., and Weissmann, C. (1993). Mice devoid of PrP are resistant to scrapie. Cell *73*, 1339-1347.

Bueler, H., Fischer, M., Lang, Y., Bluethmann, H., Lipp, H. P., DeArmond, S. J., Prusiner, S. B., Aguet, M., and Weissmann, C. (1992). Normal development and behaviour of mice lacking the neuronal cell-surface PrP protein. Nature *356*, 577-582.

Bueler, H., Raeber, A., Sailer, A., Fischer, M., Aguzzi, A., and Weissmann, C. (1994). High prion and PrPSc levels but delayed onset of disease in scrapie-inoculated mice heterozygous for a disrupted PrP gene. Mol Med *1*, 19-30.

Burthem, J., Urban, B., Pain, A., and Roberts, D. J. (2001). The normal cellular prion protein is strongly expressed by myeloid dendritic cells. Blood *98*, 3733-3738.

Cameron, H. A., Woolley, C. S., McEwen, B. S., and Gould, E. (1993). Differentiation of newly born neurons and glia in the dentate gyrus of the adult rat. Neuroscience *56*, 337-344.

Chao, M.V. (2003). Neurotrophins and their receptors: a convergence point for many signalling pathways. Nat. Rev. Neurosci. 4, 299–309.

Chapman, J., Brown, P., Goldfarb, L. G., Arlazoroff, A., Gajdusek, D. C., and Korczyn, A. D. (1993). Clinical heterogeneity and unusual presentations of Creutzfeldt-Jakob disease in Jewish patients with the PRNP codon 200 mutation. J Neurol Neurosurg Psychiatry *56*, 1109-1112.

Chen, S., Mange, A., Dong, L., Lehmann, S., and Schachner, M. (2003). Prion protein as trans-interacting partner for neurons is involved in neurite outgrowth and neuronal survival. Mol Cell Neurosci *22*, 227-233.

Chenn, A., and McConnell, S. K. (1995). Cleavage orientation and the asymmetric inheritance of Notch1 immunoreactivity in mammalian neurogenesis. Cell *82*, 631-641.

Chesebro, B. (1999). Prion protein and the transmissible spongiform encephalopathy diseases. Neuron *24*, 503-506.

Chesebro, B. (2003). Introduction to the transmissible spongiform encephalopathies or prion diseases. Br Med Bull *66*, 1-20.

Chiarini, L. B., Freitas, A. R., Zanata, S. M., Brentani, R. R., Martins, V. R., and Linden, R. (2002). Cellular prion protein transduces neuroprotective signals. Embo J *21*, 3317-3326.

Collee, J. G., Bradley, R., and Liberski, P. P. (2006). Variant CJD (vCJD) and bovine spongiform encephalopathy (BSE): 10 and 20 years on: part 2. Folia Neuropathol *44*, 102-110.

Collinge, J. (1999). Variant Creutzfeldt-Jakob disease. Lancet *354*, 317-323.

Collinge, J. (2005). Molecular neurology of prion disease. J Neurol Neurosurg Psychiatry *76*, 906-919.

Collinge, J., Beck, J., Campbell, T., Estibeiro, K., and Will, R. G. (1996a). Prion protein gene analysis in new variant cases of Creutzfeldt-Jakob disease. Lancet *348*, 56.

Collinge, J., Palmer, M. S., Sidle, K. C., Hill, A. F., Gowland, I., Meads, J., Asante, E., Bradley, R., Doey, L. J., and Lantos, P. L. (1995). Unaltered susceptibility to BSE in transgenic mice expressing human prion protein. Nature *378*, 779-783.

Collinge, J., Sidle, K. C., Meads, J., Ironside, J., and Hill, A. F. (1996b). Molecular analysis of prion strain variation and the aetiology of 'new variant' CJD. Nature *383*, 685-690.

Collinge, J., Whitfield, J., McKintosh, E., Beck, J., Mead, S., Thomas, D. J., and Alpers, M. P. (2006). Kuru in the 21st century--an acquired human prion disease with very long incubation periods. Lancet *367*, 2068-2074.

Collinge, J., Whittington, M. A., Sidle, K. C., Smith, C. J., Palmer, M. S., Clarke, A. R., and Jefferys, J. G. (1994). Prion protein is necessary for normal synaptic function. Nature *370*, 295-297.

Cotman C.W., and Berchtold N.C. (2002). Exercise: a behavioural intervention to enhance brain health and plasticity. TRENDS in Neurosciences 25 (6).

Cuille J,.Chelle PL. (1936). Pathologie animal – la maladie dite tremblante du mouton est-elle inoculable? C R Acad Sci (Paris) 203, 1552–4.

Curtis, M. A., Kam, M., Nannmark, U., Anderson, M. F., Axell, M. Z., Wikkelso, C., Holtas, S., van Roon-Mom, W. M., Bjork-Eriksson, T., Nordborg, C., *et al.* (2007). Human neuroblasts migrate to the olfactory bulb via a lateral ventricular extension. Science *315*, 1243-1249.

Daniel, P. T., Schulze-Osthoff, K., Belka, C., and Guner, D. (2003). Guardians of cell death: the Bcl-2 family proteins. Essays Biochem *39*, 73-88.

Davis, A. A., and Temple, S. (1994). A self-renewing multipotential stem cell in embryonic rat cerebral cortex. Nature *372*, 263-266.

De Gioia, L., Selvaggini, C., Ghibaudi, E., Diomede, L., Bugiani, O., Forloni, G., Tagliavini, F., and Salmona, M. (1994). Conformational polymorphism of the amyloidogenic and neurotoxic peptide homologous to residues 106-126 of the prion protein. J Biol Chem *269*, 7859-7862.

DeArmond, S. J., Mobley, W. C., DeMott, D. L., Barry, R. A., Beckstead, J. H., and Prusiner, S. B. (1987). Changes in the localization of brain prion proteins during scrapie infection. Neurology *37*, 1271-1280.

Diedrich, J. F., Bendheim, P. E., Kim, Y. S., Carp, R. I., and Haase, A. T. (1991). Scrapie-associated prion protein accumulates in astrocytes during scrapie infection. Proc Natl Acad Sci U S A *88*, 375-379.

Doetsch, F., Caille, I., Lim, D. A., Garcia-Verdugo, J. M., and Alvarez-Buylla, A. (1999). Subventricular zone astrocytes are neural stem cells in the adult mammalian brain. Cell *97*, 703-716.

Doetsch, F., (2003). A niche for adult neural stem cells. Curr Opin Genet Dev 13(5): 543-550

Doh-ura, K., Tateishi, J., Sasaki, H., Kitamoto, T., and Sakaki, Y. (1989). Pro----leu change at position 102 of prion protein is the most common but not the sole mutation related to Gerstmann-Straussler syndrome. Biochem Biophys Res Commun *163*, 974-979.

Dragatsis, I., Levine, M.S., Zeitlin, S. (2000). Inactivation of Hdh in the brain and testis results in progressive neurodegeneration and sterility in mice. Nat.Genet. 26, 300–306.

Dreyfus CF, Dai X, Lercher LD, Racey BR, Friedman WJ, Black IB. (1999) Expression of neurotrophins in the adult spinal cord in vivo. J Neurosci Res 56:1–7.

Duffy, P., Wolf, J., Collins, G., DeVoe, A. G., Streeten, B., and Cowen, D. (1974). Letter: Possible person-to-person transmission of Creutzfeldt-Jakob disease. N Engl J Med *290*, 692-693.

Eadie, B. D., Redila, V. A., and Christie, B. R. (2005). Voluntary exercise alters the cytoarchitecture of the adult dentate gyrus by increasing cellular proliferation, dendritic complexity, and spine density. J Comp Neurol *486*, 39-47.

Eriksson, P. S., Perfilieva, E., Bjork-Eriksson, T., Alborn, A. M., Nordborg, C., Peterson, D. A., and Gage, F. H. (1998). Neurogenesis in the adult human hippocampus. Nat Med *4*, 1313-1317.

Ferguson, N. M., and Donnelly, C. A. (2003). Assessment of the risk posed by bovine spongiform encephalopathy in cattle in Great Britain and the impact of potential changes to current control measures. Proc Biol Sci *270*, 1579-1584.

Flechsig E, Hegyi I., Leimeroth R., Zuniga A., Rossi D., Cozzio A., Schwarz P., Rulicke T., Gotz J., Aguzzi A. and Weissmann C.. (2003). Expression of truncated PrP targeted to Purkinje cells of PrP knockout mice causes Purkinje cell death and ataxia. The EMBO Journal 22(12), 3095-3101.

Fischer, M., Rulicke, T., Raeber, A., Sailer, A., Moser, M., Oesch, B., Brandner, S., Aguzzi, A., and Weissmann, C. (1996). Prion protein (PrP) with amino-proximal deletions restoring susceptibility of PrP knockout mice to scrapie. Embo J *15*, 1255-1264.

Forloni, G., Angeretti, N., Chiesa, R., Monzani, E., Salmona, M., Bugiani, O., and Tagliavini, F. (1993). Neurotoxicity of a prion protein fragment. Nature *362*, 543-546.

Fradkin, J. E., Schonberger, L. B., Mills, J. L., Gunn, W. J., Piper, J. M., Wysowski, D. K., Thomson, R., Durako, S., and Brown, P. (1991). Creutzfeldt-Jakob disease in pituitary growth hormone recipients in the United States. Jama *265*, 880-884.

Fraser, H., and Dickinson, A. G. (1973). Scrapie in mice. Agent-strain differences in the distribution and intensity of grey matter vacuolation. J Comp Pathol *83*, 29-40.

Fukuda, S. et al. (2003) Two distinct subpopulations of nestin-positive cells in adult mouse dentate gyrus. J. Neurosci. 23, 9357–9366.

Gabizon, R., McKinley, M. P., Groth, D., and Prusiner, S. B. (1988). Immunoaffinity purification and neutralization of scrapie prion infectivity. Proc Natl Acad Sci U S A *85*, 6617-6621.

Gauczynski, S., Peyrin, J. M., Haik, S., Leucht, C., Hundt, C., Rieger, R., Krasemann, S., Deslys, J. P., Dormont, D., Lasmezas, C. I., and Weiss, S. (2001). The 37-kDa/67-kDa laminin receptor acts as the cell-surface receptor for the cellular prion protein. Embo J *20*, 5863-5875.

Kempermann G., Jessberger S., Steiner B. and Kronenberg G.. (2004). Milestones of neuronal development in the adult hippocampus. TRENDS in Neurosciences Vol.27 No.8, 447-452.

Giese, A., Brown, D. R., Groschup, M. H., Feldmann, C., Haist, I., and Kretzschmar, H. A. (1998). Role of microglia in neuronal cell death in prion disease. Brain Pathol *8*, 449-457.

Giese, A., Groschup, M. H., Hess, B., and Kretzschmar, H. A. (1995). Neuronal cell death in scrapie-infected mice is due to apoptosis. Brain Pathol *5*, 213-221.

Gil, J.M., Mohapel, P., Araujo, I.M., Popovic, N., Li, J.Y., Brundin, P., Petersen, A. (2005). Reduced hippocampal neurogenesis in R6/2 transgenic Huntington's disease mice. Neurobiol. Dis. 20, 744–751.

Goldfarb, L. G., Brown, P., Mitrova, E., Cervenakova, L., Goldin, L., Korczyn, A. D., Chapman, J., Galvez, S., Cartier, L., Rubenstein, R., and et al. (1991). Creutzfeldt-Jacob disease associated with the PRNP codon 200Lys mutation: an analysis of 45 families. Eur J Epidemiol *7*, 477-486.

Gould, E., Cameron, H. A., Daniels, D. C., Woolley, C. S., and McEwen, B. S. (1992). Adrenal hormones suppress cell division in the adult rat dentate gyrus. J Neurosci *12*, 3642-3650.

Gray, F., Chretien, F., Adle-Biassette, H., Dorandeu, A., Ereau, T., Delisle, M. B., Kopp, N., Ironside, J. W., and Vital, C. (1999). Neuronal apoptosis in Creutzfeldt-Jakob disease. J Neuropathol Exp Neurol *58*, 321-328.

Grote, H.E., Bull, N.D., Howard, M.L., Van Dellen, A., Blakemore, C., Bartlett, P.F., Hannan, A.J. (2005). Cognitive disorders and neurogenesis deficits in Huntington's disease mice are rescued by fluoxetine. Eur. J. Neurosci. 22, 2081–2088.

Guiroy, D. C., Wakayama, I., Liberski, P. P., and Gajdusek, D. C. (1994). Relationship of microglia and scrapie amyloid-immunoreactive plaques in kuru, Creutzfeldt-Jakob disease and Gerstmann-Straussler syndrome. Acta Neuropathol (Berl) *87*, 526-530.

Guiroy, D. C., Yanagihara, R., and Gajdusek, D. C. (1991). Localization of amyloidogenic proteins and sulfated glycosaminoglycans in nontransmissible and transmissible cerebral amyloidoses. Acta Neuropathol (Berl) *82*, 87-92.

Hafiz, F. B., and Brown, D. R. (2000). A model for the mechanism of astrogliosis in prion disease. Mol Cell Neurosci *16*, 221-232.

Halban, P.A., Irminger, J.C. (1994). Sorting and processing of secretory proteins. Biochem. J. 299, 1–18.

Harper, J. D., and Lansbury, P. T., Jr. (1997). Models of amyloid seeding in Alzheimer's disease and scrapie: mechanistic truths and physiological consequences of the time-dependent solubility of amyloid proteins. Annu Rev Biochem *66*, 385-407.

Harries-Jones, R., Knight, R., Will, R. G., Cousens, S., Smith, P. G., and Matthews, W. B. (1988). Creutzfeldt-Jakob disease in England and Wales, 1980-1984: a case-control study of potential risk factors. J Neurol Neurosurg Psychiatry *51*, 1113-1119.

Hayes, N. L., and Nowakowski, R. S. (2000). Exploiting the dynamics of S-phase tracers in developing brain: interkinetic nuclear migration for cells entering versus leaving the S-phase. Dev Neurosci *22*, 44-55.

Heppner, F. L., Musahl, C., Arrighi, I., Klein, M. A., Rulicke, T., Oesch, B., Zinkernagel, R. M., Kalinke, U., and Aguzzi, A. (2001). Prevention of scrapie pathogenesis by transgenic expression of anti-prion protein antibodies. Science *294*, 178-182.

Hill, A. F., Antoniou, M., and Collinge, J. (1999). Protease-resistant prion protein produced in vitro lacks detectable infectivity. J Gen Virol *80 (Pt 1)*, 11-14.

Hill, A. F., Butterworth, R. J., Joiner, S., Jackson, G., Rossor, M. N., Thomas, D. J., Frosh, A., Tolley, N., Bell, J. E., Spencer, M., *et al.* (1999). Investigation of variant Creutzfeldt-Jakob disease and other human prion diseases with tonsil biopsy samples. Lancet *353*, 183-189.

Hill, A. F., Desbruslais, M., Joiner, S., Sidle, K. C., Gowland, I., Collinge, J., Doey, L. J., and Lantos, P. (1997a). The same prion strain causes vCJD and BSE. Nature *389*, 448-450, 526.

Hill, A. F., Zeidler, M., Ironside, J., and Collinge, J. (1997b). Diagnosis of new variant Creutzfeldt-Jakob disease by tonsil biopsy. Lancet *349*, 99-100.

Hofer, M., Pagliusi, S.R., Hohn, A., Leibrock, J., Barde, Y.A. (1990). Regional istribution of brain-derived neurotrophic factor mRNA in the adult mouse brain. EMBO J. 9, 2459–2464.

Hoshino, S., Inoue, K., Yokoyama, T., Kobayashi, S., Asakura, T., Teramoto, A., and Itohara, S. (2003). Prions prevent brain damage after experimental brain injury: a preliminary report. Acta Neurochir Suppl *86*, 297-299.

Houston, F., Foster, J. D., Chong, A., Hunter, N., and Bostock, C. J. (2000). Transmission of BSE by blood transfusion in sheep. Lancet *356*, 999-1000.

Hsiao, K., Baker, H. F., Crow, T. J., Poulter, M., Owen, F., Terwilliger, J. D., Westaway, D., Ott, J., and Prusiner, S. B. (1989). Linkage of a prion protein missense variant to Gerstmann-Straussler syndrome. Nature *338*, 342-345.

Hsiao, K. K., Groth, D., Scott, M., Yang, S. L., Serban, H., Rapp, D., Foster, D., Torchia, M., Dearmond, S. J., and Prusiner, S. B. (1994). Serial transmission in rodents of neurodegeneration from transgenic mice expressing mutant prion protein. Proc Natl Acad Sci U S A *91*, 9126-9130.

Imai, Y., Ibata, I., Ito, D., Ohsawa, K., and Kohsaka, S. (1996). A novel gene iba1 in the major histocompatibility complex class III region encoding an EF hand protein expressed in a monocytic lineage. Biochem Biophys Res Commun *224*, 855-862.

Ivanova T., Beyer C. (2001). Pre- and postnatal expression of brain-derived neurotrophic factor mRNA/protein and tyrosine protein kinase receptor B mRNA in the mouse hippocampus, Neuroscience Letters 307, 21-24

Jackson, G. S., Beck, J. A., Navarrete, C., Brown, J., Sutton, P. M., Contreras, M., and Collinge, J. (2001). HLA-DQ7 antigen and resistance to variant CJD. Nature *414*, 269-270.

Jendroska, K., Heinzel, F. P., Torchia, M., Stowring, L., Kretzschmar, H. A., Kon, A., Stern, A., Prusiner, S. B., and DeArmond, S. J. (1991). Proteinase-resistant prion protein accumulation in Syrian hamster brain correlates with regional pathology and scrapie infectivity. Neurology *41*, 1482-1490.

Jin, K., Sun, Y., Xie, L., Peel, A., Mao, X. O., Batteur, S., and Greenberg, D. A. (2003). Directed migration of neuronal precursors into the ischemic cerebral cortex and striatum. Mol Cell Neurosci *24*, 171-189.

Joaquín C., Saá P., Hetz C., and Soto C.. (2005) In Vitro Generation of Infectious Scrapie Prions. Cell 121: 195-206.

Jobling, M. F., Stewart, L. R., White, A. R., McLean, C., Friedhuber, A., Maher, F., Beyreuther, K., Masters, C. L., Barrow, C. J., Collins, S. J., and Cappai, R. (1999). The hydrophobic core sequence modulates the neurotoxic and secondary structure properties of the prion peptide 106-126. J Neurochem *73*, 1557-1565.

Johansson, C. B., Momma, S., Clarke, D. L., Risling, M., Lendahl, U., and Frisen, J. (1999). Identification of a neural stem cell in the adult mammalian central nervous system. Cell *96*, 25-34.

Kanaani, J., Prusiner, S. B., Diacovo, J., Baekkeskov, S., and Legname, G. (2005). Recombinant prion protein induces rapid polarization and development of synapses in embryonic rat hippocampal neurons in vitro. J Neurochem *95*, 1373-1386.

Kawamoto Y, Nakamura S, Nakano S, Oka N, Akiguchi I, Kimura J. (1996) Immunohistochemical localization of brain-derived neurotrophic factor in adult rat brain. Neuroscience 74:1209–1226.

Kempermann, G., Gast, D., Kronenberg, G., Yamaguchi, M., and Gage, F. H. (2003). Early determination and long-term persistence of adult-generated new neurons in the hippocampus of mice. Development *130*, 391-399.

Kempermann, G., Kuhn, H. G., and Gage, F. H. (1997a). Genetic influence on neurogenesis in the dentate gyrus of adult mice. Proc Natl Acad Sci U S A *94*, 10409-10414.

Kempermann, G., Kuhn, H. G., and Gage, F. H. (1997b). More hippocampal neurons in adult mice living in an enriched environment. Nature *386*, 493-495.

Kimberlin, R. H., Cole, S., and Walker, C. A. (1987). Pathogenesis of scrapie is faster when infection is intraspinal instead of intracerebral. Microb Pathog *2*, 405-415.

Kimberlin, R. H., and Walker, C. A. (1986). Pathogenesis of scrapie (strain 263K) in hamsters infected intracerebrally, intraperitoneally or intraocularly. J Gen Virol *67 (Pt 2)*, 255-263.

Kimberlin, R. H., and Walker, C. A. (1988). Pathogenesis of experimental scrapie. Ciba Found Symp *135*, 37-62.

Kirschenbaum B, Goldman SA (1995) Brain-derived neurotrophic factor promotes the survival of neurons arising from the adult rat forebrain subependymal zone. Proc Natl Acad Sci USA 92:210–214.

Klamt, F., Dal-Pizzol, F., Conte da Frota, M. J., Walz, R., Andrades, M. E., da Silva, E. G., Brentani, R. R., Izquierdo, I., and Fonseca Moreira, J. C. (2001). Imbalance of antioxidant defense in mice lacking cellular prion protein. Free Radic Biol Med *30*, 1137-1144.

Klein, M. A., Frigg, R., Flechsig, E., Raeber, A. J., Kalinke, U., Bluethmann, H., Bootz, F., Suter, M., Zinkernagel, R. M. & Aguzzi, A. (1997). A crucial role for B cells in neuroinvasive scrapie. Nature (London) 390, 687–690.Kornack, D. R., and Rakic, P. (1999). Continuation of neurogenesis in the hippocampus of the adult macaque monkey. Proc Natl Acad Sci U S A *96*, 5768-5773.

Kretzschmar, H. A., Giese, A., Brown, D. R., Herms, J., Keller, B., Schmidt, B., and Groschup, M. (1997). Cell death in prion disease. J Neural Transm Suppl *50*, 191-210.

Kretzschmar, H. A., Prusiner, S. B., Stowring, L. E., and DeArmond, S. J. (1986). Scrapie prion proteins are synthesized in neurons. Am J Pathol *122*, 1-5.

Kreutzberg, G. W. (1996). Microglia: a sensor for pathological events in the CNS. Trends Neurosci *19*, 312-318.

Kuczius, T., and Groschup, M. H. (1999). Differences in proteinase K resistance and neuronal deposition of abnormal prion proteins characterize bovine spongiform encephalopathy (BSE) and scrapie strains. Mol Med *5*, 406-418.

Kuczius, T., Haist, I., and Groschup, M. H. (1998). Molecular analysis of bovine spongiform encephalopathy and scrapie strain variation. J Infect Dis *178*, 693-699.

Kuhn, H. G., Dickinson-Anson, H., and Gage, F. H. (1996). Neurogenesis in the dentate gyrus of the adult rat: age-related decrease of neuronal progenitor proliferation. J Neurosci *16*, 2027-2033.

Kuwahara, C., Takeuchi, A. M., Nishimura, T., Haraguchi, K., Kubosaki, A., Matsumoto, Y., Saeki, K., Matsumoto, Y., Yokoyama, T., Itohara, S., and Onodera, T. (1999). Prions prevent neuronal cell-line death. Nature *400*, 225-226.

Lasmezas, C. I., Deslys, J. P., Demaimay, R., Adjou, K. T., Lamoury, F., Dormont, D., Robain, O., Ironside, J., and Hauw, J. J. (1996). BSE transmission to macaques. Nature *381*, 743-744.

Lasmezas, C. I., Fournier, J. G., Nouvel, V., Boe, H., Marce, D., Lamoury, F., Kopp, N., Hauw, J. J., Ironside, J., Bruce, M., *et al.* (2001). Adaptation of the bovine spongiform encephalopathy agent to primates and comparison with Creutzfeldt-- Jakob disease: implications for human health. Proc Natl Acad Sci U S A *98*, 4142-4147.

Lazic, S.E., Grote, H., Armstrong, R.J., Blakemore, C., Hannan, A.J., Van Dellen, A., Barker, R.A. (2004). Decreased hippocampal cell proliferation in R6/1 Huntington's mice. Neuroreport 15, 811–813.

Legname Giuseppe, Ilia V. Baskakov, Hoang-Oanh B. Nguyen, Detlev Riesner, Fred E. Cohen, Stephen J. DeArmond, Stanley B. Prusiner. (2004). Synthetic Mammalian Prions. Science 305: 673-6.

Lemaire-Vieille, C., Schulze, T., Podevin-Dimster, V., Follet, J., Bailly, Y., Blanquet-Grossard, F., Decavel, J. P., Heinen, E., and Cesbron, J. Y. (2000). Epithelial and endothelial expression of the green fluorescent protein reporter gene under the control of bovine prion protein (PrP) gene regulatory sequences in transgenic mice. Proc Natl Acad Sci U S A *97*, 5422-5427.

Lendahl, U., Zimmerman, L. B., and McKay, R. D. (1990). CNS stem cells express a new class of intermediate filament protein. Cell *60*, 585-595.

Li, A., Sakaguchi, S., Atarashi, R., Roy, B. C., Nakaoke, R., Arima, K., Okimura, N., Kopacek, J., and Shigematsu, K. (2000). Identification of a novel gene encoding a PrP-like protein expressed as chimeric transcripts fused to PrP exon 1/2 in ataxic mouse line with a disrupted PrP gene. Cell Mol Neurobiol *20*, 553-567.

Lim D.A., Tramontin A.D., Trevejo J.M., Herrera D.G., García-Verdugo J.M., and Alvarez-Buylla A. (2000). Noggin antagonizes BMP signaling to create a niche for adult neurogenesis. Neuron, Vol. 28, 713–726.

Liu, J., Solway, K., Messing, R. O., and Sharp, F. R. (1998). Increased neurogenesis in the dentate gyrus after transient global ischemia in gerbils. J Neurosci *18*, 7768-7778.

Liu, Q.R., Lu, L., Zhu, X.G., Gong, J.P., Shaham, Y., Uhl, G.R. (2006). Rodent BDNF genes, novel promoters, novel splice variants, and regulation by cocaine. Brain Res. 1067, 1–12.

Llewelyn, C. A., Hewitt, P. E., Knight, R. S., Amar, K., Cousens, S., Mackenzie, J., and Will, R. G. (2004). Possible transmission of variant Creutzfeldt-Jakob disease by blood transfusion. Lancet *363*, 417-421.

Lois, C., and Alvarez-Buylla, A. (1993). Proliferating subventricular zone cells in the adult mammalian forebrain can differentiate into neurons and glia. Proc Natl Acad Sci U S A *90*, 2074-2077.

Lowenstein, D.H. and Arsenault, L., The effects of growth factors on the survival and differentiation of cultured dentate gyrus neurons, J. Neurosci., 16 (1996) 1759-1769.

Lu, K., Wang, W., Xie, Z., Wong, B. S., Li, R., Petersen, R. B., Sy, M. S., and Chen, S. G. (2000). Expression and structural characterization of the recombinant human doppel protein. Biochemistry *39*, 13575-13583.

Luskin, M. B. (1993). Restricted proliferation and migration of postnatally generated neurons derived from the forebrain subventricular zone. Neuron *11*, 173-189.

Luthi Carter R, Hanson SA, Strand AD, Bergstrom DA, Chun W, Peters NL, Woods AM, Chan EY, Kooperberg C, Krainc D, Young AB, Tapscott SJ, Olson JM (2002) Dysregulation of gene expression in the R6/2 model of polyglutamine disease: parallel changes in muscle and brain. Hum Mol Genet 11:1911–1926.

Mabbott, N. A., Mackay, F., Minns, F., and Bruce, M. E. (2000). Temporary inactivation of follicular dendritic cells delays neuroinvasion of scrapie. Nat Med *6*, 719-720.

Mabbott, N. A., and MacPherson, G. G. (2006). Prions and their lethal journey to the brain. Nat Rev Microbiol *4*, 201-211.

Mabbott, N. A., Young, J., McConnell, I., and Bruce, M. E. (2003). Follicular dendritic cell dedifferentiation by treatment with an inhibitor of the lymphotoxin pathway dramatically reduces scrapie susceptibility. J Virol *77*, 6845-6854.

Mackenzie, A. (1983). Immunohistochemical demonstration of glial fibrillary acidic protein in scrapie. J Comp Pathol *93*, 251-259.

Mallucci, G., Dickinson, A., Linehan, J., Klohn, P. C., Brandner, S., and Collinge, J. (2003). Depleting neuronal PrP in prion infection prevents disease and reverses spongiosis. Science *302*, 871-874.

Mallucci, G. R., Ratte, S., Asante, E. A., Linehan, J., Gowland, I., Jefferys, J. G., and Collinge, J. (2002). Post-natal knockout of prion protein alters hippocampal CA1 properties, but does not result in neurodegeneration. Embo J *21*, 202-210.

Manson, J. C., Clarke, A. R., Hooper, M. L., Aitchison, L., McConnell, I., and Hope, J. (1994). 129/Ola mice carrying a null mutation in PrP that abolishes mRNA production are developmentally normal. Mol Neurobiol *8*, 121-127.

Manson, J. C., Hope, J., Clarke, A. R., Johnston, A., Black, C., and MacLeod, N. (1995). PrP gene dosage and long term potentiation. Neurodegeneration *4*, 113-114.

Manuelidis, L., Tesin, D. M., Sklaviadis, T., and Manuelidis, E. E. (1987). Astrocyte gene expression in Creutzfeldt-Jakob disease. Proc Natl Acad Sci U S A *84*, 5937-5941.

Marella, M., and Chabry, J. (2004). Neurons and astrocytes respond to prion infection by inducing microglia recruitment. J Neurosci *24*, 620-627.

Marella, M., Gaggioli, C., Batoz, M., Deckert, M., Tartare-Deckert, S., and Chabry, J. (2005). Pathological prion protein exposure switches on neuronal mitogen-activated protein kinase pathway resulting in microglia recruitment. J Biol Chem *280*, 1529-1534.

Markakis, E. A., and Gage, F. H. (1999). Adult-generated neurons in the dentate gyrus send axonal projections to field CA3 and are surrounded by synaptic vesicles. J Comp Neurol *406*, 449-460.

Marsh, R. F., Bessen, R. A., Lehmann, S., and Hartsough, G. R. (1991). Epidemiological and experimental studies on a new incident of transmissible mink encephalopathy. J Gen Virol *72 (Pt 3)*, 589-594.

Marshall Christine A.G., Satoshi O. Suzuki and James E. Goldman. (2003). Gliogenic and neurogenic progenitors of the subventricular zone: who are they, where did they come from, and where are they going? Glia 43:52–61.

Milhavet, O., Casanova, D., Chevallier, N., McKay, R. D., and Lehmann, S. (2006). Neural stem cell model for prion propagation. Stem Cells.

Miller, M. W., Wild, M. A., and Williams, E. S. (1998). Epidemiology of chronic wasting disease in captive Rocky Mountain elk. J Wildl Dis *34*, 532-538.

Ming Guo-li and Song Hongjun. (2005). Adult neurogenesis in the mammalian central nervous system. Annu. Rev. Neurosci. 28:223–50

Mione, M. C., Cavanagh, J. F., Harris, B., and Parnavelas, J. G. (1997). Cell fate specification and symmetrical/asymmetrical divisions in the developing cerebral cortex. J Neurosci *17*, 2018-2029.

Miyata, T., Kawaguchi, A., Okano, H., and Ogawa, M. (2001). Asymmetric inheritance of radial glial fibers by cortical neurons. Neuron *31*, 727-741.

Miyata, T., Kawaguchi, A., Saito, K., Kawano, M., Muto, T., and Ogawa, M. (2004). Asymmetric production of surface-dividing and non-surface-dividing cortical progenitor cells. Development *131*, 3133-3145.

Miyazono, M., Iwaki, T., Kitamoto, T., Kaneko, Y., Doh-ura, K., and Tateishi, J. (1991). A comparative immunohistochemical study of Kuru and senile plaques with a special reference to glial reactions at various stages of amyloid plaque formation. Am J Pathol *139*, 589-598.

Montrasio, F., Frigg, R., Glatzel, M., Klein, M. A., Mackay, F., Aguzzi, A., and Weissmann, C. (2000). Impaired prion replication in spleens of mice lacking functional follicular dendritic cells. Science *288*, 1257-1259.

Montrasio F., Cozzio A., Flechsig E., Rossi D., Klein M.A., Ru¨ licke T., Raeber A.J., Vosshenrich C.A.J., Proft J., Aguzzi A., and Weissmann C. (2001). B lymphocyte-restricted expression of prion protein does not enable prion replication in prion protein knockout mice. PNAS 98(7), 4034–4037.

Moore, R. C., Lee, I. Y., Silverman, G. L., Harrison, P. M., Strome, R., Heinrich, C., Karunaratne, A., Pasternak, S. H., Chishti, M. A., Liang, Y., *et al.* (1999). Ataxia in prion protein (PrP)-deficient mice is associated with upregulation of the novel PrP-like protein doppel. J Mol Biol *292*, 797-817.

Morshead, C. M., Craig, C. G., and van der Kooy, D. (1998). In vivo clonal analyses reveal the properties of endogenous neural stem cell proliferation in the adult mammalian forebrain. Development *125*, 2251-2261.

Nakajima, K., and Kohsaka, S. (1993). Functional roles of microglia in the brain. Neurosci Res *17*, 187-203.

Nakatomi, H., Kuriu, T., Okabe, S., Yamamoto, S., Hatano, O., Kawahara, N., Tamura, A., Kirino, T., and Nakafuku, M. (2002). Regeneration of hippocampal pyramidal neurons after ischemic brain injury by recruitment of endogenous neural progenitors. Cell *110*, 429-441.

Nathanson, N., Wilesmith, J., and Griot, C. (1997). Bovine spongiform encephalopathy (BSE): causes and consequences of a common source epidemic. Am J Epidemiol *145*, 959-969.

Noctor, S. C., Flint, A. C., Weissman, T. A., Dammerman, R. S., and Kriegstein, A. R. (2001). Neurons derived from radial glial cells establish radial units in neocortex. Nature *409*, 714-720.

Ohsawa, F., Widmer, H.R., Knusel, B., Denton, T.L. and Hefti, F., Response of embryonic rat hippocampal neurons in culture to neurotrophin-3, brain-derived neurotrophic factor and basic fibroblast growth factor, Neuroscience, 57 (1993) 67-77

Palmer, M. S., Dryden, A. J., Hughes, J. T., and Collinge, J. (1991). Homozygous prion protein genotype predisposes to sporadic Creutzfeldt-Jakob disease. Nature *352*, 340-342.

Palmer, T. D., Willhoite, A. R., and Gage, F. H. (2000). Vascular niche for adult hippocampal neurogenesis. J Comp Neurol *425*, 479-494.

Pan, K. M., Baldwin, M., Nguyen, J., Gasset, M., Serban, A., Groth, D., Mehlhorn, I., Huang, Z., Fletterick, R. J., Cohen, F. E., and et al. (1993). Conversion of alpha-helices into beta-sheets features in the formation of the scrapie prion proteins. Proc Natl Acad Sci U S A *90*, 10962-10966.

Papassotiropoulos, A., Wollmer, M. A., Aguzzi, A., Hock, C., Nitsch, R. M., and de Quervain, D. J. (2005). The prion gene is associated with human long-term memory. Hum Mol Genet *14*, 2241-2246.

Parent, J. M., Yu, T. W., Leibowitz, R. T., Geschwind, D. H., Sloviter, R. S., and Lowenstein, D. H. (1997). Dentate granule cell neurogenesis is increased by seizures and contributes to aberrant network reorganization in the adult rat hippocampus. J Neurosci *17*, 3727-3738.

Peden, A. H., Head, M. W., Ritchie, D. L., Bell, J. E., and Ironside, J. W. (2004). Preclinical vCJD after blood transfusion in a PRNP codon 129 heterozygous patient. Lancet *364*, 527-529.

Peretz, D., Williamson, R. A., Kaneko, K., Vergara, J., Leclerc, E., Schmitt-Ulms, G., Mehlhorn, I. R., Legname, G., Wormald, M. R., Rudd, P. M., *et al.* (2001). Antibodies inhibit prion propagation and clear cell cultures of prion infectivity. Nature *412*, 739-743.

Peyrin, J. M., Lasmezas, C. I., Haik, S., Tagliavini, F., Salmona, M., Williams, A., Richie, D., Deslys, J. P., and Dormont, D. (1999). Microglial cells respond to amyloidogenic PrP peptide by the production of inflammatory cytokines. Neuroreport *10*, 723-729.

Picard-Riera, N., Decker, L., Delarasse, C., Goude, K., Nait-Oumesmar, B., Liblau, R., Pham-Dinh, D., and Evercooren, A. B. (2002). Experimental autoimmune encephalomyelitis mobilizes neural progenitors from the subventricular zone to undergo oligodendrogenesis in adult mice. Proc Natl Acad Sci U S A *99*, 13211-13216.

Pincus D, Harrison C, Goodman R, Edgar M, Keyoung HM, Fraser R, Nedergaard M, Goldman SA (1998) FGF2/BDNF-associated maturation of new neurons generated from adult human subependymal cells. Ann Neurol 43:576–585.

Pocchiari, M. (1994). Prions and related neurological diseases. Mol Aspects Med *15*, 195-291.

Prusiner, S. B. (1982). Novel proteinaceous infectious particles cause scrapie. Science *216*, 136-144.

Prusiner, S. B. (1991). Molecular biology of prion diseases. Science *252*, 1515-1522.

Prusiner, S. B. (1997). Prion diseases and the BSE crisis. Science *278*, 245-251.

Prusiner, S. B. (1998). Prions. Proc Natl Acad Sci U S A *95*, 13363-13383.

Prusiner, S. B., Scott, M., Foster, D., Pan, K. M., Groth, D., Mirenda, C., Torchia, M., Yang, S. L., Serban, D., Carlson, G. A., and et al. (1990). Transgenetic studies implicate interactions between homologous PrP isoforms in scrapie prion replication. Cell *63*, 673-686.

Quinones-Hinojosa, A., Sanai, N., Soriano-Navarro, M., Gonzalez-Perez, O., Mirzadeh, Z., Gil-Perotin, S., Romero-Rodriguez, R., Berger, M. S., Garcia-Verdugo, J. M., and Alvarez-Buylla, A. (2006). Cellular composition and cytoarchitecture of the adult human subventricular zone: a niche of neural stem cells. J Comp Neurol *494*, 415-434.

Race R.E., Priola S.A., Bessen R.A., Ernst D., Dockter J., Rall G.F., Mucke L., Chesebro B., and Oldstonet M.B.A.. (1995). Neuron-specific expression of a hamster prion protein minigene in transgenic mice induces susceptibility to hamster scrapie agent. (1995). Neuron 15, 1183-1191.

Race, R., and Chesebro, B. (1998). Scrapie infectivity found in resistant species. Nature *392*, 770.

Race, R., Raines, A., Raymond, G. J., Caughey, B., and Chesebro, B. (2001). Long-term subclinical carrier state precedes scrapie replication and adaptation in a resistant species: analogies to bovine spongiform encephalopathy and variant Creutzfeldt-Jakob disease in humans. J Virol *75*, 10106-10112.

Raeber, A. J., Race, R. E., Brandner, S., Priola, S. A., Sailer, A., Bessen, R. A., Mucke, L., Manson, J., Aguzzi, A., Oldstone, M. B., *et al.* (1997). Astrocyte-specific expression of hamster prion protein (PrP) renders PrP knockout mice susceptible to hamster scrapie. Embo J *16*, 6057-6065.

Raeber, A. J., Klein, M. A., Frigg, R., Flechsig, E., Aguzzi, A. & Weissmann, C. (1999a). PrP-dependent association of prions with splenic but not circulating lymphocytes of scrapie-infected mice. EMBO J. **18,** 2702–2706.

Raeber A.J., Sailer A., Hegyu I., Klein M.A., Licke T.R.U., Fischer M., Brandner S., Aguzzi A. and Weissmann C. (1999b). Ectopic expression of prion protein (PrP) in T lymphocytes or hepatocytes of PrP knockout mice is insufficient to sustain prion replication. *Proc. Natl. Acad. Sci. USA,* 96, 3987–3992.

Reiner, A., Albin, R.L., Anderson, K.D., D'Amato, C.J., Penney, J.B., Young, A.B. (1988). Differential loss of striatal projection neurons in Huntington disease. Proc. Natl. Acad. Sci. U.S.A. 85, 5733–5737.

Reynolds, B. A., and Weiss, S. (1992). Generation of neurons and astrocytes from isolated cells of the adult mammalian central nervous system. Science *255*, 1707-1710.

Rieger, R., Edenhofer, F., Lasmezas, C. I., and Weiss, S. (1997). The human 37-kDa laminin receptor precursor interacts with the prion protein in eukaryotic cells. Nat Med *3*, 1383-1388.

Rietze, R. L., Valcanis, H., Brooker, G. F., Thomas, T., Voss, A. K., and Bartlett, P. F. (2001). Purification of a pluripotent neural stem cell from the adult mouse brain. Nature *412*, 736-739.

Rossi, D., Cozzio, A., Flechsig, E., Klein, M. A., Rulicke, T., Aguzzi, A., and Weissmann, C. (2001). Onset of ataxia and Purkinje cell loss in PrP null mice inversely correlated with Dpl level in brain. Embo J *20*, 694-702.

Roucou, X., Gains, M., and LeBlanc, A. C. (2004). Neuroprotective functions of prion protein. J Neurosci Res *75*, 153-161.

Rubio, N. (1997). Mouse astrocytes store and deliver brain-derived neurotrophic factor using the non-catalytic gp95trkB receptor. Eur. J. Neurosci. 9, 1847–1853.

Sailer, A., Bueler, H., Fischer, M., Aguzzi, A., and Weissmann, C. (1994). No propagation of prions in mice devoid of PrP. Cell *77*, 967-968.

Sakaguchi, S., Katamine, S., Nishida, N., Moriuchi, R., Shigematsu, K., Sugimoto, T., Nakatani, A., Kataoka, Y., Houtani, T., Shirabe, S., *et al.* (1996). Loss of cerebellar Purkinje cells in aged mice homozygous for a disrupted PrP gene. Nature *380*, 528-531.

Sakakibara, S., and Okano, H. (1997). Expression of neural RNA-binding proteins in the postnatal CNS: implications of their roles in neuronal and glial cell development. J Neurosci *17*, 8300-8312.

Sanai, N., Tramontin, A. D., Quinones-Hinojosa, A., Barbaro, N. M., Gupta, N., Kunwar, S., Lawton, M. T., McDermott, M. W., Parsa, A. T., Manuel-Garcia Verdugo, J., *et al.* (2004). Unique astrocyte ribbon in adult human brain contains neural stem cells but lacks chain migration. Nature *427*, 740-744.

Santuccione, A., Sytnyk, V., Leshchyns'ka, I., and Schachner, M. (2005). Prion protein recruits its neuronal receptor NCAM to lipid rafts to activate p59fyn and to enhance neurite outgrowth. J Cell Biol *169*, 341-354.

Scharfman, H. E., Goodman, J. H., and Sollas, A. L. (2000). Granule-like neurons at the hilar/CA3 border after status epilepticus and their synchrony with area CA3 pyramidal cells: functional implications of seizure-induced neurogenesis. J Neurosci *20*, 6144-6158.

Schinder, A. F., and Gage, F. H. (2004). A hypothesis about the role of adult neurogenesis in hippocampal function. Physiology (Bethesda) *19*, 253-261.

Schmitt-Ulms, G., Legname, G., Baldwin, M. A., Ball, H. L., Bradon, N., Bosque, P. J., Crossin, K. L., Edelman, G. M., DeArmond, S. J., Cohen, F. E., and Prusiner, S. B. (2001). Binding of neural cell adhesion molecules (N-CAMs) to the cellular prion protein. J Mol Biol *314*, 1209-1225.

Schmidtke, K., Manner, H., Kaufmann, R., Schmolck, H. (2002). Cognitive procedural learning in patients with fronto-striatal lesions. Learn. Mem. 9, 419–429.

Schoenherr, C.J., Paquette, A.J., Anderson, D.J. (1996). Identification of potential target genes for the neuron-restrictive silencer factor. Proc. Natl. Acad. Sci. U.S.A. 93, 9881–9886.

Seri, B., Garcia-Verdugo, J. M., McEwen, B. S., and Alvarez-Buylla, A. (2001). Astrocytes give rise to new neurons in the adult mammalian hippocampus. J Neurosci *21*, 7153-7160.

Sharif, A., Legendre, P., Prevot, V., Allet, C., Romao, L., Studler, J. M., Chneiweiss, H., and Junier, M. P. (2006). Transforming growth factor alpha promotes sequential conversion of mature astrocytes into neural progenitors and stem cells. Oncogene.

Shyu, W. C., Lin, S. Z., Chiang, M. F., Ding, D. C., Li, K. W., Chen, S. F., Yang, H. I., and Li, H. (2005). Overexpression of PrPC by adenovirus-mediated gene targeting reduces ischemic injury in a stroke rat model. J Neurosci *25*, 8967-8977.

Silverman, G. L., Qin, K., Moore, R. C., Yang, Y., Mastrangelo, P., Tremblay, P., Prusiner, S. B., Cohen, F. E., and Westaway, D. (2000). Doppel is an N-glycosylated, glycosylphosphatidylinositol-anchored protein. Expression in testis and ectopic production in the brains of Prnp(0/0) mice predisposed to Purkinje cell loss. J Biol Chem *275*, 26834-26841.

Solforosi, L., Criado, J. R., McGavern, D. B., Wirz, S., Sanchez-Alavez, M., Sugama, S., DeGiorgio, L. A., Volpe, B. T., Wiseman, E., Abalos, G., *et al.* (2004). Cross-linking cellular prion protein triggers neuronal apoptosis in vivo. Science *303*, 1514-1516.

Somerville, R. A., Chong, A., Mulqueen, O. U., Birkett, C. R., Wood, S. C., and Hope, J. (1997). Biochemical typing of scrapie strains. Nature *386*, 564.

Song, H., Kempermann, G., Overstreet Wadiche, L., Zhao, C., Schinder, A. F., and Bischofberger, J. (2005). New neurons in the adult mammalian brain: synaptogenesis and functional integration. J Neurosci *25*, 10366-10368.

Song, H., Stevens, C. F., and Gage, F. H. (2002). Astroglia induce neurogenesis from adult neural stem cells. Nature *417*, 39-44.

Spencer, M. D., Knight, R. S., and Will, R. G. (2002). First hundred cases of variant Creutzfeldt-Jakob disease: retrospective case note review of early psychiatric and neurological features. Bmj *324*, 1479-1482.

Spires T.L., Grote H.E., Varshney N.K., Cordery P.M., Dellen A., Blakemore C., and Hannan A.J. (2004). Environmental enrichment rescues protein deficits in a mouse model of Huntington's Disease, indicating a possible disease mechanism. J Neurosci. 24(9):2270 –2276.

Steele, A. D., Emsley, J. G., Ozdinler, P. H., Lindquist, S., and Macklis, J. D. (2006). Prion protein (PrPc) positively regulates neural precursor proliferation during developmental and adult mammalian neurogenesis. Proc Natl Acad Sci U S A *103*, 3416-3421.

Stekel, D. J., Nowak, M. A., and Southwood, T. R. (1996). Prediction of future BSE spread. Nature *381*, 119.

Sullivan FR, Bird ED, Alpay M, Cha JH (2001) Remotivation therapy and Huntington's disease. J Neurosci Nurs 33:136–142.

Sun, Y.M., Greenway, D.J., Johnson, R., Street, M., Belyaev, N.D., Deuchars, J., Bee, T., Wilde, S., Buckley, N.J. (2005). Distinct profiles of REST interactions with its target genes at different stages of neuronal development. Mol.Biol. Cell 16, 5630–5638.

Szpak, G. M., Lewandowska, E., Lechowicz, W., Wierzba-Bobrowicz, T., Kulczycki, J., Bertrand, E., Pasennik, E., and Dymecki, J. (2006). The brain immune response in human prion diseases. Microglial activation and microglial disease. I. Sporadic Creutzfeldt-Jakob disease. Folia Neuropathol *44*, 202-213.

Tagliavini, F., Prelli, F., Verga, L., Giaccone, G., Sarma, R., Gorevic, P., Ghetti, B., Passerini, F., Ghibaudi, E., Forloni, G., and et al. (1993). Synthetic peptides homologous to prion protein residues 106-147 form amyloid-like fibrils in vitro. Proc Natl Acad Sci U S A *90*, 9678-9682.

Tateishi, J., Kitamoto, T., Hoque, M. Z., and Furukawa, H. (1996). Experimental transmission of Creutzfeldt-Jakob disease and related diseases to rodents. Neurology *46*, 532-537.

Telling, G. C., Haga, T., Torchia, M., Tremblay, P., DeArmond, S. J., and Prusiner, S. B. (1996). Interactions between wild-type and mutant prion proteins modulate neurodegeneration in transgenic mice. Genes Dev *10*, 1736-1750.

Thackray, A. M., Klein, M. A., Aguzzi, A., and Bujdoso, R. (2002). Chronic subclinical prion disease induced by low-dose inoculum. J Virol *76*, 2510-2517.

Thellung, S., Florio, T., Corsaro, A., Arena, S., Merlino, M., Salmona, M., Tagliavini, F., Bugiani, O., Forloni, G., and Schettini, G. (2000). Intracellular mechanisms mediating the neuronal death and astrogliosis induced by the prion protein fragment 106-126. Int J Dev Neurosci *18*, 481-492.

Thellung, S., Florio, T., Villa, V., Corsaro, A., Arena, S., Amico, C., Robello, M., Salmona, M., Forloni, G., Bugiani, O., *et al.* (2000). Apoptotic cell death and impairment of L-type voltage-sensitive calcium channel activity in rat cerebellar granule cells treated with the prion protein fragment 106-126. Neurobiol Dis *7*, 299-309.

Thellung, S., Villa, V., Corsaro, A., Arena, S., Millo, E., Damonte, G., Benatti, U., Tagliavini, F., Florio, T., and Schettini, G. (2002). p38 MAP kinase mediates the cell death induced by PrP106-126 in the SH-SY5Y neuroblastoma cells. Neurobiol Dis *9*, 69-81.

Timmusk, T., Palm, K., Metsis, M., Reintam, T., Paalme, V., Saarma, M., Persson, H. (1993). Multiple promoters direct tissue-specific expression of the rat BDNF gene. Neuron 10, 475–489.

Timmusk, T., Belluardo, N., Persson, H., Metsis, M. (1994). Developmental regulation of brain-derived neurotrophic factor messenger RNAs transcribed from different promoters in the rat brain. Neuroscience 60, 287–291.

Timmusk, T., Lendahl, U., Funakoshi, H., Arenas, E., Persson, H., Metsis, M. (1995). Identification of brain-derived neurotrophic factor promoter regions mediating tissue-specific, axotomy-, and neuronal activity-induced expression in transgenic mice. J. Cell Biol. 128, 185–199.

Tozuka, Y., Fukuda, S., Namba, T., Seki, T., and Hisatsune, T. (2005). GABAergic excitation promotes neuronal differentiation in adult hippocampal progenitor cells. Neuron *47*, 803-815.

Ueki T., Tanaka M., Yamashita K., Mikawa S., Qiu Z., Maragakis N.J., Hevner R.F., Miura N., Sugimura H., and Sato K.. (2003). A novel secretory factor, Neurogenesin-1, provides neurogenic environmental cues for neural stem cells in the adult hippocampus. J. Neurosci. 23(37):11732–11740.

Van Everbroeck B, Pals P, Martin JJ, Cras P (1999) Antigen retrieval in prion protein immunohistochemistry. J Histochem Cytochem 47:1465-1470

Van Everbroeck, B., Dewulf, E., Pals, P., Lubke, U., Martin, J. J., and Cras, P. (2002). The role of cytokines, astrocytes, microglia and apoptosis in Creutzfeldt-Jakob disease. Neurobiol Aging *23*, 59-64.

van Praag, H., Christie, B. R., Sejnowski, T. J., and Gage, F. H. (1999). Running enhances neurogenesis, learning, and long-term potentiation in mice. Proc Natl Acad Sci U S A *96*, 13427-13431.

van Praag, H., Kempermann, G., and Gage, F. H. (1999). Running increases cell proliferation and neurogenesis in the adult mouse dentate gyrus. Nat Neurosci *2*, 266-270.

van Praag, H., Schinder, A. F., Christie, B. R., Toni, N., Palmer, T. D., and Gage, F. H. (2002). Functional neurogenesis in the adult hippocampus. Nature *415*, 1030-1034.

Veerhuis, R., Hoozemans, J. J., Janssen, I., Boshuizen, R. S., Langeveld, J. P., and Eikelenboom, P. (2002). Adult humán microglia secrete cytokines when exposed to neurotoxic prion protein peptide: no intermediary role for prostaglandin E2. Brain Res *925*, 195-203.

Wadsworth, J. D., Hill, A. F., Beck, J. A., and Collinge, J. (2003). Molecular and clinical classification of human prion disease. Br Med Bull *66*, 241-254.

Weise, J., Crome, O., Sandau, R., Schulz-Schaeffer, W., Bahr, M., and Zerr, I. (2004). Upregulation of cellular prion protein (PrPc) after focal cerebral ischemia and influence of lesion severity. Neurosci Lett *372*, 146-150.

Weise, J., Sandau, R., Schwarting, S., Crome, O., Wrede, A., Schulz-Schaeffer, W., Zerr, I., and Bahr, M. (2006). Deletion of cellular prion protein results in reduced Akt activation, enhanced postischemic caspase-3 activation, and exacerbation of ischemic brain injury. Stroke *37*, 1296-1300.

Weissmann, C. (1996). PrP effects clarified. Curr Biol *6*, 1359.

Westaway, D., DeArmond, S.J., Cayetano-Canlas, J., Groth, D., Foster, D., Yang, S.L., Torchia, M., Carlson, G.A., and Prusiner, S.B. (1994). Degeneration of skeletal muscle, peripheral nerves, and the central nervous system in transgenic mice overexpressing wildtype prion proteins. Cell *76*, 117–129.White, A. R., Enever, P., Tayebi, M., Mushens, R., Linehan, J., Brandner, S., Anstee, D., Collinge, J., and Hawke, S. (2003). Monoclonal antibodies inhibit prion replication and delay the development of prion disease. Nature *422*, 80-83.

Whittington, M. A., Sidle, K. C., Gowland, I., Meads, J., Hill, A. F., Palmer, M. S., Jefferys, J. G., and Collinge, J. (1995). Rescue of neurophysiological phenotype seen in PrP null mice by transgene encoding human prion protein. Nat Genet *9*, 197-201.

Wieser, H. G., Schindler, K., and Zumsteg, D. (2006). EEG in Creutzfeldt-Jakob disease. Clin Neurophysiol *117*, 935-951.

Will, R. G. (1993). Epidemiology of Creutzfeldt-Jakob disease. Br Med Bull *49*, 960-970.

Will, R. G., Ironside, J. W., Zeidler, M., Cousens, S. N., Estibeiro, K., Alperovitch, A., Poser, S., Pocchiari, M., Hofman, A., and Smith, P. G. (1996). A new variant of Creutzfeldt-Jakob disease in the UK. Lancet *347*, 921-925.

Williams, A., Lucassen, P. J., Ritchie, D., and Bruce, M. (1997). PrP deposition, microglial activation, and neuronal apoptosis in murine scrapie. Exp Neurol *144*, 433-438.

Williams, A. E., Lawson, L. J., Perry, V. H., and Fraser, H. (1994). Characterization of the microglial response in murine scrapie. Neuropathol Appl Neurobiol *20*, 47-55.

Wroe, S. J., Pal, S., Siddique, D., Hyare, H., Macfarlane, R., Joiner, S., Linehan, J. M., Brandner, S., Wadsworth, J. D., Hewitt, P., and Collinge, J. (2006). Clinical presentation and pre-mortem diagnosis of variant Creutzfeldt-Jakob disease associated with blood transfusion: a case report. Lancet *368*, 2061-2067.

Zawlik, I., Witusik, M., Hulas-Bigoszewska, K., Piaskowski, S., Szybka, M., Golanska, E., Liberski, P. P., and Rieske, P. (2006). Regulation of PrPC expression: nerve growth factor (NGF) activates the prion gene promoter through the MEK1 pathway in PC12 cells. Neurosci Lett *400*, 58-62.

Zhang, C. C., Steele, A. D., Lindquist, S., and Lodish, H. F. (2006). Prion protein is expressed on long-term repopulating hematopoietic stem cells and is important for their self-renewal. Proc Natl Acad Sci U S A *103*, 2184-2189.

Zigova Tanja, Viorica Pencea, Stanley J. Wiegand, and Marla B. Luskin. (1998). Intraventricular administration of BDNF increases the number of newly generated neurons in the adult olfactory bulb. Molecular and Cellular Neuroscience 11, 234–245.

Zuccato C, Ciammola A, Rigamonti D, Leavitt BR, Goffredo D, Conti L, MacDonald ME, Friedlander RM, Silani V, Hayden MR, Timmusk T, Sipione S, Cattaneo E (2001) Loss of huntingtin-mediated BDNF gene transcription in Huntington's disease. Science 293:493–498.

Zuccato, C., Tartari, M., Crotti, A., Goffredo, D., Valenza, M., Conti, L., Cataudella, T., Leavitt, B.R., Hayden, M.R., Timmusk, T., Rigamonti, D., Cattaneo, E. (2003). Huntingtin interacts with REST/NRSF to modulate the transcription of NRSE-controlled neuronal genes. Nat. Genet. 35, 76–83.

Zuccato, C., Tartari, M., Goffredo, D., Cattaneo, E., Rigamonti, D. (2005). From target identification to drug screening assays for neurodegenerative diseases. Pharmacol. Res. 52, 245–251.

Zuccato C, Cattaneo E. (2007). Role of brain-derived neurotrophic factor in Huntington's disease. Prog Neurobiol. 81(5-6):294-330.

Appendix 1. Reagents, prepared solutions and equipment

Tail DNA extraction

Tail Lysis Buffer:

Tris pH 8	50mM
EDTA pH 8	100mM
NaCl	100mM
SDS	1 %

TE 10x stock (sterile):

Tris pH 7.5	100mM
EDTA	10mM

Chemicals:

EDTA	Sigma	cat. no. 3609
NaCl	Fisher	cat. no. S3120/63
Proteinase K (PK)	Roche	cat. no. 1 373 200
Trizma Base	Sigma	cat. no. T1503
SDS (sodium dodecyl sulphate)	Fluka/Sigma	cat. no. 71729

PCR

Reagents:

dNTPs	Promega	cat. no. C1145
Taq DNA Polymerase	Promega	cat. no. 17549322
$MgCl_2$ (25mM)	Promega	cat. no. 17039751
10x $MgCl_2$ buffer (thermophilic DNA)	Promega	cat. no. 17039843

Primers:

Primer B (PDG246), Primer D (PDG247), Primer RBF, Primer RBR.

all primers were purchased from MWG and dissolved in autoclaved distilled water (volume as indicated in the product instructions),then shaken at the appropriate temperature for 8 mins (Eppendorf Thermomixer, 900 rpm).

Agarose gel

PBS solution:

NaCl	137 mM
KCl	2.7 mM
Na_2HPO_4	10mM
KH_2PO_4	2mM

50x TAE (Tris Acetate EDTA) solution:

trizma base	242.2g
glacial acetic acid	57.1 ml
0.5M EDTA pH 8	100ml
ddH_2O	bring to 1 litre

Glacial Acetic Acid:

tris acetate	2M
EDTA pH 8	0.05M

6x Loading Buffer:

Tris pH 7.5	10mM
EDTA	50mM
Ficoll 400	15%
Bromophenolblue	0.03%
XyleneCylol FF	0.03%
Orange G	0.4%

Ethidium Bromide: dissolved in water at a concentration of 10 mg/ml

Chemicals:

Agarose	Sigma	cat. no. A9539
DNA Ladder 100bp	Promega	cat. no. G2101
Ethidium Bromide MB Grade	Sigma	cat. no. E2515
KCl	Fluka/Sigma	cat. no. 60132
Bromophenolblue	Fisher	cat. no. B/P620/44
XyleneCyanol FF	Sigma	cat. no. X 4126
Orange G	Sigma	cat. no. O 3756
Ethidium Bromide	Sigma	cat. no E2515

Prion infection

Animals were anaesthetized with isoflurane using Vettech Compact Anaesthesia System

I4096: 1% RML inoculum

I5035: 1% CD1 Mock inoculum (normal brain homogenate)

BrdU injections

BrdU (5' Bromo-2'deoxyuridine) cat no B5002 from Sigma: stock of 5 and 10 µg/µl BrdU in ddH_2O was prepared and stored in dark at 4 °C.

Sectioning on the vibratome and storage of brain sections

10% buffered formal saline (formalin) from Pioneer Research Chemicals Limited, cat. no. PRC/R/2
Sodium azide from Sigma, cat. no. S 2002

BrdU/DAB stainings for vibratome brain sections

Hydrochloric Acid Solution:

PBS	0.1M
HCl	2N
triton x-100	1%

DAB Solution:

DAB	1ml
PBS	25 mls
H_2O_2	10-15 µl

H_2O_2 was added immediately before use

Borate Buffer:

0.1 M boric acid in ddH2O, pH 8.4

PBST solution:

PBS solution containing 0.05% Tween 20

Haematoxylin solution:

Haematoxylin diluted 1:4 in distilled water and filtered before use.

Acid solution:

1% HCl in 100% ethanol

Chemicals:

ABC Complex/ HPR	DakoCytomation	cat.no. K0355
Ethanol AnalaR 99.7 %	VWR	cat. no. 10107 EP
DAB	Fluka	cat. no. 32741-5G-F
Xylene GPR	BIOS EUROPE	cat. no. LS81950/G
Pertex Mounting Medium (60% xylene)	Medite Gmb	cat. no. H PER 4000
Boric acid	Sigma	cat. no. B6768
Haematoxylin, Harris	BDH	cat. no. 351946T

Immuno-fluorescent double stainings

TSA blocking solution:

TSA blocking reagent	0.5%
Tris-HCl	0.1 M
NaCl	0.15M

Prepared by heating to 60 °C and continuous stirring. Adjust to pH 7.5 and store at -20 °C.

Chemicals:

TSA blocking reagent	Perkin Elmer	cat. no. FP1020
ABC Complex/ HPR	DakoCytomation	cat. no. K0355
Hoechst 33342	Molecular Probes	cat. no. H1399
Dako Fluorescent mounting medium	Dakocytomation	cat. no. S3023
DMSO	Fluka/Sigma	cat. no. 41644
TSA Plus Cyanine 3 System	Perkin Elmer	cat. no. NEL744

Each aliquot of TSA-Cy3 powder as supplied was dissolved in 250µl DMSO. Immediately before use, TSA-Cy3 was further diluted 1:50 in the diluent solution supplied.

Histology of paraffin-embedded sections

Tris-EDTA citrate buffer pH 7.8 (x10):

H_2O	1 l
EDTA	5g
Trizma base	2.5g
Tri-sodium citrate	3.2g

2M sodium hydroxide:

Sodium hydroxide	80g
H_2O	1 l

Chemicals:

Superblock	Pierce	cat. no. 3754577
Protease 1	NexES	cat. no. 760-2018
IViewDAB Detection Kit [containing an inhibitor solution (3 % hydrogen peroxide) (4 min), universal biotinylated secondary antibody (10 min), streptavidin-horseradish peroxidase solution (10 min) DAB and hydrogen peroxide (20 min), copper solution (4 min)].	Ventana Medical Systems	cat. no. 760-091
DAB-MAP kit	Ventana	
Eosin	VWR	cat. no. 352654T
Harris Haematoxylin	VWR	cat. no. 351946T
10 % Buffered formal-Saline	Pioneer Research Ltd	cat. no. PRC/R/2
98 % Formic acid	VWR	cat. no. 284305N
Sodium hydroxide pellets	VWR	cat. no. 30167 4M
Industrial methylated spirits	JM Loveridge Ltd	cat. no. 102-3795
Pure Paraffin Wax	R A Lamb	cat. no. W2
Methanol GPR	VWR	cat. no. 101586B
EDTA	Sigma	cat. no. E-1644
Trizma Base	Sigma	cat. no. T-1503
Tri-sodium citrate	Sigma	cat. no. S461

Strept ABComplex/HRP Duet kit	Dako	cat. no. K0492

Other:

Biopsy cassettes	R.A.Lamb	cat. no. E10/BMW/colour
SuperFrost Microscope Slides	VWR	cat. no. 631-0108

Antibodies

Primary Antibodies:

Rat anti-BrdU	abcam	cat. no. 6326
Mouse anti-β III tubulin (TUJ1)	Chemicon	cat. no. MAB 1637
Rabbit anti-GFAP	Dako	cat. no. Z0334
Rabbit anti-iba1	Wako	cat. no. 019-19741
biotinylated swine a-rabbit	DAKOcytomation	cat. no. E0353

Secondary Antibodies:

Biotinylated rabbit anti-rat	dakocytomation	cat. no. E0468
Alexa anti-mouse 488 (H+L)	Molecular Probes	cat. no. A11001
Alexa anti-rabbit 488 (H+L)	Molecular Probes	cat. no. A11008
biotinylated swine a-rabbit	dakocytomation	cat. no. E0353

Protein determination

Chemicals:

BSA (bovine serum albumin)	Sigma	cat.no. A 1470
BCA Protein Assay Reagent Kit	Pierce (Perbio Science	cat.no. 23225

BDNF Elisa

Carbonate coating buffer pH 9.7::

sodium bicarbonate	0.025 M
sodium carbonate	0.025 M

DPBS pH 7.3::

ddH_2O	200mls
KCl	0.04 g
NaCl	1.6 g
KH_2PO4	0.04g
Na_2HPO_4	0.23g
$CaCl_2.2H_20$	26.6 mg
$MgCl_2.6H_2O$	20mg

Water was added to the KCl, NaCl, KH_2PO_4, and Na_2HPO_4

pH was then adjusted to 7.3 and the other two chemicals were added and the solution mixed thoroughly

PBST ::

PBS solution containing 0.05% Tween 20

ddH_2O	200mls
KCl	0.04 g
NaCl	1.6 g
KH_2PO4	0.04g
Na_2HPO_4	0.23g
$CaCl_2.2H_20$	26.6 mg
$MgCl_2.6H_2O$	20mg

Lysis buffer::

ddH_2O	50mls
Tris-HCl pH 8.0	0.1576 g
NaCl	0.4g
NP40	0.5 ml
Glycerol	5mls
PMSF	8.7mg
Aprotinin	500mg
Leupeptin	50mg
Sodium Vanadate	4.57 mg

Neural stem cell culture

Reconstituted papain solution::

EBSS (vial1 of papain dissociation system)	5mls
Papain (vial2 of papain dissociation system	All content of vial 2
DNAseI (vial3 of papain dissociation system	250 µl

Vial 1 contains sterile Earle's Balanced Salt Solution (EBSS)

Vial 3 (DNAseI) is reconstituted with 0.5ml of EBSS (vial 1)

For the reconstituted papain solution vial 2 (papain) was mixed initially with 5mls of EBSS (vial 1) until papain was completely dissolved and the solution appeared clear and then 250 µl of DNAseI (vial 3) was added.

DNAse-albumin inhibitor mixture::

EBSS (vial1 of papain dissociation system)	2.7mls
Albumin-ovomucoid inhibitor solution (vial4 of papain dissociation system	300 µl
DNAseI (vial3 of papain dissociation system	150 µl

Glucose medium::

NaCl	120 mM
KCl	5 mM
HEPES	25 mM
Glucose	9.1 mM

pH was set up at 7.4 and the medium was stored at 4°C

Neurosphere medium::

DMEM / HamF12 media	50mls
P/S	1%
B27	1ml
EGF	10 µl
bFGF	10 µl

The medium needs to be warmed up at 37°C before added to the cells.

Stock solutions of EGF and bFGF were prepared at a concentration of 100µg/ml in 0.1% BSA each.

Papain solution for dissociation of neurospheres::

Papain	35.5 µl
DMEM / HamF12 media	1ml

L-cystein	24mg L-cystein / ml MEM

Trypsin inhibitor solution::

L15 media	13ml
BSA	15mg
Tyrpsin stopper	7mg
DNAse	16mg

Chemicals::

Papain DissociationSystem (contains vial 1(EBSS), vial 2 (papain), vial 3 (DNAse) and vial 4 (Ovomucoid protease inhibitor with BSA)	Worthington	cat. no.LK003150 1kit
DMEM / HamF12	Sigma	cat.no. D8437
P/S (antibiotic)	Invitrogen	cat.no. 15140-122
B27	Invitrogen	cat.no. 17504-044
EGF	Calbiochem	cat.no. 324851
bFGF	PreproTech	cat.no. 100-18B
L15 media	Sigma	cat.no. 5520
BSA	Sigma	cat.no. A1470
Tyrpsin stopper	Roche	cat.no. 109878
DNAse	Roche	cat.no. 104159
Papain	Worthington	cat.no. LS 003124
Trypsin/EDTA (1x)	Invitrogen	cat.no. 25300-054

green needle (21G)	BD	cat.no. 304432

Equipment and software:

Peloris dual retort rapid tissue processor, Vision Biosystems

RA Lamb Embedding station

Leica RM 2135 microtome

Benchmark Staining Machine, Ventana Medical Systems Inc., Tucson, Arizona (http://www.ventanamed.com/).

Cox Pro-Mounter RCM 2000

Microplate reader BioRad

Eppendorf centrifuge 5415D

Eppendorf Thermomixer Comfort

Autoclave Boxer 200L (121 °C for 20')

Bio-Rad Gel Doc 1000

AB Applied Biosystems GeneAmp PCR System 9700

Vibratome 1500, Vibratome instruments GS-044026

Zeiss LSM510 META Confocal microscope

Axioskop 2 Mot Light microscope

Bio-Rad Power Pac 2000

Appendix 2. Study of Proliferation – number of mice examined

Study of proliferation in the hippocampus of mice - Number of mice examined.

Mouse Line	Inoculation	Time point of single BrdU injection	BrdU latency	No of mice examined	Sagittal area analysed per animal
wt	mock	various	30'	8	160µm
wt	RML	110 days p.i.	30'	3	160µm
wt	RML	Onset of symptoms	30'	3***	160µm
tg37	mock	various	30'	4	160µm
tg37	RML	8 wk p.i.	30'	3	160µm
tg37	RML	11 wk p.i.	30'	3	160µm
tg37	RML	12 wk p.i.	30'	3	160µm
NFH-Cre/tg37	RML	12 wk p.i.	30'	3	160µm
NFH-Cre/tg37	RML	13 wk p.i.	30'	3	160µm
NFH-Cre/tg37	RML	37 wk p.i.	30'	2*	160µm
NFH-Cre/tg37	none	9 wk of age	30'	3	160µm
NFH-Cre/tg37	none	15 wk of age	30'	3	160µm
NFH-Cre/tg37	none	22 wk of age	30'	3**	160µm
Prnp $^{0/0}$	none	12-24 wk	30'	6	160µm

* PCR data confirming the genotype of the 2 animals examined could not be located.
** PCR data confirming the genotype of 1 of the 3 animals examined could not be located.
*** 1 mouse developed symptoms at 111 days p.i. and the other 2 at 124 days p.i.

Appendix 3. Characterisation of BrdU-labelled cells – number of mice examined

Characterisation of BrdU-labelled cells in the dentate gyrus of mice.
Number of mice examined and number of sections (per mouse) analysed on the confocal microscope.

Mouse Strain	Inoculation	Time point of single BrdU inj.	BrdU latency	Double staining	No. of mice examined	Total no. of 40 µm sections analyzed
wt	RML	110 d p.i.	8 days	BrdU/β tubulin	3	5
wt	RML	110 d p.i.	8 days	BrdU/GFAP	3	6
wt	RML	110 d p.i.	8 days	BrdU/Iba-1	3	6
tg37	mock	11 wk p.i.	7 days	BrdU/β tubulin	3	7
tg37	mock	11 wk p.i.	7 days	BrdU/GFAP	4	6
tg37	mock	12 wk p.i.	5 days	BrdU/GFAP	2	4
tg37	mock	11 wk p.i.	7 days	BrdU/Iba-1	4	7
tg37	RML	11 wk p.i.	7 days	BrdU/β tubulin	4	7
tg37	RML	11 wk p.i.	7 days	BrdU/GFAP	4	7
tg37	RML	12 wk p.i.	5 days	BrdU/GFAP	3	6
tg37	RML	11 wk p.i.	7 days	BrdU/Iba-1	4	8
NFH-Cre/tg37	RML	13 wk p.i.	7 days	BrdU/β tubulin	3	6
NFH-Cre/tg37	RML	13 wk p.i.	7 days	BrdU/GFAP	3	6
NFH-Cre/tg37	RML	13 wk p.i.	7 days	BrdU/Iba-1	3	6